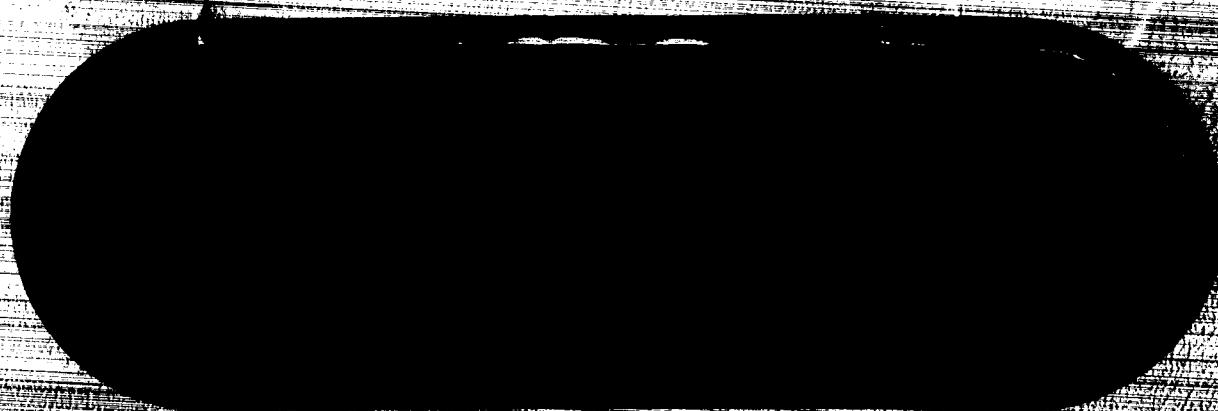


BOEING



GPO PRICE \$ _____
CFSTI PRICE(S) \$ _____
Hard copy (HC) 4.00
Microfiche (MF) 1.00

ff 853 July 85

FACILITY FORM 802

<u>N66-14278</u> (ACCESSION NUMBER)	_____ (THRU)
<u>148</u> (PAGES)	<u>1</u> (CODE)
<u>CR 68983</u> (NASA CR OR TMX OR AD NUMBER)	<u>03</u> (CATEGORY)

SEATTLE, WASHINGTON

DEVELOPMENT AND TESTING OF A LOW-TEMPERATURE HYDRAULIC SYSTEM

Final Report

Volume II

HYDRAULIC SYSTEM ANALYSIS AND TEST PROGRAM

D2-90795-2

Prepared under

George C. Marshall Space Flight Center Contract NAS8-11722

by

The Boeing Company, Aerospace Group

September 1965

CONTENTS

	<u>Page</u>
ABSTRACT	v
1.0 INTRODUCTION	1
2.0 SUMMARY	2
2.1 Development	2
2.2 Design and Fabrication	3
2.3 Test Program	3
2.4 Conclusions	5
3.0 HYDRAULIC SYSTEM ANALYSIS	6
3.1 Fluid and Seal Evaluation	6
3.2 Materials Evaluation	27
3.3 Thermal Protection	29
4.0 TEST SYSTEM DESIGN	51
4.1 Application Requirements	51
4.2 System Design	60
4.3 Test Facility Equipment	69
5.0 TEST PROGRAM	76
5.1 Test Plan	76
5.2 Low-Temperature Tests	88
5.3 Combined-Effects Tests	111
5.4 Thermal Cycling Test	124
5.5 Vacuum Tests	131
6.0 TEST PROGRAM CONCLUSIONS	141
7.0 INVENTIONS	143
REFERENCES	144

FIGURES

<u>Figure</u>		<u>Page</u>
1	Seal Material Deflection Characteristics	9
2	Effect of Temperature on Load Deflection	10
3	Fluid Thermal Stability Apparatus	12
4	Physical Properties of Low-Temperature Fluids	13
5	Low-Temperature Fluids Thermal Stability and Material Compatibility	14
6	Contraction of Low-Temperature Hydraulic Fluids	16
7	Viscosity of Various Fluids	17
8	Properties of Heat-Transfer Fluids	19
9	Static O-Ring Test System	20
10	Elastomer Swell Test Results	21
11	Fluid-Elastometer Compatibility	23
12	Dynamic Nonelastomeric Seals	26
13	Material Characteristics at Low Temperature	28
14	Power Penalty — Batteries and Solar Cells	31
15	Power Penalty — Hydrogen-Oxygen Fuel Cells	33
16	Power Penalty — Isotope Heat Sources	34
17	Power Penalty Summary for Vehicles with Fuel Cell Power Source	35
18	Power Penalty Summary for Vehicles Without Fuel Cell Power Source	36
19	Radiation Heat Loss — No Insulation	39
20	Radiation Heat Loss — Multilayer Insulation	41
21	Radiation Heat Loss — Glass Fiber Insulation	42
22	Thermal Protection System Weight for Vehicles with Fuel Cell Power Source	43
23	Thermal Protection System Weight for Vehicles Without Fuel Cell Power Source	44
24	Conduction Heat Loss Through Actuator Bearing	46
25	Thermal Protection System Weight Including Conduction Losses for Vehicles with Fuel Cell Power Source	47
26	Thermal Protection System Weight Including Conduction Losses for Vehicles with Fuel Cell Power Source	48
27	Thermal Protection System Weight Including Conduction Losses for Vehicles Without Fuel Cell Power Source	49
28	Thermal Protection System Weight Including Conduction Losses for Vehicles Without Fuel Cell Power Source	50
29	Actuator Position Selection	54
30	Actuation Requirement Variation with Actuator Position	55
31	Test System Design Alternates	58
32	Basic Test-System Schematic	61
33	Hydraulic Cart	62
34	Test Actuator Parts	64
35	Chipped Plating Example	66
36	Pitted Plating Example	67

FIGURES (Cont)

<u>Figure</u>		<u>Page</u>
37	Actuator Installation in Vacuum Container	70
38	Loading Device Cross Section	73
39	Test System Components	75
40	Test Program Outline	77
41	Data Acquisition Schematic	79
42	Operational Test System	81
43	Hot Cathode Ionization Vacuum Gage	82
44	Test System Schematic	84
45	Low-Temperature Test Facilities and Instrumentation	89
46	Test System Installation-Low Temperature Tests	91
47	Flow Coefficient vs Temperature	95
48	Low-Temperature Actuator Dynamic Seal Wear	97
49	System Response, +75 to -50°F	100
50	System Response, +75 to -100°F (Only Valve No. 4)	101
51	System Response, +75 to -100°F (Both No. 4 and No. 5 Valves)	102
52	System Response, +75 to -140°F	103
53	Actuator Checkout Test Data	105
54	Open-Loop Frequency Response, +75 to -140°F	106
55	Actuation System Low Temperature Step Response	108
56	Fluid Pressure and Temperature During a Typical Low Temperature Test Run	109
57	Low Temperature Tests-Temperature History	110
58	Space Simulator Facility	113
59	Automatic Cooling System	114
60	Automatic Temperature Controller	115
61	Environmental History — Simulated Flight Test	118
62	Simulated Flight Test System Response Data	119
63	Frequency Response — High Temperature Test ($\Delta p = 2000$ psi)	122
64	Frequency Response — High Temperature Test	123
65	Thermal Cycling Temperature Control	125
66	Typical Thermal Cycle	127
67	Thermal Cycling History	128
68	System Response-Thermal Cycle Test	129
69	Seal-Wear Actuator Number 1	130
70	Vacuum Storage Station Schematic	132
71	Vacuum Storage Station	133
72	Leakage Effects on Vacuum-Container Pressure	136
73	Vacuum Storage Pressure Log	137
74	Vacuum Storage Test-Fluid Leakage	138
75	System Response with Vacuum Stored Actuator	140

ABSTRACT

This document is Volume II of the final report for Contract NAS8-11722. Abstracts for both volumes are included below for continuity.

Volume I — The stages of space exploration leading to placement of men on the Moon require Earth-orbiting vehicles, with and without re-entry capability, and lunar surface vehicles, with and without roving capability. Actuation tasks must be performed during operation of each of these four types of vehicles. The comparison of various actuation systems to satisfy these space tasks is determined in this study by the use of a parametric trade evaluation.

Eighty candidate space actuation tasks are considered from which 10 are selected as having the most trade-study value. From these 10, one task associated with each of the above four vehicle types is investigated in detail.

The evaluation considers hydraulic, pneumatic, and electromechanical actuation systems to satisfy the requirements of each task. Provisions for power and thermal conditioning for each system are considered. The results of the trade study are in the form of a numerical rating summary showing the comparison of systems, for the same task, on the basis of weight, reliability, cost, availability, and performance margin.

Volume II — The effective use of hydraulic systems in space applications depends mainly on the compatibility of these systems with space temperature and pressure environments. The results of testing some of the more important compatibility aspects are presented in this report. Advanced fluids and seal compounds are evaluated to provide a basis for the selection of these items for a hydraulic system operating in a space thermal environment of -240 to $+275^{\circ}\text{F}$ and a hard vacuum of 10^{-8} torr. Strength properties of metals are analyzed to select materials for component fabrication. A single-pass linear-actuator test system and supporting equipment are designed to simulate the operational characteristics of a study task evaluated as described in Volume I.

Results of the test program show how reducing the fluid temperature affects the operation of the system and the minimum operating temperature for the test fluid selected. The results of operation in a simulated space flight show the system's capability for intermittent use associated with many space actuation duty cycles. The effects of high temperature on system operation are reported, as are the effects of 100 hours of system thermal cycling at temperatures from -240 to $+275^{\circ}\text{F}$. Environmental effects on seals and system operation following long-term (5-month) hard-vacuum storage of the linear actuator are reported. A thermal analysis is also presented that describes, using parametric data, the protection required for various hydraulic applications in space.

1.0 INTRODUCTION

Power-amplified actuation systems for space applications are becoming a necessity with the advent of manned space vehicles. The power magnitudes required for advanced space-actuation applications on such vehicles indicate a weight and reliability advantage if hydraulic power can be employed. Past hydraulic-equipment development programs for missile and aircraft applications provide extensive design experience that is not available with either electromechanical or pneumatic actuation systems. This vast experience is, however, limited to systems designed for operation in Earth-atmosphere environments. The effective employment of hydraulics in space, therefore, depends on the compatibility of fluid power systems with space environments, particularly the temperature and pressure environments.

The limitations of hydraulic systems in space temperature and pressure environments are not firmly known. Previous test experience has mainly been associated with materials and component evaluations rather than complete system performance. It is known that state-of-the-art hydraulic fluids limit low-temperature testing of a system to approximately -65°F . Advanced fluids are, therefore, necessary for evaluations to be conducted in simulated space environments.

One of the problems associated with space vehicles is whether environmental protection of a hydraulic system required to operate at low temperature is preferable to designing for the use of low-temperature fluids and seals. The need for resolution of this and such problems as the effect of long-term hard-vacuum storage on hydraulic actuation equipment is emphasized by the timetable of planned interplanetary travel in the 1970's when space vehicles could effectively incorporate hydraulic actuation equipment. The program presented in this report provides a significant initial step toward this goal.

2.0 SUMMARY

Fluid-power-system applications that encounter severe lunar-surface or space environments have been few to date. Requirements for only short operational periods in space, or use of environment-protection schemes, have alleviated facing the temperature- and hard-vacuum-environment problem. Most of the applicable efforts aimed at combating thermal environments stem from heat-transfer-loop work, which, because of the space-radiator freezing problem, has brought about investigation of new low-temperature fluids and seals also applicable to hydraulic power systems.

This report contains the results of a program to design, develop, and fabricate a hydraulic actuation system and to test that system in simulated space-temperature and pressure environments. The development portion of the program included evaluation of fluids, seals, and materials for use in space environments as well as an analysis of thermal-protection methods to isolate equipment from the full effects of the extremely low space temperatures. The fabrication portion of the program was concerned with selection or manufacture of components for the actuation-system design selected — a single-pass blowdown test system. The test phase of the program provided an evaluation of the operational characteristics of the fabricated system. The characteristics investigated were determined during system operation at fluid temperatures as low as -165°F and under hard-vacuum storage at 10^{-6} torr for 5 months. Other testing investigated intermittent usage during a simulated lunar flight, operation at 275°F , and inactive thermal cycling between 275 and -240°F lunar-surface temperatures.

2.1 DEVELOPMENT

As the result of an inquiry to fluid suppliers, five low-viscosity dielectric coolants were selected and evaluated for application to low-temperature hydraulic use. Tests were performed to determine pour point, low-temperature volume change, temperature-viscosity characteristics, wear and lubricity characteristics, and thermal stability. In a similar fashion, five elastomeric phenyl silicone seal polymers were evaluated for use at low temperatures. Tests to determine swell of the unrestrained polymer and of the polymer in seal-gland configurations were performed, as well as an evaluation of seal leakage and chemical compatibility with the five selected fluids.

From the above evaluations, DuPont E-3, with an ASTM pour point of -155°F , was selected for use as the test fluid and Parker S-424-7 compound for the elastomeric seal material. Isopropyl alcohol was determined to be the best solvent for the E-3 fluid.

Materials that had adequate strength properties at low temperature were analyzed for use in fabrication of the test system. Impact strength was a determining factor in selecting stainless steel 304LC for the actuator. Titanium is used in the reservoir where impact is not a consideration.

2.2 DESIGN AND FABRICATION

The space actuation task selected for simulation in the test program was the thrust-vector-control gimbaling of an RL-10 propulsion engine, as required for a typical lunar landing vehicle. This task is one of four tasks evaluated in the trade-study portion of the contract, reported in Volume I. The test system design used to perform this simulation was a single-pass blowdown type using a linear actuator. The design chosen used a 3000-psig system pressure. An inertia/friction load of 559 pounds provided the resistance to actuator motion, simulating the 3915 inch-pounds of torque required in the flight application.

The actuator design used has a stroke of 4 inches and an effective area of 0.39 square inch. This provided a 1.4 factor over the required actuation force for the application. The design also incorporated removable piston seal glands and had provisions for measurement of leakage past the primary seal in each of these glands. The secondary seal used to implement leakage measurement was a spring-loaded teflon "omniseal." Chrome plating was used on the piston and piston rod and nickel plating on the housing bore and rod glands. Two identical actuators were fabricated. One was used for the system tests and the other for the long-term-storage test in a hard vacuum.

The reservoir was designed with an 850-cubic-inch capacity providing a 1.2 factor over the fluid volume required to perform the operational sequence, which was repeated numerous times during the test program. The operational sequence performed simulated the flight application by testing at actuation frequencies between 0.5 and 6 cps in a continuous sweep. This operation evaluated the full-flow capability of the test system, which had a 3-cps break frequency design requirement.

Fabrication of special equipment was necessary to support the test program. A load fixture was fabricated to provide the structural support for the test system and the inertia/friction load. A special container to isolate the servoactuator during the 5-month vacuum-storage period was designed and fabricated so that the servoactuator could be operated without being removed from the container. Other support equipment was provided to implement fluid handling and transfer.

Because the test program was not conducted using thermal-protection devices, an analysis was provided showing the thermal penalties involved in protecting any hydraulic system to -50, -100, and -150°F fluid operational temperatures. The analysis considered that a system may be allowed to freeze, and preheating could be used to restore the system to operational temperatures. Heating sources to provide electrical energy, such as batteries, solar cells, and fuel cells, were studied, as was direct heating by radioisotope. The choice of which heat source should be used in any application is dependent on the application and the availability of such a source on the vehicle. Data to assist in making selections of thermal-protection systems is presented.

2.3 TEST PROGRAM

The first series of tests performed was to evaluate the system operational characteristics at low temperature and determine the minimum operational temperature using

E-3 fluid. Tests were performed at fluid temperatures of 75, 0, and -50°F, and in subsequent decreasing 25°F increments to -150°F. The temperature of -140°F was determined to be the practical limitation for use of the E-3 fluid, with -165°F being the temperature where cycling equal to or greater than 0.5 cps was not possible. Fluid performance of the low-response breadboard test system degraded rapidly beyond -100°F. Seal leakage was minor and well within acceptable tolerance limits established for missiles and aircraft. Residual contamination, not generated in the system, caused a serious flow restriction through filters at high fluid viscosities. A major system pressure drop was also noticed at high viscosities because of increased losses through the system pressure line filter. There was no permanent degradation within the system resulting from operation at low temperature.

A simulated lunar flight test was performed to evaluate intermittent operation of the hydraulic system during exposure to both low temperature and hard vacuum. Operational sequences were performed after 72 hours of exposure to -140°F and 10^{-6} torr and again after a total of 144 hours of exposure. The test was successfully completed after cleaning the filters of residual contaminants. There were no permanent changes in operational characteristics resulting from the test. Seal leakage was well within tolerable limits.

A test at 275°F was performed to evaluate the capability of a system to operate at high lunar-surface temperatures. The test was completed successfully with insignificant dynamic seal leakage. Fluid utilization was excessive because of the low fluid viscosity, forcing the operational sequence to be performed at selected frequencies rather than by sweeping the range of frequencies. The effects on operational characteristics during high-temperature operation were comparable with those at low temperature.

The thermal cycling test was performed to determine the changes that might occur in a hydraulic system's operational characteristics as a result of 100 hours of cycling between temperatures of 275 and -240°F with the system inactive. Comparison of the operational characteristics before and after the test showed that there were no permanent changes as a result of the test. No leakage was found in the collection tubes following the test.

A vacuum storage test was performed to determine the deteriorating effects of 5 months of continuous hard-vacuum exposure on seals and other outgassing materials in the actuation system. The vacuum storage was conducted at a pressure of approximately 10^{-6} torr. A harder vacuum was not possible because of partial blocking of the storage container pumping port by the actuator and because of actuator seal leakage. Total leakage for the 5-month period was only 1.23 cubic inches, or an average of 0.01 cc per hour, which was insignificant from a hydraulic system standpoint. Operation of the stored actuator after the storage period revealed no system performance effects attributable to the storage.

Disassembly of the Number 1 servoactuator for seal changes after the low-temperature series and for final disassembly after thermal cycling revealed abrasion on the dynamic

seals. Similar but much less severe wear patterns on seals were evidenced with the Serial Number 2 actuator as a result of vacuum testing.

2.4 CONCLUSIONS

The leakage and sealing problems that might have been expected as a result of exposure to space environments were not encountered. A nominal 20 percent squeeze was used in the design of components which is approximately 10 percent greater than normal. Improvements in sealing not incorporated in these tests may be used to further reduce leakage if this appears desirable.

Fluid and seal studies need to be continued toward the goal of evaluating system operation at lunar-surface temperatures without thermal protection. Although protection can be provided for hydraulic systems at these temperatures, the improved system reliability, if conditioning is not needed, deserves much consideration. The minimum temperature at which flat system response may be obtained can be reduced by increasing the servovalve amplifier gain, thus increasing the break frequency. The minimum limiting temperature for flat response is expected to be near -125°F . This limit should be investigated in future evaluations. The probable existence of a system performance relationship with fluid viscosity also needs further study by evaluating other advanced fluids.

Although the test results of this program all show an affirmative conclusion that hydraulic systems are adequate in space environments, the proof of such a conclusion rests in further environmental testing using a recirculating system. The development of a pump that will both pressurize fluid at 0.3-centistoke viscosity and provide flow with the same fluid at a viscosity greater than 3000 centistokes is a major problem. The applications for hydraulic systems in space shown in Volume I are only a few of the possible uses for such systems. The existence of this relatively untapped field of hydraulic applications indicates the need for continuation of investigations that will lead to the development of hydraulic hardware for space actuation flight systems.

3.0 HYDRAULIC SYSTEM ANALYSIS

The anticipated use of hydraulically operated devices on the lunar surface requires systems capable of operating at temperatures as low as -240°F . Fluid temperatures in radiators or exposed hydraulic systems on orbiting vehicles are expected to reach a minimum of -180°F or lower. Until these recent requirements, operation of aircraft and missiles at temperatures of -65°F on arctic bases established the requirement for service. Most elastomeric seals lose their resilience and, therefore, their sealing capabilities below -65°F . Nonelastomeric seals have not provided adequate dynamic sealing for long-duration missions or for positive sealing after limited cycling. These concerns about fluids and seals indicate the need for an analysis in this area of low-temperature capability.

Machinable materials that can be used at space temperatures must be selected by not only considering the ultimate tensile strength, but also by giving special attention to the impact-loading considerations, because of the major changes in impact strength with decreasing temperature.

Thermal protection for spacecraft hydraulic systems must be considered part of the system analysis until development of low-temperature hydraulic systems makes protection unnecessary.

3.1 FLUID AND SEAL EVALUATION

None of the current fluids formulated for hydraulic use have low-temperature properties adequate for space use. Reference 1 contains the results of testing in which -75°F was determined to be the minimum temperature for operation of a recirculating system using MIL-H-5606A fluid. Such fluids as MIL-H-5606A can be used in space systems by keeping the fluid warm through constant circulation and the use of insulation. Heat can also be applied either internally or externally in the form of electrical or nuclear energy. From the standpoints of reliability and weight, it is more desirable to design systems that can be started in the ambient thermal environment of the vehicle. Progress toward this goal is advanced in this contract by the evaluation of a number of candidate low-temperature fluids for hydraulic use.

The use of hydraulic systems at low temperatures depends as much on the adequacy of seals as on the properties of fluids. Nonelastomeric seals, because of leakage, have not been completely acceptable as a primary seal at low temperatures. The elastomeric sealing polymers that maintain their elasticity below -100°F are limited to the phenyl silicone compounds. The thus-limited number of acceptable seal compounds places an additional constraint on fluids for hydraulic use — that of compatibility between the seals and selected fluids.

3.1.1 SCREENING TESTS

The temperature range of the lunar environment (-240°F to 275°F) cannot be spanned by any known fluid without special system-design innovations. Candidate fluids, such as hexane or pentane, that could span the temperature range require high return pressures (approximately 300 psi) at high temperature to maintain a fluid state. Long-term storage in space environments before use, or intermittent use typical of many applications, prohibits the consideration of high return pressures that would increase leakage rates.

An inquiry was made among the following major fluid suppliers concerning off-the-shelf or pilot-plant fluids that might have application in a low-temperature hydraulic system.

- 1) Oronite Division of California Chemical Company.
- 2) Dow Corning Corporation.
- 3) Organic Chemicals Division of the DuPont Company.
- 4) Esso Research and Engineering Company.
- 5) General Electric Company.
- 6) Halocarbon Products Company.
- 7) Minnesota Mining and Manufacturing Company, Chemical Division.
- 8) Monsanto Chemical Company.
- 9) Shell Oil Company.
- 10) Texaco, Incorporated.
- 11) Union Carbide and Chemicals Company.

A number of samples of readily available low-viscosity dielectric coolants were obtained for evaluation. These fluids were capable of low-temperature operation within the range of -130°F to -180°F . The associated high-temperature capabilities were within the range of 120°F to 450°F .

The five fluids selected for detail-evaluation testing were:

- 1) Dow Corning — DC 331, a low-viscosity dimethyl silicone;
- 2) DuPont — E-3, a fluorinated ether;
- 3) Halocarbon — 208, a halogenated branched-chain aliphatic hydrocarbon;
- 4) Minnesota Mining and Manufacturing — FX-81, a cyclic fluorinated ether;
- 5) Monsanto — MCS-198, a silicate ester.

The Boeing Company wishes to express its appreciation to these companies for their cooperation in supplying fluid samples for evaluation, comparative data on most fluid characteristics checked by Boeing, and data on such other characteristics as specific

heat, thermal conductivity, density, hydrolytic stability, and surface tension. These fluids represent the best selection of available low-temperature fluids as of December 1964, with an extended capability for moderate-high-temperature use.

The results of Boeing-sponsored research (Reference 2) to evaluate seals for space applications are shown in Figure 1 and clearly indicate the superiority of phenyl silicone seals at low temperatures. Figure 2 shows the effect of temperature on the loaded deflection for the general category of methyl phenyl silicone compounds. These results demonstrate that a phenyl silicone compound can be used to approximately -170°F if the 10-percent deflection point at 400-psi load is considered the allowable limit for stiffness.

Samples of Dow Corning and Parker Seal phenyl silicone compounds were evaluated for compatibility with each of the fluids previously mentioned. In some tests, teflon and 3-2013 Buna N were included for comparison. The particular phenyl silicones evaluated were:

- 1) Dow Corning — DC 960;
- 2) Dow Corning — DC 651;
- 3) Dow Corning — DC 675;
- 4) Parker Seal — S-383-7;
- 5) Parker Seal — S-424-7.

The Boeing Company wishes to express its appreciation to Dow Corning and Parker Seal for their cooperation in furnishing material samples and information regarding use of their particular compounds in the environments specified by the contract.

3.1.1.1 Fluid Test Description

The following tests and evaluations were performed on the fluids noted above.

Pour Point — A modified ASTM D97-57 pour-point test was run after making slight changes in the pour-point apparatus to allow the use of liquid nitrogen as the cooling agent rather than the conventional dry ice and acetone. An air gap was used to insulate the liquid nitrogen from direct contact with the fluid. The rate of cooling was more rapid than that employed in the standard ASTM D97-57 procedure (Reference 3).

Low-Temperature Soak Test — The fluids, in 150-ml beakers, were placed in a desiccator to prevent condensation and formation of ice crystals during cooling. The desiccator was placed in a cold box operating at -90°F and cooled for 8 hours. At the end of this period, the fluids were moved from the cold box and examined for crystals or solids of any type.

Low-Temperature Volume Change — Two of the most promising fluids (DC 331 and DuPont E-3) were cooled to -250°F (or complete solidification) in a tall graduate to observe volume change with temperature. Cooling was done with liquid nitrogen insulated from the test fluid by an air gap.

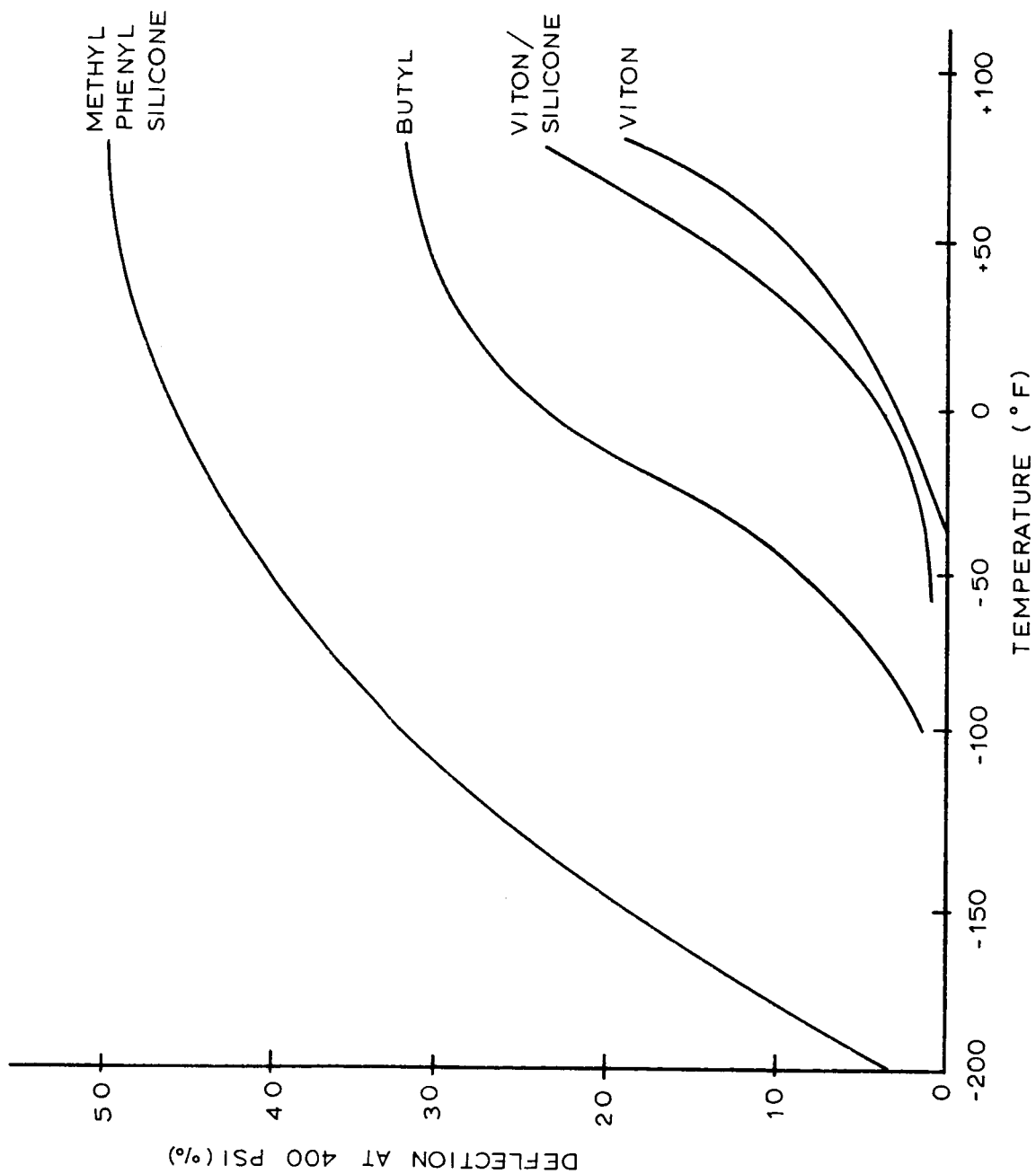


Figure 1: Seal Material Deflection Characteristics

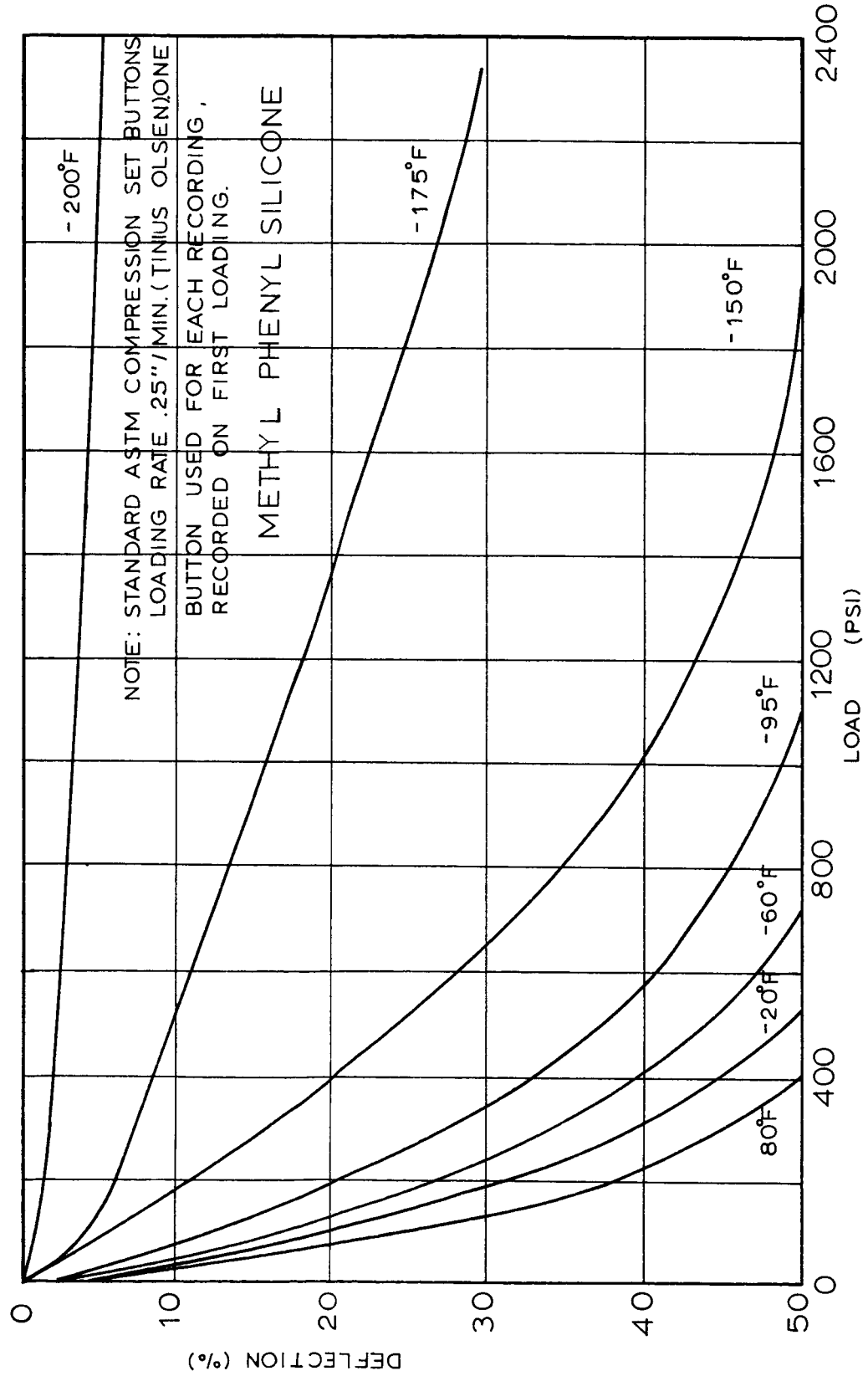


Figure 2: Effect Of Temperature On Load Deflection

Viscosity-Temperature Characteristics — A viscosity-temperature curve was constructed by measuring viscosities at -100, +100, and 210°F and utilization of supplier data. The viscosities at 100 and 210 were measured by ASTM D445-60 (Reference 3) procedures while the measurements at -100°F were made with a specially constructed low-temperature bath. Denatured ethyl alcohol was used as the bath fluid and dry ice and liquid nitrogen for cooling. The standard modified Ostwald glass viscosimeters were used with suitable corrections in the calibration constant because of the low test temperature. Viscosities at 325°F were obtained by extrapolation on the ASTM chart. Studies by Penn State University (Reference 4) have shown this procedure to yield values that could deviate a maximum of 10 percent from measured values throughout the temperature range of 210 to 325°F.

Flash Points — The Cleveland open cup procedure according to ASTM D92-57 (Reference 3) was used to make this measurement.

Wear and Lubricity Characteristics — Lubricity of the various fluids was determined with the Shell four-ball wear tester using a load of 10 kg, 167°F temperature, and a speed of 1200 rpm for 2 hours. The test balls were 52100 steel. The conditions employed in this test have been found to correlate best with wear in hydraulic pumps.

Thermal Stability — This test consisted of heating the fluid in a closed stainless-steel bomb, with a dry-nitrogen atmosphere, for periods of 20 or 48 hours at 275°F. During testing, the bomb was constantly rocked to keep fresh fluid in contact with the corrosion specimens, which consisted of 0.5-inch-diameter ball bearings of metals representative of those found in hydraulic systems. Where ball bearings of a desired metal were not available, 0.5- by 0.25-inch disks were used and alternated with the 0.5-inch-diameter balls. The corrosion specimens were held in a specimen holder to prevent movement as the bomb was rocked. The assembled thermal stability bomb is illustrated in Figure 3.

Viscosity, flash point, and solids content of the fluids were measured before and after this test. Balls and disks were weighed to the nearest 0.1 milligram to determine weight change during exposure to the fluid. In some cases, the metal specimens were sectioned and examined for intergranular corrosion.

3.1.1.2 Fluid Test Results

The results of the fluid screening tests described in Section 3.1.1.1 are tabulated on Figures 4 and 5. Figure 4 shows the fluid physical properties and Figure 5 reports data on fluid thermal stability and compatibility with materials. A discussion of these results follows.

Pour Point — Several of the fluids had pour points of approximately -150°F, with FX-81 having the lowest pour point at -172°F. The pour of the first batch of Halocarbon 208 was -103°F instead of the -140°F quoted in company literature. Halocarbon, Inc., investigated this problem and supplied a second sample, which had a pour point of -148°F.

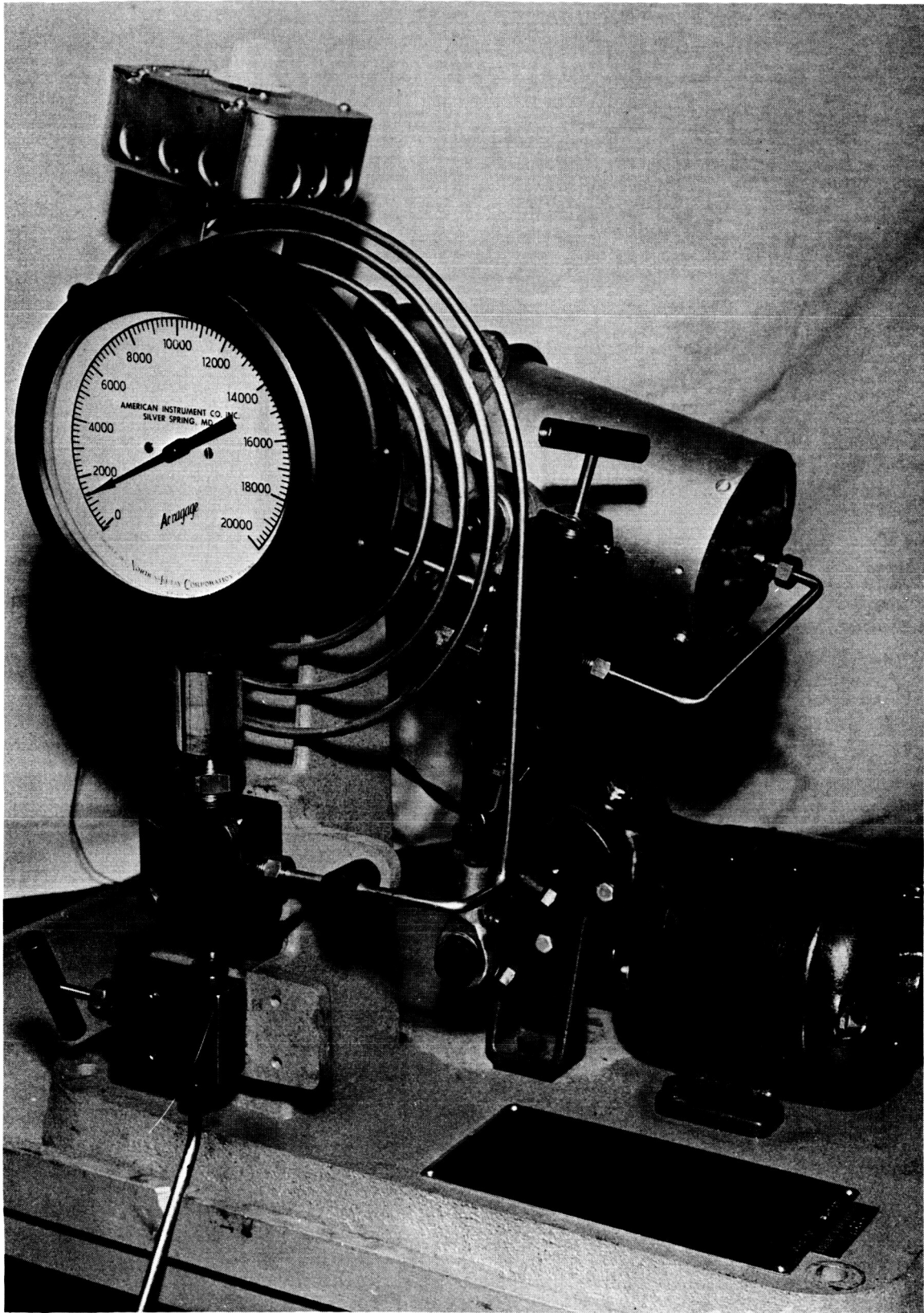


Figure 3: Fluid Thermal Stability Apparatus

Fluid	① Pour Point °F	-90°F Low-Temperature Soak Test	② Viscosity, CS				④ Flash Point (°F)	⑤ Shell 4 Ball Wear Test, Scar Dia (Millimeters)
			-100°F	100°F	210°F	325°F		
MSC-198	-142	No effect	85.5	1.66	0.80	0.49	180	1.06
DC-331	-130	60% of fluid solidified	678.9	12.09	5.01	2.8	420	0.56
H-208	-148	No effect	510	2.38	1.14	0.71	None	0.44
FX-81	-172	No effect	21.4	0.66	0.4	>0.4	None	0.73 ^⑥
E-3	-155	No effect	223.7	0.99	0.43	>0.4	None	0.39

① ASTM Procedure D97-57 (Modified)

② ASTM Procedure D445-60

③ Extrapolated from ASTM Viscosity Temperature Chart

④ ASTM Procedure D92-57

⑤ Run at 167°F, 10 Kg, 2 hours, 1200 RPM, 52100 Balls,

MIL-H-5606 gives value of 0.28 under these conditions

⑥ Run at 80°F because of excessive evaporation loss at 167°F

Figure 4: Physical Properties Of Low-Temperature Fluids

	Time (hrs)	Temp (°F)	① Viscosity Change (%)	Change in Flash (°F)	Change in Solids (mg)	Weight Change in Metals (mg/cm ²)								
						4130	Bearium Bronze	440C	M-10	Naval Bronze	Titan- ium GAL-4v	Be-Cu	304S.S.	321S.S.
Fluid														
MCS-198	20	275	-4.2	-5	+0.7	-0.177	-0.276	-0.079	-0.256	-0.336				
DC-331	20	275	-0.33	+15	+0.6	0.00	0.00	-0.02	0.00	-0.02				
E-3	20	275	0.0	—	+0.05	-0.177	-0.059	-0.198	-0.198	-0.079				
H-208	① 48	275	+0.3	—	—	—	—	-0.019		-0.059	0.0 ^②	—	0.0 ^②	-0.019
E-3	① 48	275	+21.0	—	—	—	—	0.0			-0.019	-0.059	+0.039 ^②	+0.019

① DC 675 O rings present in bomb during run.

② These metals sectioned for intergranular corrosion inspection. None found.

Figure 5: Low-Temperature Fluids Thermal Stability And Material Compatibility

Low-Temperature Soak Test — When subjected to the procedure in Section 3.1.1.1, DC 331 developed solids that filled approximately 60 percent of the fluid volume in the sample container. Fluids for the first tests were in beakers open to the atmosphere in the cold box. When solids were noted in the DC 331 it was thought that condensed water was freezing in the beaker. However, subsequent tests on specimens in dessicators placed in the cold box demonstrated that the solid formation in DC 331 was due to solidification of fluid constituents. The test was repeated several times with similar results. When Dow Corning Corporation was contacted concerning this phenomenon, they stated that this behavior was common with certain batches of DC 331, but that in their experience the solidification had not occurred at such high temperatures. They did state that partial solidification usually occurred at temperatures above the ASTM pour point of the fluid.

Low-Temperature Volume Change — E-3 fluid was subjected to this test to ensure that no expansion would occur upon solidification and damage sections of the low-temperature hydraulic system. DC 331 was also evaluated to determine if unusual volume changes occurred in the region of -90 to -130°F where solidification had occurred in the low-temperature soak test. It can be noted in Figure 6 that no volume increase occurred in either fluid at any time during the cooling period.

Viscosity-Temperature Characteristics — Viscosity-temperature curves for the five fluids and a comparison with MIL-H-5606A have been plotted in Figure 7. These results show that the approximate low-temperature limitation of both DC 331 and E-3 fluids should be less than -125°F. This value was based on an extrapolated viscosity of 3000 centistokes, which was the limiting viscosity for recirculating MIL-H-5606A system operation observed during the Boeing test program reported in Reference 1. The limiting condition for operation with a single-pass blowdown system should be a viscosity greater than 3000 centistokes. The minimum permissible viscosity at high temperature is not known. If a 0.5-centistoke minimum is assumed for operation of a recirculating system, MCS-198, Halocarbon 208, and DC 331 would be satisfactory at 325°F and E-3 at approximately 175°F.

Flash Point — Flash point is a measure of the fire hazard involved with the handling of the fluid, which may be of major concern on manned spacecraft. However, this characteristic is of little significance in respect to this program's test system. The halogenated fluids — E-3, FX-81, and Halocarbon 208 — were nonflammable under the condition of the Cleveland open cup flash point test because they are inert fluids. Both DC 331 and MCS-198 had high enough flash points to make handling safe under normal conditions.

Wear and Lubricity Characteristics — Results of this test show that E-3 fluid had the best lubricity of any of the fluids tested. E-3 wear-scar diameters were slightly larger than those of MIL-H-5606A, which has given adequate pump life at temperatures up to 375°F for missile systems. It will be noted that it was not possible to run FX-81 at 167°F in the four-ball wear tester because of excessive evaporation from the open ball chamber. However, by adding fluid several times during the test and restricting the temperature to 80°F the run was completed.

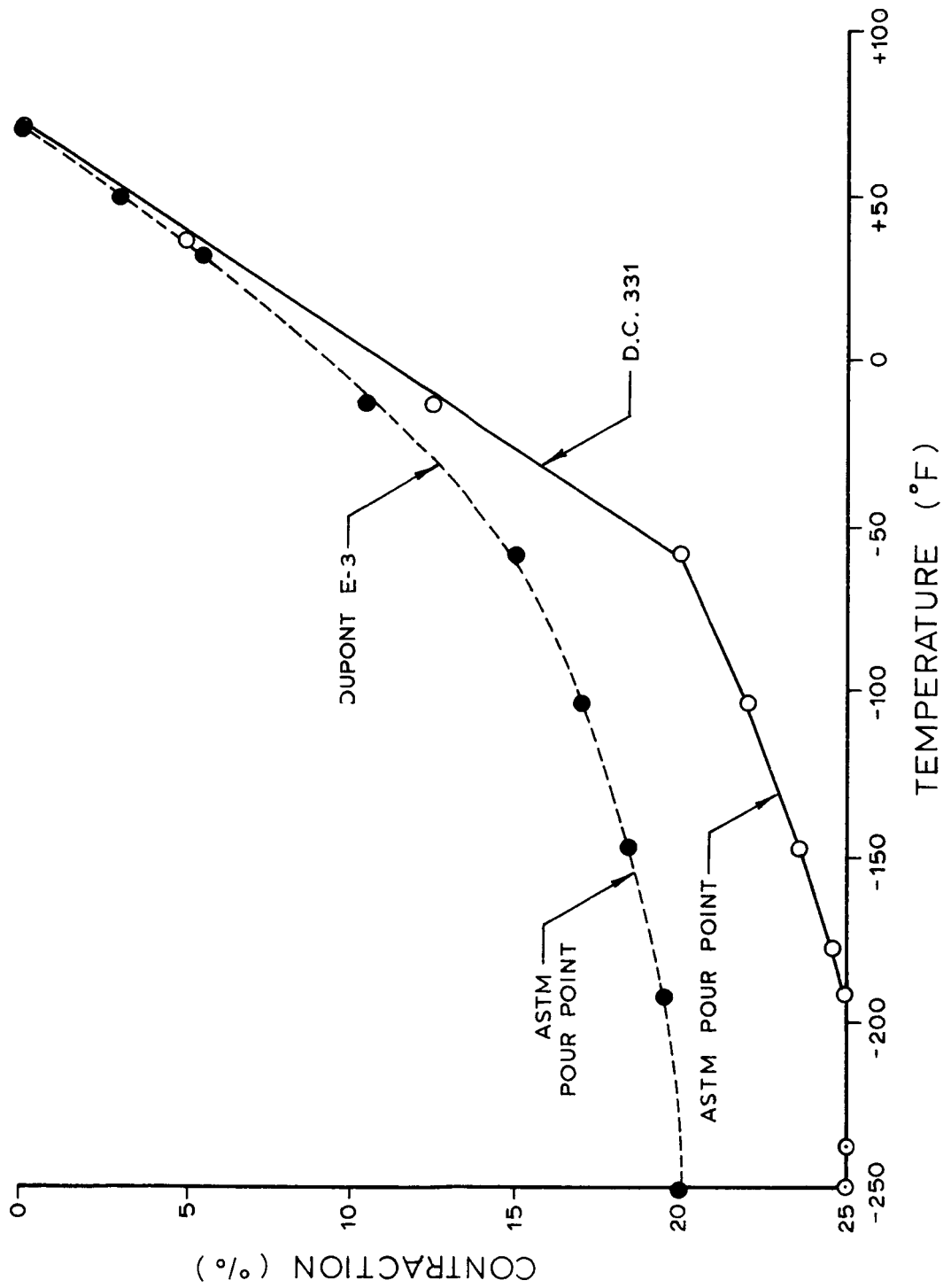


Figure 6: Contraction Of Low-Temperature Hydraulic Fluids

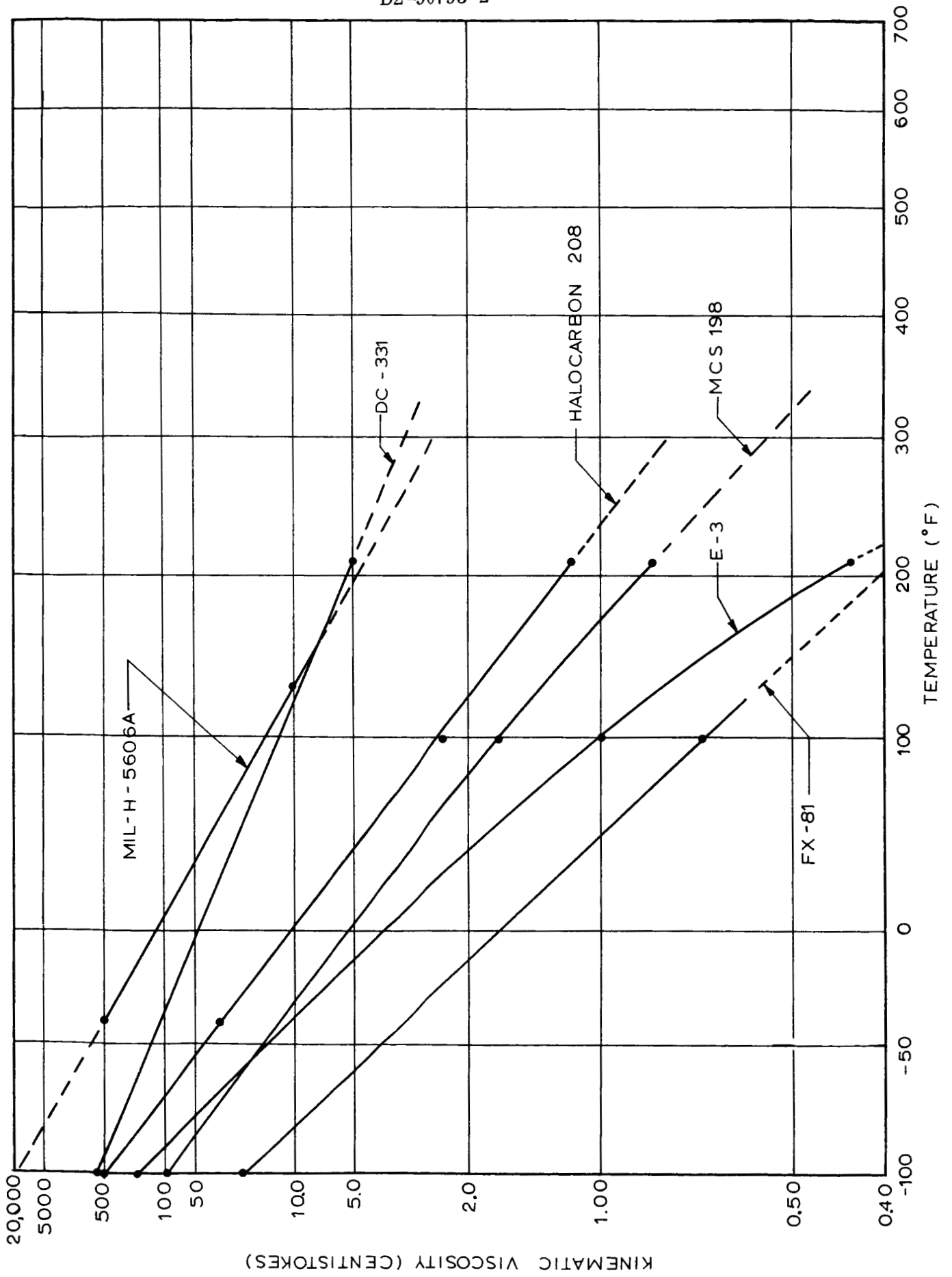


Figure 7: Viscosity Of Various Fluids

Thermal Stability — Results of the thermal stability tests demonstrated that all fluids evaluated were stable enough to be employed at 275°F for at least 20 hours. The common hydraulic system metals present in the fluids during exposure in no case showed weight changes more than the 0.4 mg/cm² allowable for copper-based alloys and the 0.2 mg/cm² for other metals.

3.1.1.3 Comparison of Fluids as Heat-Transfer Media

A comparison of the five fluids evaluated in this program as heat-transfer fluids is shown in Figure 8. Several other low-temperature fluids, received too late for evaluation in this program, are also shown. Measurements made by Boeing are marked with an asterisk. No conclusions were drawn as to the superiority of any one material because of a lack of data and verification of vendor values.

3.1.1.4 Elastomer Test Description

The following tests and evaluations were performed on the phenyl silicone elastomers specified in Section 3.1.1.

Immersion Tests — A 1- by 1-inch square of the elastomer was soaked in a covered beaker of fluid for 72 hours at 160°F, and the size of the squares was measured after testing. This initial compatibility test was useful for detecting large increases in volume and for selecting the best phenyl silicone compound. Elastomers satisfactory in the immersion test were then subjected to the following standard ASTM tests.

Fluid-Elastomer Compatibility Tests — A number of Dow Corning and Parker compounds were immersed in the test fluids for 72 hours at 160°F. ASTM tensile and elongation (D 412) and durometer (D 676) tests were performed on the elastomers before and after immersion in the fluids. The volume changes of the elastomers were determined by ASTM procedure D 412 (Reference 5).

Static Seal Tests — A low-temperature sealing test was performed with several of the fluids by employing the static seal test apparatus shown in Figure 9. O-rings were assembled wet with the test fluid and the test apparatus pressurized to 4000 psi to determine initial leakage. The apparatus was soaked for 48 hours at 160°F in an oven and pressurized to first 4000, then 100 psi, the pressure being held for 10 minutes at each level. The assembly was next cooled to -100°F and the pressure test repeated. The assembly was then warmed to room temperature, tested again for leakage, and disassembled for inspection of O-rings.

3.1.1.5 Elastomer Test Results

The results of the elastomer screening tests described in Section 3.1.1.4 are reported below.

Immersion Tests — Results of the immersion tests are shown in Figure 10. DC 675 provided the smallest volume change of the three phenyl silicone elastomers evaluated. This test also demonstrated that MCS-198, DC 331, and Halocarbon 208 would be

Fluid	Viscosity (cs) at -100°F 100°F	Spec. Heat, 77°F Btu/(lb)(°F)	Thermal Conductivity Btu/(hr)(ft ²)(°F)(ft)	Density (Gm/cc at 77°F)	Surface Tension (Dynes/cm at 77°F)	Lubricity, Wear Scar Dia. (mm) (167°F, 1200 rpm, 10 kg)	Type of Fluid
MCS-198	85.5* 1.66*	0.46	0.063	0.898	24.0	1.06*	Silicate ester
DC 331	697* 12.09*	0.35	0.071	0.940	20.0	0.56*	Methyl silicone
H206	510* 2.38*	0.24	0.044	1.830	32.6	0.44*	Chloro- fluorocarbon
FX-81	21.4* 0.66*	0.248	0.079	1.79	15.0	0.73	Fluorinated ether
E-3	224* 0.99*	0.243	0.041	1.725	18.1	0.39*	Fluoro- carbon
Esso Res. & Engr. LO 3174	202 1.60	0.480	0.071	0.756	-	0.27	Petroleum Derivative
G.E. 716-42- 253	400 -	-	-	0.95	-	0.6	Methyl silicone
Dupont Fluoro- Com- pound II	16			1.659			Fluoro- carbon
Oronite 8786	1000 4.32	0.41	0.0794	-	-	-	Silicate ester
Glycol- H2O- 60-40 (Min. F.P.)	F.P. 3 -60	0.780	0.21	1.09	-	-	Ethylene Glycol & Water

* Run at Boeing

Figure 8: PROPERTIES OF HEAT-TRANSFER FLUIDS

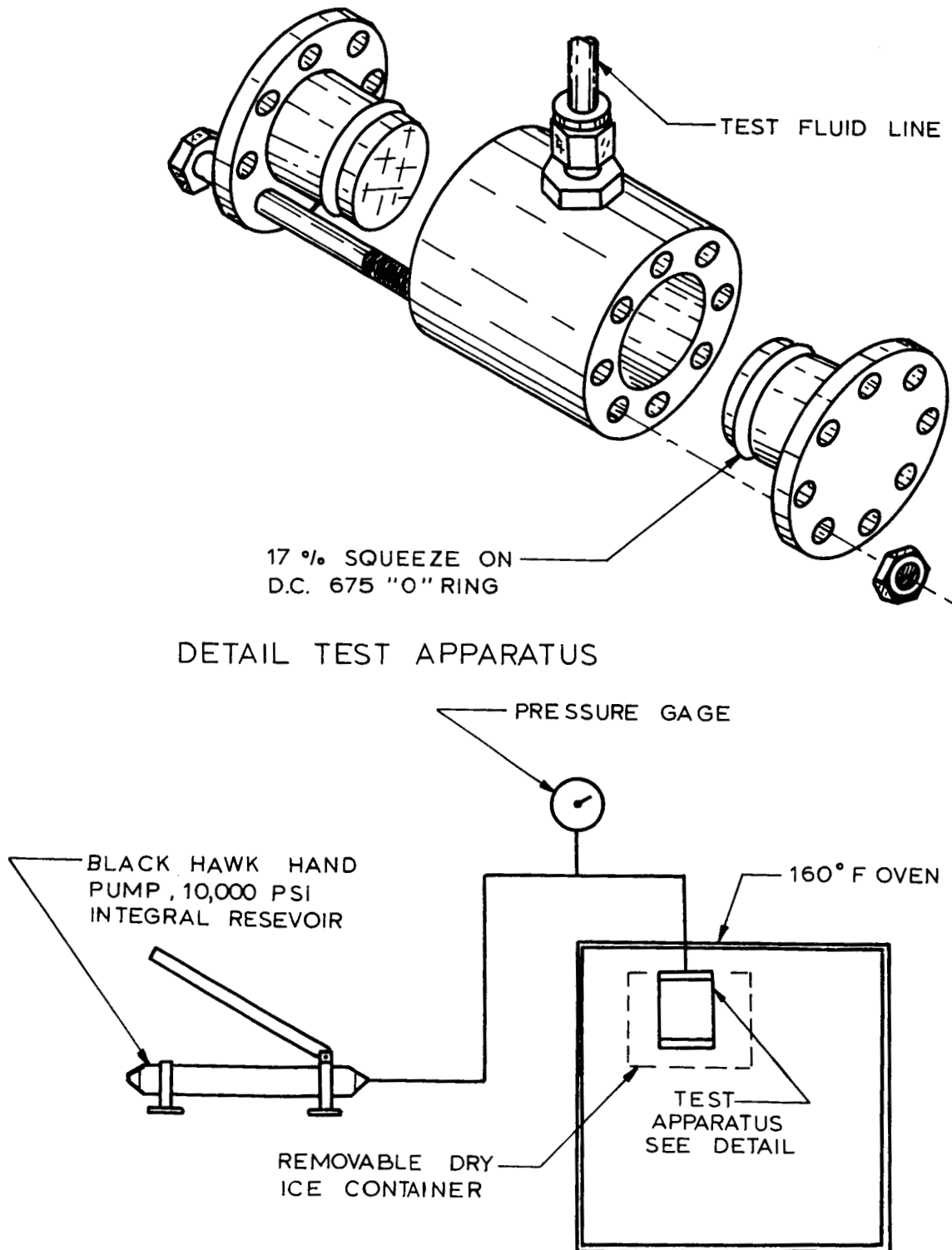


Figure 9: Static O-Ring Test System

Fluid	Polymer or Elastomer	Initial Size	Final Size	Rating	Remarks
MCS-198	DC 960	1 x 1	1.5 x 1.5	Poor	
	DC 651	1 x 1	1.75 x 1.75	Very Poor	
	DC 675	1 x 1	1.4 x 1.4	Poor	
	Teflon	1 x 1	1 x 1	Good	
DC 331	DC 960	1 x 1	1.75 x 1.75	Very Poor	
	DC 651	1 x 1	1.5 x 1.5	Poor	
	DC 675	1 x 1	1.2 x 1.2	Fair	
Halo- carbon 208	DC 960	1 x 1	1.5 x 1.5	Poor	
	DC 651	1 x 1	1.5 x 1.5	Poor	
	DC 675	1 x 1	1.3 x 1.3	Fair	
FX-81	DC 960	1 x 1	1 x 1	Good	
	DC 651	1 x 1	1 x 1	Good	
	DC 675	1 x 1	1 x 1	Good	
E-3	DC 960	1 x 1	1 x 1	Good	White precipitate in fluid
	DC 651	1 x 1	1 x 1	Good	White precipitate in fluid
	DC 675	1 x 1	1 x 1	Good	White precipitate in fluid
	Teflon	1 x 1	1 x 1	Good	

Exposure — 72 hours at 160°F in beaker

Figure 10: ELASTOMER SWELL TEST RESULTS

marginal at best, while FX-81 and E-3 would cause little volume change in the phenyl silicone elastomers. Also, MCS-198 and E-3 did not have any effect on teflon at 160°F.

Fluid Elastomer Compatibility Tests — ASTM tensile and elongation, durometer, and volume change test results are shown in Figure 11. The data from this figure shows that Parker S-424-7 had the best tensile values of any compound hard enough for O-rings. This compound also demonstrated a slight increase in volume, a desirable characteristic, when immersed in E-3 fluid.

A sample of Buna N elastomer, representative of that used in MIL-H-5606 systems, was evaluated with Halocarbon 208 for comparison with the silicones. It will be noted that the initial tensile values of this elastomer were more than double those of Parker S-424-7, the silicone elastomer selected for use in the breadboard test to be built. A white flocculent precipitate was formed when DC 675, 651, and 960 elastomers compounded at Dow Corning were exposed to E-3 fluid. This precipitate was not present when similar phenyl silicone elastomers compounded by Parker were exposed to E-3 fluid. After infrared analysis of the precipitate, it was concluded that a mold release compound, used exclusively by Dow Corning, was causing the precipitate. The compound selected, Parker S-424-7, did not demonstrate any precipitate formation in exposure tests with E-3 fluid.

Static Seal Tests — These tests were made primarily to determine the limits of allowable elastomer volume change and as a final check of E-3 compatibility with phenyl silicone O-rings in an actual seal application. O-rings made from DC 675 were assembled into the apparatus shown in Figure 9 with a squeeze of 17 percent and the tests described in Section 3.1.1.4 were performed, using E-3 and DC 331 fluids.

DC 331 produced what was estimated to be a maximum allowable swell (80.5 percent) with the DC 675 elastomer in the ASTM tests tabulated in Figure 11. E-3 fluid, with a 0.9-percent swell, represented the minimum swell noted with any of the fluids evaluated.

No leakage occurred with either fluid and the O-rings showed no sign of damage due to cutting or tearing. The cross-sectional diameter of the O-rings used in DC331 had increased to only 50 percent of the change noted when the same rings were immersed in a beaker of fluid for 48 hours at 160°F. This indicated that the swell measured in a noncapsulated state may be considerably greater than the swell that will occur in an actual gland configuration.

As expected, no measurable increase in cross-sectional diameter of the rings exposed to E-3 fluid was noted.

3.1.2 FLUID AND ELASTOMER SEAL SELECTION

Fluids were eliminated from consideration as the test system fluid when deficiencies in fluid properties or seal compatibility were uncovered. Fluids rejected and the reasons for rejection are as follows.

Elastomer	Fluid	Before Exposure				After Exposure of 72 hours @ 160°F				Volume Change (%)	Remarks
		Tensile (psi)	Elong (%)	Dur		Tensile (psi)	Elong (%)	Dur			
DC 675	MCS-198									+183.5	
DC 675	DC-331									+ 80.5	
DC 675	H-208	632	200	74		245	60	60		+191	
DC 675	E-3	752	131	72		739	128	72		+ 0.9	White precipitate in fluid
DC 651	E-3	1180	473	53		1079	418	53		+ 1.2	Compound soft for best O - rings
DC 960	E-3	1392	543	59		1384	500	62		+ 0.6	Compound soft for best O - rings
Parker S-383-7	E-3	1096	360	66		1112	353	68		- 7.5	No precipitate
Parker S-424-7	E-3	892	200	73		915	170	73		+ 1.1	No white pre- cipitate
3-2013 Buna-N	H-208	2228	220	70		2084	180	60		+ 14.5	

Tensile and elongation by ASTM D412.

Durometer by ASTM D676.

Volume Change by ASTM D471.

Figure 11: Fluid-Elastomer Compatibility

- 1) FX-81 had a very low viscosity at high temperatures, which would have made its use in hydraulic piston pumps doubtful. In addition, its lubricity was poor even at 80°F. FX-81, however, is an excellent low-temperature heat-transfer fluid or is usable as a hydraulic fluid if high temperatures are not encountered.
- 2) DC 331 was marginal in elastomer swell characteristics and solidifies at -90°F, disqualifying it as a true low-temperature fluid.
- 3) MCS-198 has poor lubricity and seriously swelled the phenyl silicone type elastomers used in the system.
- 4) Halocarbon 208 has a very deleterious effect on phenyl silicone elastomers.

The above considerations left E-3 as the one fluid without serious deficiencies except at high temperatures. This fluid, because of its low viscosity at high temperatures, will probably be usable to only 170°F in a system containing a present high-pressure piston pump. Because the contract test system is a single-pass blowdown system, no problems are anticipated using the E-3 fluid at 275°F.

Parker S-424-7 elastomer was selected for use with the E-3 fluid in both static and dynamic O-ring configurations.

3.1.3 SOLVENT COMPATIBILITY

The solubility of the selected DuPont E-3 test fluid in various solvents was determined as a method to select a solvent for component cleaning purposes during the course of the test program. The results of this testing are shown in the following table and include the effect of exposure of the S-424-7 elastomer to the selected solvent, isopropyl alcohol.

E-3 SOLUBILITY

<u>Fluid 1</u>	<u>Fluid 2</u>	<u>Solubility at Room Temperature</u>	<u>Remarks (Relative to Fluid 2)</u>
E-3	Aliphatic naptha BMS 3-3	None	
E-3	Acetone	Complete solubility	Destructive to most elastomers
E-3	Methyl ethyl ketone	Complete solubility	Very destructive to most elastomers
E-3	Denatured ethyl alcohol	None	Mild effect on elastomers
E-3	Methyl alcohol	10% by volume solubility of alcohol in E-3	
E-3	Isopropyl alcohol	20% by volume solubility of E-3 in alcohol	Mild effect on most elastomers
MIL-H-5606	Isopropyl alcohol	Complete solubility when fluids agitated	

EXPOSURE TEST

<u>Fluid</u>	<u>Elastomer</u>	<u>Time</u>	<u>Temperature</u>	<u>Results</u>
Isopropyl alcohol	Parker S-424-7	48 hours	Room temperature	1- by 1-inch piece of elastomer increased to 1.094- by 1.094-inch, durometer changed from 73 to 56

The test results show that aliphatic naptha and denatured ethyl alcohol were not suitable since E-3 was not soluble in either solvent. Acetone and methyl ethyl ketone were not suitable solvents due to their destructive action on elastomers. Methyl alcohol was soluble in E-3 and was therefore not a solvent for E-3. Isopropyl alcohol was selected as a solvent for E-3 because of its mild effect on phenyl silicones, as shown by the results of the exposure test reported above. In addition, isopropyl alcohol is a solvent for MIL-H-5606 and has a mild effect on Buna N elastomers.

3.1.4 SECONDARY DYNAMIC SEAL SELECTION

A test requirement to measure fluid leakage past the primary dynamic gland seals at each end of the double-acting linear actuator established a need for a secondary seal in each rod gland. An investigation was conducted to select a nonelastomeric seal configuration for use in the secondary seal installation. Metal seals were considered undesirable from a leakage standpoint because of the hard-vacuum environment to be encountered. Figure 12 shows the six most promising configurations reviewed and comments related to the review. The "omniseal" was selected for the application on the basis of acceptable previous use and what appeared to be an easier installation in the internal seal application.

3.1.5 CONCLUSIONS

The fluid evaluation revealed that only one fluid of those tested, DuPont E-3, appeared to be satisfactory for the test program. It also revealed that even this fluid is not ideal for use in deep space or in lunar-surface applications because of limitations at high temperature. It is concluded that additional fluid evaluations of potentially applicable fluids such as Allied Chemical fluid FY-64, Esso Research fluid LO-3174, and others that have recently become available need to be conducted. It is also suggested that development be conducted to improve the low-temperature characteristics of fluids such as DuPont E-3 and Dow Corning DC 331, which are acceptable for limited space application.

The need for improved elastomeric seals will always be present when the use of hydraulic systems is considered. An elastomer is not presently available that will maintain adequate elasticity at temperatures less than approximately -180°F. Development of new compounds for dynamic seals are needed to continue the investigation of low-temperature fluids compatible with a -240°F requirement. Cooperation between fluid and seal manufacturers is necessary to ensure compatibility of low-temperature seal compounds with the fluids to be used in space actuation systems.



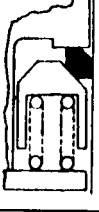



Seal Trade Name	Vendor	Dynamic Seals Proposed for use with E-3	
		Type	Rod Seal Configuration
Omniseal	Aeroquip Corp.	Teflon with dual 304 springs.	
Bal-Seal	Bal-Seal Engrg Co.	Teflon with a single stainless steel spring.	
Delta-Seal	R. Krueger Co.	Teflon-graphite with a spring-loaded wedge ring.	
Pacific	Pacific Piston Ring Co.	Step-gap teflon with 17-4PH contacting ring.	
Raco	Raco Engineering	Teflon cap strip with O-ring.	
Cook	Dover Corp., Cook Airtomic Div.	Outer ring AMS 5643 inner ring. Teflon and O-ring.	
			<p>Information indicates that the seals would perform satisfactorily.</p> <p>Similar to the "omni-seal," but contains only one load spring.</p> <p>Relatively new. Difficult to design into the actuator.</p> <p>No information available on seal performance.</p> <p>The swell characteristics of the elastomer may result in excessive rod friction.</p> <p>Four sets of seals were required for each rod gland.</p> <p>The elastomer may result in excessive rod friction.</p>

Figure 12: DYNAMIC NONELASTOMERIC SEALS

3.2 MATERIALS EVALUATION

Because the hydraulic system tested was the first of its type used for extreme-low-temperature and hard-vacuum testing, it was important that versatile materials be selected with capabilities somewhat beyond the operating temperature range of the fluid selected in Section 3.1.2. An analysis was, therefore, conducted to select materials for use in the manufacture of the actuator and reservoir. Additional analysis was conducted to evaluate the compatibility of materials used in off-the-shelf servovalves with the E-3 fluid.

3.2.1 STEELS AND TITANIUM

As shown in Figure 13, the tensile strength of materials considered for the high-pressure-fluid power system presents no problem. The tensile-strength data actually shows a significant improvement with low-temperature operation. When impact strength is also of importance, as within the actuator, the fact that the impact strength of some materials decreases rapidly at low temperatures is an important consideration. The most commonly used actuator material, 4340 steel, has strength capabilities adequate for temperatures above -150°F, as shown in Figure 13. The impact energy data taken from References 6 and 7 for temperatures between -65°F and cryogenic temperatures indicate that a material showing a flatter slope than that for 4340 is preferable.

The material selected for manufacture of the actuator was 304 LC stainless steel. This material has the disadvantage of having low tensile strength at room temperature, which necessitates extreme care in the handling of surfaces with fine finishes. Using the second choice, Inconel X, would have alleviated this problem, but would have resulted in higher material and fabrication costs. Selection of actuator material in an actual flight application would depend on the handling problem in comparison to fabrication costs. In the majority of flight applications, the advantages of using Inconel X outweigh the disadvantage of higher cost.

Titanium is a recommended material for pressure vessels and other components that do not carry high impact loads (refer to the tensile strength curve in Figure 13). The strength of a titanium pressure vessel is not the only requirement, as sharp cracks and some defects can cause brittle failure below yield or ultimate. From data of Reference 8, cracks ranging from 0.015- to 0.037-inch deep and having lengths of ∞ and 0.074 inch, respectively, would be required to cause failure at burst pressure. These would be small cracks, but could be readily found. At the working pressure, very much larger cracks could be tolerated. Cracks having depths ranging from 0.17 to 0.45 inch and with respective lengths of ∞ and 0.90 inch would be required to cause failure in the absence of a corrosive environment. These defects would easily be picked up by the inspection procedure required. The welds, being annealed, are more resistant to cracks than the base metal and are stressed lower due to the local reinforcement. The conclusion reached was that the proposed titanium vessel should be quite reliable and meet the service requirements, provided corrosive environments are not encountered.

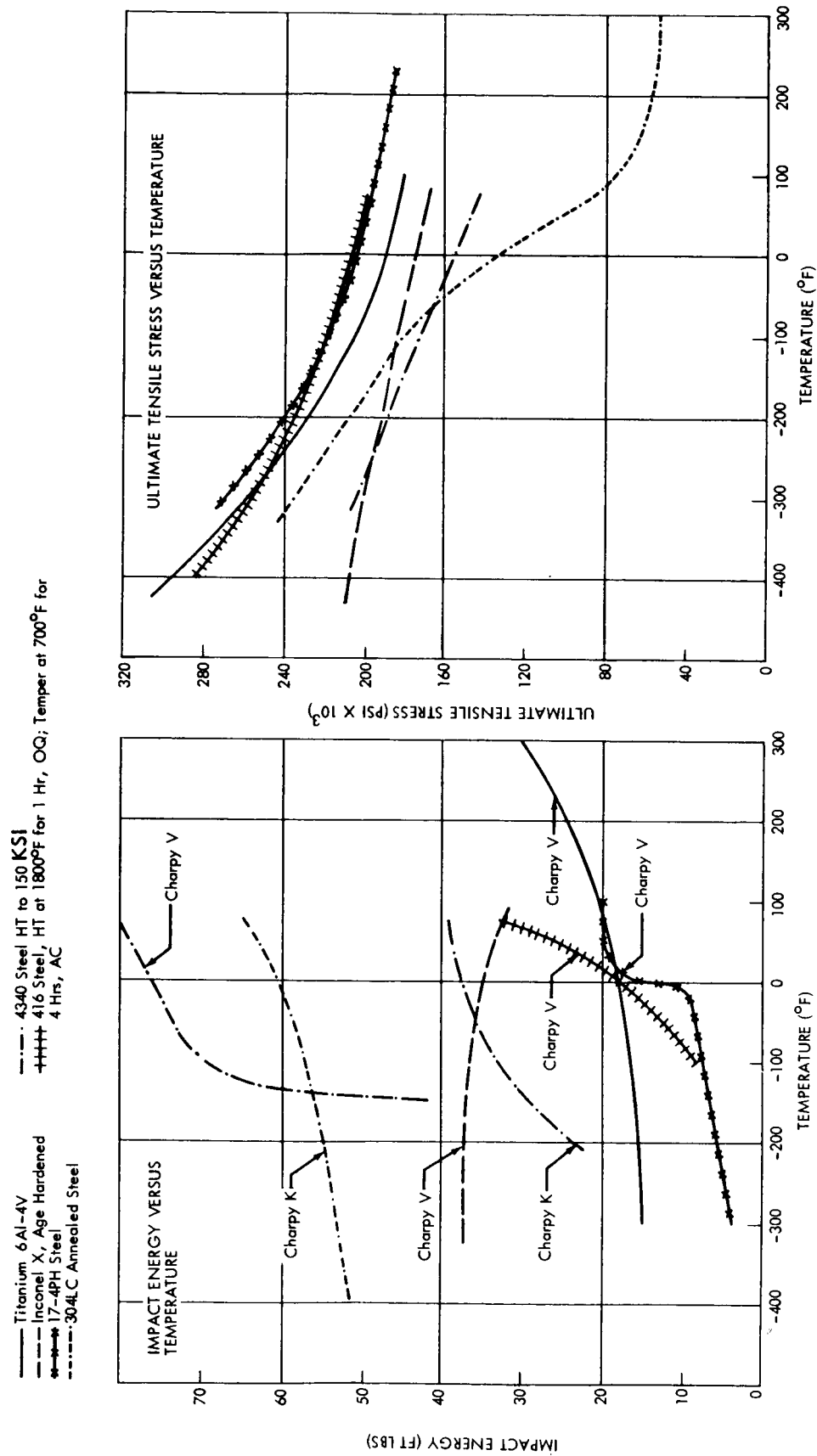


Figure 13: Material Characteristics At Low Temperature

3.2.2 PLATING

It was considered essential to plate the internal surfaces of the actuator housing and glands as well as the actuator rod and piston. The plating would not only provide harder contact surfaces at room temperature but would also eliminate the galling tendencies of using stainless steel on stainless steel. Samples of 304 LC stainless steel were plated with both electroless nickel and chrome to investigate whether the plating processes were satisfactory. Tool cuts were made in the plated surfaces to determine whether the plating would flake off. It was determined that acceptable plating could be obtained on 304 LC stainless steel. A disadvantage of plating chrome and electroless nickel on 304 LC was that the plating could not be removed for repair of parts by reversing the plating process. Reversing the plating process leaves an undesirable etched surface because of the chrome and nickel in the base material. Machine grinding is, therefore, required to remove or reduce undesired plating depth.

3.3 THERMAL PROTECTION

The severe low temperatures of outer space exceeds the present operational temperature capability of hydraulic actuation systems. For these extreme environments, a thermal protection system must be provided that will maintain the equipment above the minimum operational temperature. The purpose of this section is to analyze the weight penalty for this thermal-protection system. The environmental temperature selected for this analysis is -240°F with minimum component temperatures of -100 and -150°F . It is assumed that the equipment is installed in a vacuum and, therefore, that conduction and radiation will be the modes of heat transfer from the components to the environment. The results of the study are presented on the basis of the amount of surface area that must be protected and are, therefore, applicable to any actuation system once the minimum allowable component temperature is known.

In addition to maintaining the components above a minimum operating temperature, a thermal-protection system should be considered that allows the component to cool to environmental temperatures and is then preheated prior to usage. The weight penalty of the preheat system depends on the thermal capacitance of the system to be heated and the minimum allowable component temperatures. The penalty may also depend on the total number of preheats. The penalty can be calculated using the power penalties and insulation weights presented in this section. Examples of the preheat thermal-protection system are included with the actuation system trade studies in Volume I.

This section is separated into two parts. The first part discussed the power sources that can be used for providing the heat required to maintain the desired component temperature. The second part presents the heat-transfer analyses and the results of the thermal protection system study.

3.3.1 THERMAL-PROTECTION-SYSTEM HEAT SOURCES

Two basic types of heat sources were considered. The first, which includes batteries, solar cells, and fuel cells, provides electrical energy that is used to operate resistance

heaters. The second source was the direct heat from a radioisotope. Conduction rods were used to conduct the heat from the isotope capsule to the component, or some designs allow the isotope capsule to be installed directly on the component.

The battery considered for this study is the silver-zinc cell. A constant specific weight of 90 watt-hours per pound was used for the battery power penalty. This penalty is for a relatively slow withdrawal rate from the battery such as would be used with a thermal-protection system and includes the provisions for operation in a vacuum environment. The battery must be maintained at approximately 80°F for maximum performance and, thus the penalty for thermal protection of the battery is also included. The resulting penalty versus mission time and power level is shown in Figure 14.

The solar-cell penalty was selected as 1.0 pound per watt. This is typical of a cell with negligible drag penalty, but does include a silver-zinc battery allowance for some operation when in the shadow (if orbiting vehicle) or for poor orientation of the cells. The penalty versus mission time is shown in Figure 14.

Hydrogen-oxygen fuel cells were also included as a heat source. Three possible fuel-cell configurations were considered.

Dependent Fuel Cell — The fuel cell would be installed in the vehicle primarily for other than the thermal-protection system. Probably the best example of this is a fuel cell installed to supply power for the actuation system. The thermal protection would not require power when the primary system required power and thus none of the installed weight would be charged to the thermal-protection system. A penalty for the reactants and associated tankage would be charged to the thermal-protection system for the dependent-fuel-cell system.

Semidependent Fuel Cells — This fuel cell supplies power for other systems; however, an installed weight penalty of 0.11 pound per watt is included with the reactants and tankage penalty. The 0.11 pound per watt is based on a cell of 2-kilowatt size.

Independent Fuel Cell — The independent fuel cell supplies the power required by the thermal-protection system only. Two fuel-cell manufacturers have developed space-vehicle fuel cells of 40- to 50-watt size. One of the cells weighs approximately 15 pounds without tankage. This weight could be reduced to an estimated 12 pounds. A minimum weight of 10 pounds was assumed for fuel cells. This cell was assumed to be provided reactants from tanks installed primarily for other than the fuel cell. An example would be reactants supplied from hydrogen and oxygen tankage of a propulsion system. If storage is not available on the vehicle, the penalty for reactants will somewhat exceed the values assumed for this study. The reactants and tankage are included as a penalty; however, the system would be more attractive if the reactants were vented fluids from propulsion tankage, which would not be chargeable to the thermal-protection system.

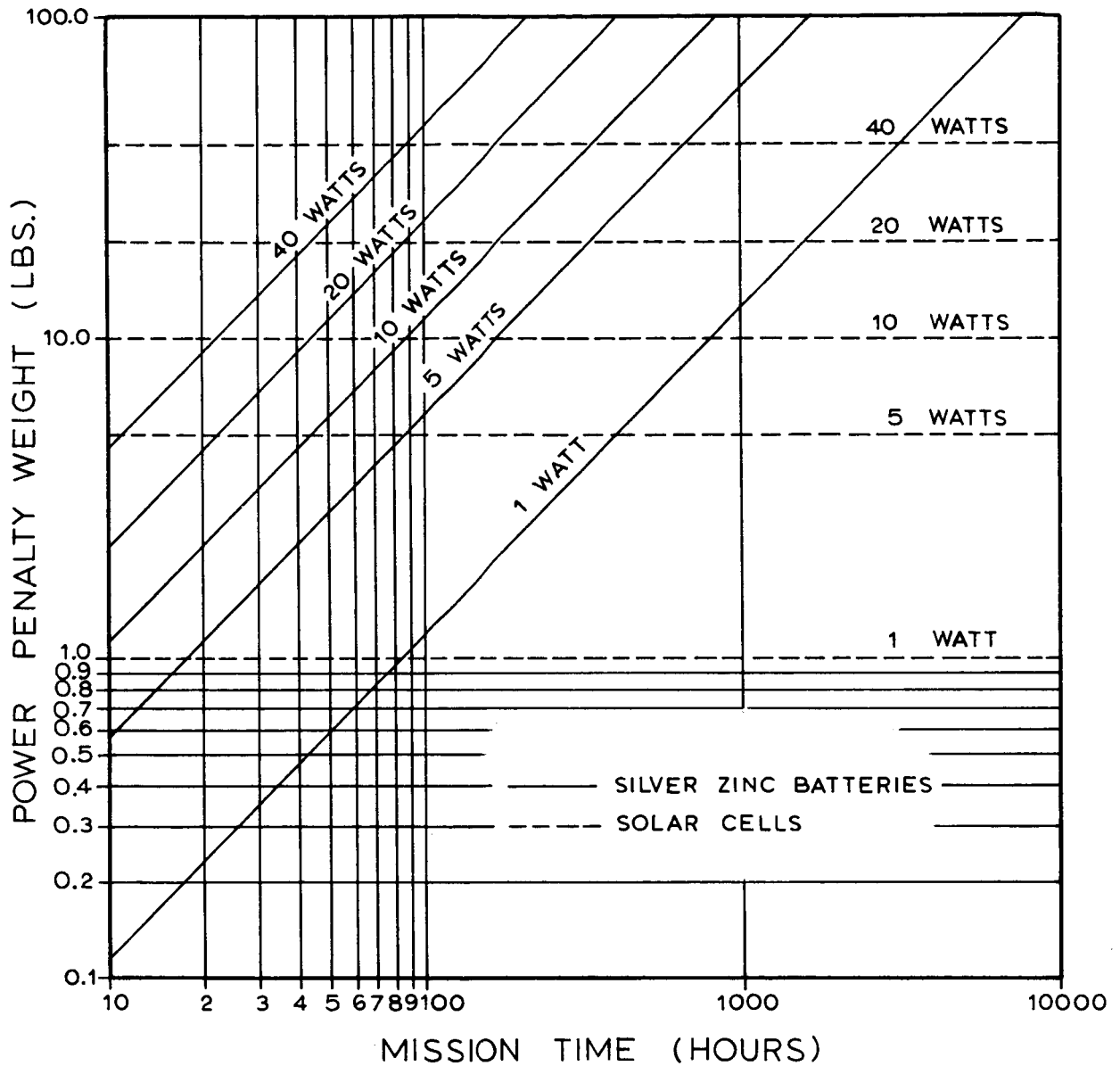


Figure 14: Power Penalty — Batteries And Solar Cells

Figure 15 shows the resulting weight penalties for the three fuel-cell systems versus mission time.

Two isotopes were considered as heat sources, polonium 210 and plutonium 238. Both isotopes emit primarily alpha particles and therefore can be shielded relatively easily. The amount of shielding required by the polonium 210 isotope is about 0.4 inch of depleted uranium and no shielding is required for the plutonium 238. This limits dose rates to 1 to 2 mrad per hour at 1 meter from the source.

The major penalty for the isotope heat source is to encase the isotope material so that it is not dispersed if a vehicle failure occurs. This study assumed that a 1-inch-thick molybdenum casing would provide suitable protection. This is a problem area and requires additional study, especially if failures involving re-entry are considered. Polonium 210 costs roughly 20 to 200 dollars per watt and plutonium 238 costs 500 to 900 dollars per watt. The availability of both isotopes is poor, but there are indications that the availability may become better in the future. The life of polonium is satisfactory for missions of about 6 months; for longer missions, the initial power level has to be increased. This increased initial power level could cause overheating problems at the first of the mission. Figure 16 shows the weight comparison between polonium 210 and plutonium 238.

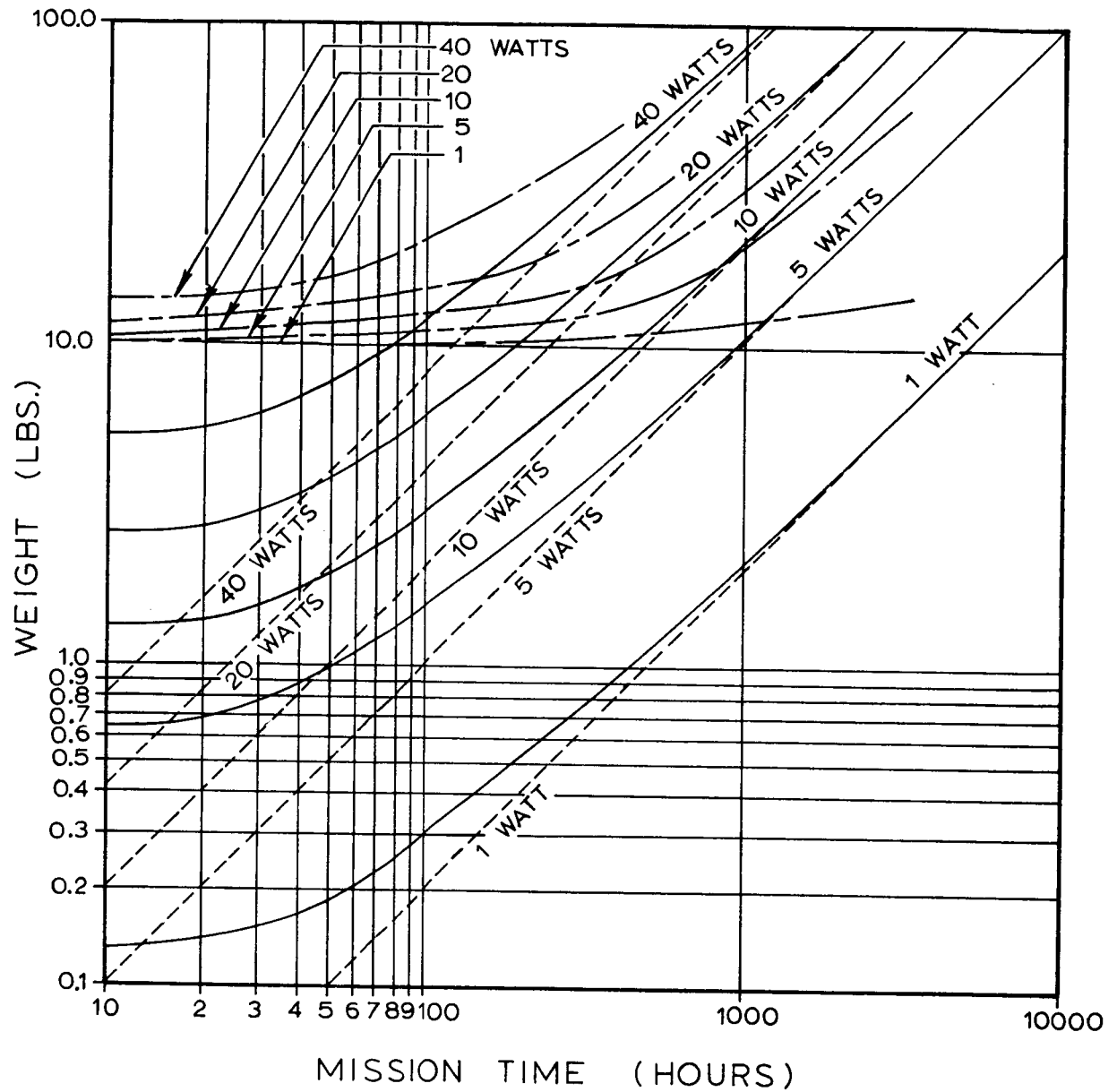
The weight penalties for the various power sources were combined to show the minimum-weight heat source. If a dependent fuel cell is installed on the vehicle primarily for other systems, the summary is shown in Figure 17. If such a fuel cell is not on the vehicle, Figure 18 presents the power source summary. Comparison of Figures 17 and 18 shows that, if a fuel cell is on the vehicle, less penalty results by using this source rather than batteries. If the fuel cell is not on the vehicle, batteries provide the least-penalty power for missions of several days. The power sources of Figures 17 and 18 will be used for the thermal-protection weight trade study following.

3.3.2 THERMAL-PROTECTION-SYSTEM HEAT-TRANSFER ANALYSIS

Since it was assumed that the actuation system would be installed in an unpressurized section of the vehicle, the radiation and conduction heat-transfer mechanisms need to be considered and convection can be neglected. The analysis is covered in two parts. The first part considers conduction through the insulation and radiation from the insulation surface to the surroundings. The second part considers conduction through fittings that penetrate the insulation. Finally, the weight penalties for the overall heat transfer are presented.

The radiation heat transfer from the actuation system package was calculated with the following assumptions:

- 1) Steady-state conditions prevail;
- 2) One-dimensional heat transfer through the insulation covering the package;
- 3) The surfaces surrounding the actuation system package are at a constant temperature and act as an infinitely large black body;
- 4) Component temperature maintained at a constant value.



- DEPENDENT FUEL CELL (PENALTY FOR REACTANTS AND TANKAGE ONLY).
- SEMI-DEPENDENT FUEL CELL (PENALTY FOR INSTALLED WEIGHT, REACTANTS AND TANKAGE FOR FUEL CELL SUPPLYING POWER FOR OTHER VEHICLE SYSTEMS ALSO).
- · — · — INDEPENDENT FUEL CELL (PENALTY FOR INSTALLED WEIGHT, REACTANTS AND TANKAGE FOR FUEL CELL SUPPLYING POWER FOR ONLY THERMAL PROTECTION).

Figure 15: Power Penalty — Hydrogen-Oxygen Fuel Cells

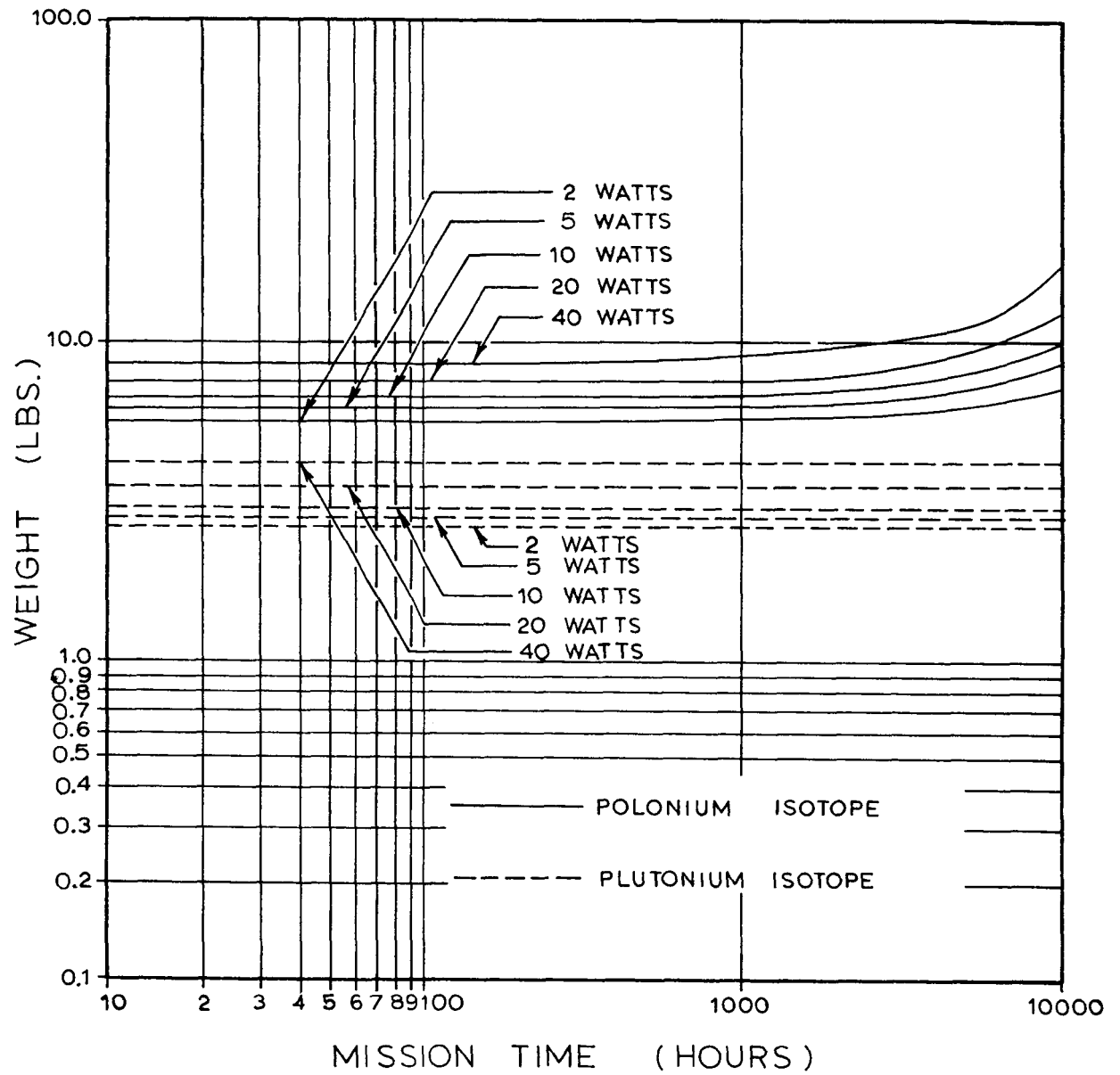
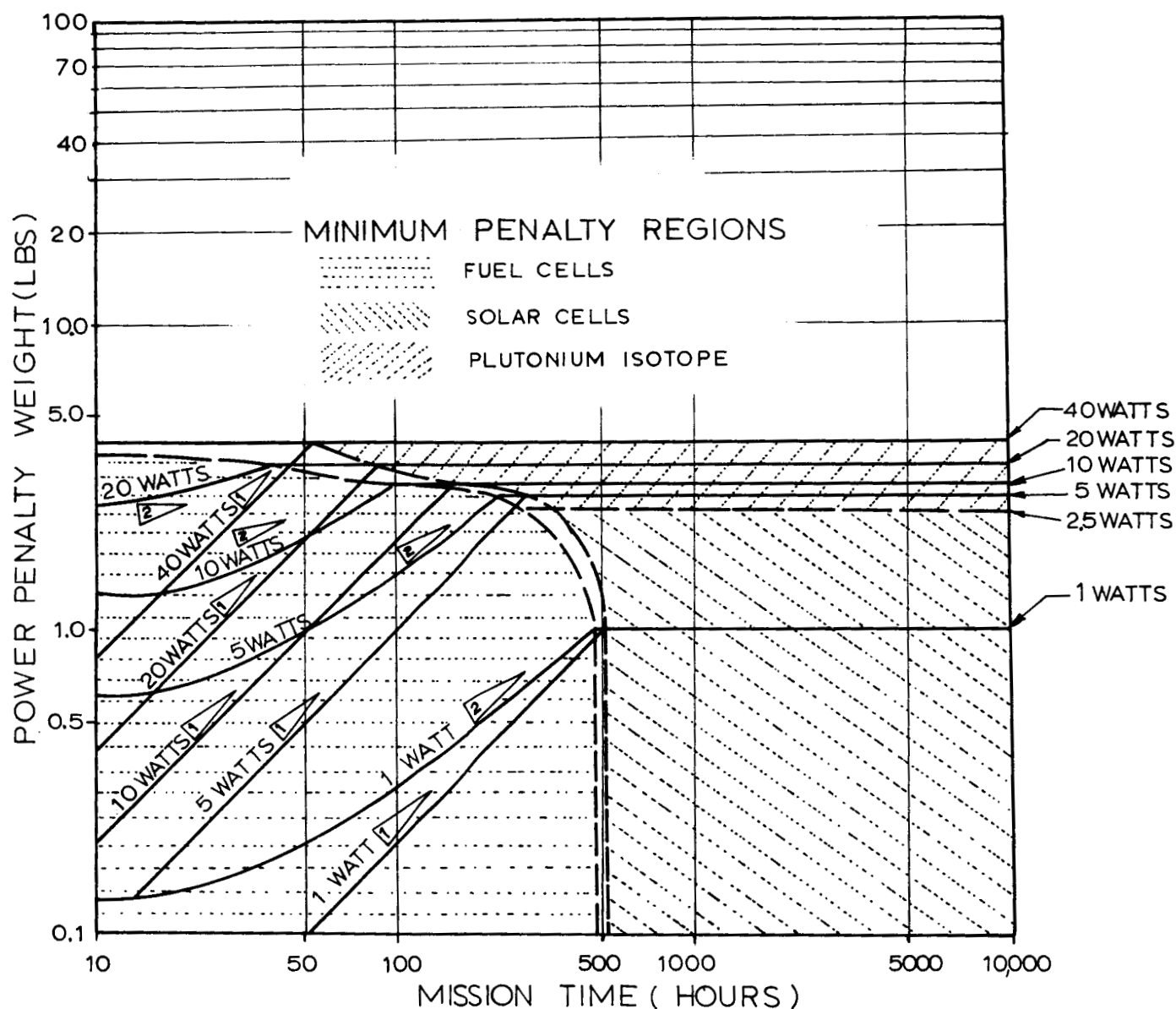


Figure 16: Power Penalty — Isotope Heat Sources



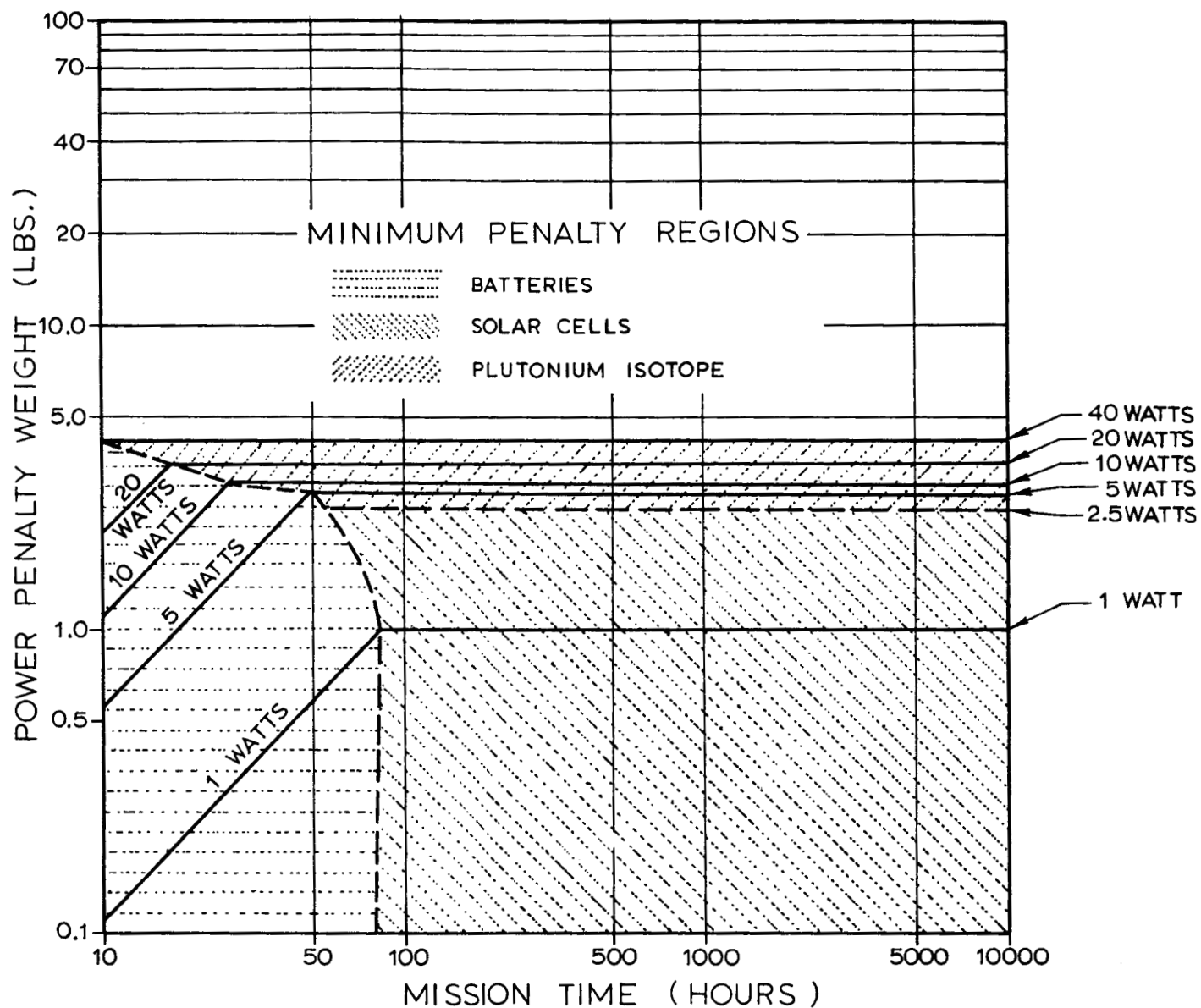
ENERGY SOURCES CONSIDERED

- SILVER ZINC BATTERIES
- SOLAR CELLS
- POLONIUM ISOTOPE
- PLUTONIUM ISOTOPE
- DEPENDENT FUEL CELL 1
- SEMI-DEPENDENT FUEL CELL 2

Figure 17: Power Penalty Summary for Vehicles With Fuel Cell Power Source *

- 1 DEPENDENT FUEL CELL - PENALTY FOR REACTANTS AND TANKAGE ONLY.
- 2 SEMI-DEPENDENT FUEL CELL - PENALTY FOR INSTALLED WEIGHT, REACTANTS AND TANKAGE FOR FUEL CELL SUPPLYING POWER FOR OTHER VEHICLE SYSTEMS ALSO.

* IF VEHICLE DOES NOT HAVE A FUEL CELL POWER SOURCE SUPPLYING POWER TO OTHER SYSTEMS USE PENALTIES SHOWN ON FIGURE 18 .



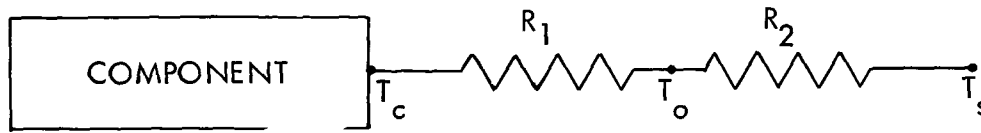
ENERGY SOURCES CONSIDERED

- SILVER ZINC BATTERIES
- SOLAR CELLS
- POLONIUM ISOTOPE
- PLUTONIUM ISOTOPE
- INDEPENDENT FUEL CELLS (SUPPLIES POWER FOR ONLY THERMAL PROTECTION)

Figure 18: Power Penalty Summary For Vehicles Without Fuel Cell Power Source *

* IF VEHICLE HAS A FUEL CELL POWER SOURCE SUPPLYING POWER TO OTHER SYSTEMS USE PENALTIES SHOWN ON FIGURE 17.

The thermal analog used for determining the radiation heat losses is shown below:



where:

T_c = component temperature, °R

T_o = external temperature of the insulation covering the package, °R

T_s = sink temperature to which package radiates, °R

R_1 = thermal resistance of insulation covering the package, hr-°R/Btu

R_2 = radiation resistance between the package and its surroundings, hr-°R/Btu

The following equations were used in determining the values of the analog resistors.

R_1 insulation:

$$R_1 = \frac{\Delta X_{ins}}{K_{ins} A_{ins}}$$

R_2 radiation:

$$R_2 = \frac{1}{\sigma \epsilon_o A_{rad} (T_o^2 + T_s^2) (T_o + T_s)}$$

where:

ΔX_{ins} = insulation thickness, in.

K_{ins} = insulation thermal conduction, Btu/hr-ft²-°R/in.

A_{ins} = area of insulation, ft²

σ = Stefan-Boltzmann constant, 0.171×10^{-8} Btu/hr-ft²-°R⁴

ϵ_o = emissivity

A_{rad} = surface area, ft²

Also, since we assume steady-state conditions;

$$q_{ins} = q_{rad}$$

where:

$$\begin{aligned} q_{\text{ins}} &= \text{heat transferred through insulation, Btu/hr} \\ &= \frac{T_c - T_o}{R_1} \end{aligned}$$

$$\begin{aligned} q_{\text{rad}} &= \text{heat radiated from surface, Btu/hr} \\ &= \frac{T_o - T_s}{R_2} \end{aligned}$$

so:

$$\frac{K_{\text{ins}} A_{\text{ins}}}{\Delta X_{\text{ins}}} (T_c - T_o) = \sigma \epsilon_o A_{\text{rad}} (T_o^4 - T_s^4)$$

but, since one-dimensional slab heat flow was assumed

$$A_{\text{ins}} = A_{\text{rad}}$$

Therefore:

$$T_o + \frac{\sigma \epsilon_o \Delta X_{\text{ins}}}{K_{\text{ins}}} T_o^4 = T_c + \frac{\sigma \epsilon_o \Delta X_{\text{ins}}}{K_{\text{ins}}} T_s^4$$

The radiation heat loss from the actuation system package (equivalent to the heater requirement) can be calculated using the above equation to solve for T_o and substituting into the following equation.

$$q_{\text{rad}} = \sigma \epsilon_o A_{\text{rad}} (T_o^4 - T_s^4)$$

The radiation heat loss from the hydraulic equipment was calculated for several different conditions. The cases considered were:

- 1) Sink temperature — -50 to -460°F
- 2) Insulation type — multilayer, glass fiber
- 3) External package emissivity — 0.06, 0.9
- 4) Hydraulic component temperature — -50, -100, -150°F.

The effect of various sink temperatures on the radiation heat loss is shown in Figure 19. Since the magnitude of the radiation heat loss is dependent on the fourth power of the absolute temperature, the sink temperature has relatively little effect on the radiation heat loss at the lower temperatures. This is demonstrated by the data plotted in Figure 19. For example, the heat loss for a component with a temperature of -50°F

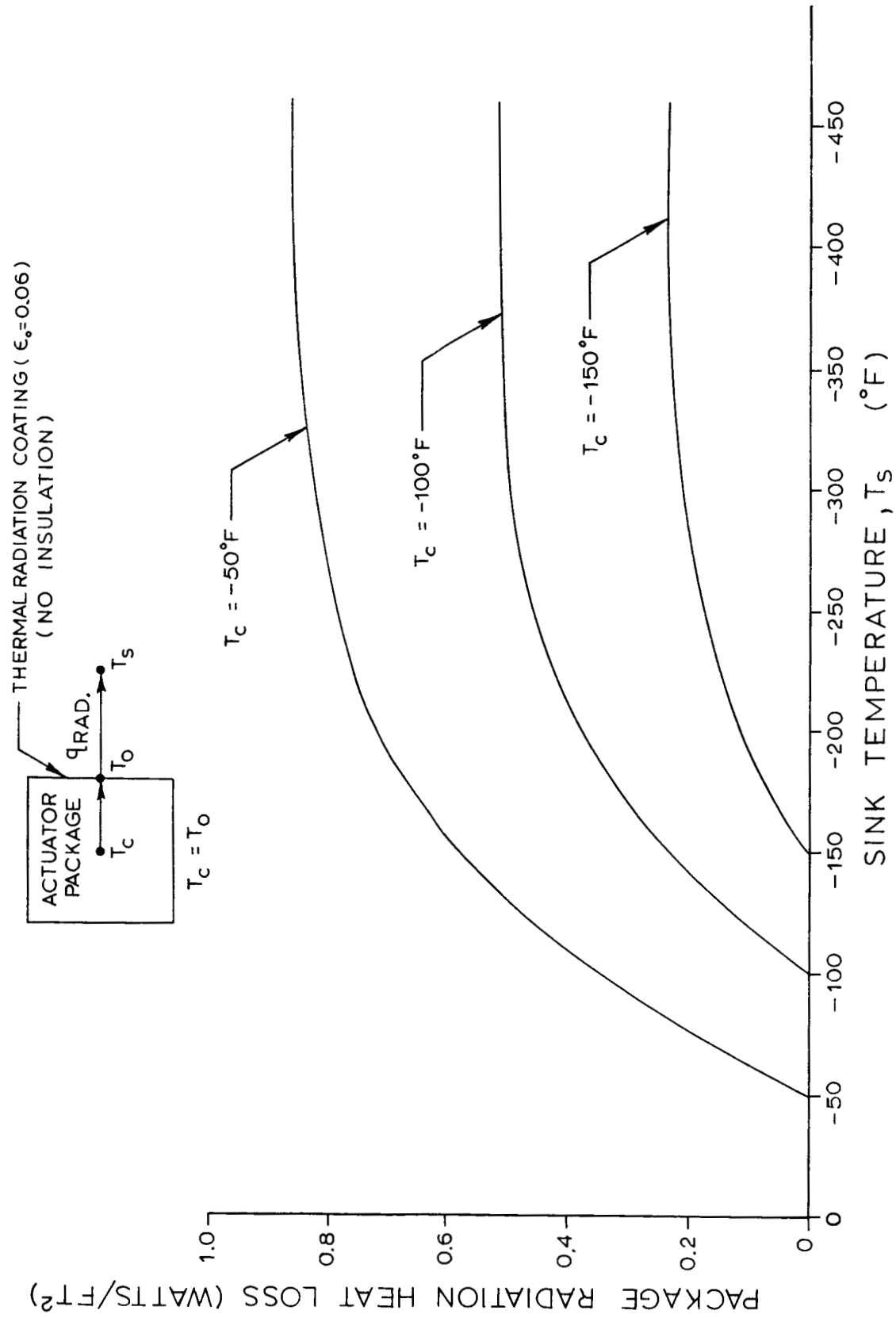


Figure 19: Radiation Heat Loss — No Insulation

and a sink temperature of -460°F is 0.86 watt per square foot of surface area. If this sink temperature were raised to -240°F , the corresponding effect would be to lower the heat loss to 0.78 watt, or about 9-percent reduction. If the component temperature was -150°F rather than -50°F , the lowering of heat loss by changing the sink temperature from -460°F to -240°F is about 29 percent. Hence, the lower sink temperatures do not appreciably affect the component heat loss when the temperature is significantly greater than the sink temperature.

Two basic types of insulation were investigated in this study. These were multilayer and glass-fiber insulation. The multilayer insulation consists of layers of highly reflective metal foil separated by glass-fiber spacer material. Other multilayer combinations have also been used, but have similar thermal characteristics. A weight of 5.0 pounds per cubic foot was assumed for both insulations. This includes the installation weight.

For a given insulation thickness, the multilayer insulation is much more effective than the glass fiber, because the thermal conductivity of glass-fiber insulation is roughly 100 times greater than that of multilayer insulation. A comparison of the two insulations at various thicknesses is shown in Figures 20 and 21.

The significant point is that a half-inch of multilayer insulation reduces the heat leak of a package with a temperature of -50°F from 0.78 watt per square foot to 0.045 watt per square foot, compared to 2.5 inches of glass fiber, which reduces the heat leak only from 0.78 watt to 0.34 watt. Therefore, where long mission durations are encountered, larger weight penalties are associated with glass-fiber insulation, along with large volume penalties. The volume will be important in space vehicles because minimizing volume is an important design criterion.

Techniques need to be developed to allow efficient installation of the multilayer insulations. If heat shorts occur from the attachments, the effective conductivity can be very much greater than that of the insulation.

The effect of varying the package outer surface emissivity is also shown in Figures 20 and 21. The external package emissivity has a significant effect on heat loss where no insulation is required. With a component temperature of -50°F and a sink temperature of -240°F , the radiation heat loss is 12 watts per square foot with an emissivity of 0.90, whereas the heat loss is 0.78 watt with an emissivity of 0.06. The lower emissivity value of 0.06 can be achieved by the use of highly reflective aluminum foil. Hence, this value of emissivity will be used for determining package heat loss and the optimum thermal-protection system.

The optimum insulation thickness was determined using the power penalties in Figures 17 and 18 and the heat loss of Figures 20 and 21. These results are shown in Figures 22 and 23. Figure 22 corresponds to the vehicle power penalties of Figure 17, which is for a vehicle with fuel cell installed for other systems. Figure 23 is for a vehicle without an installed fuel cell. The isotope power source cannot be included on these figures since the weight depends on the total power requirement, which is a function

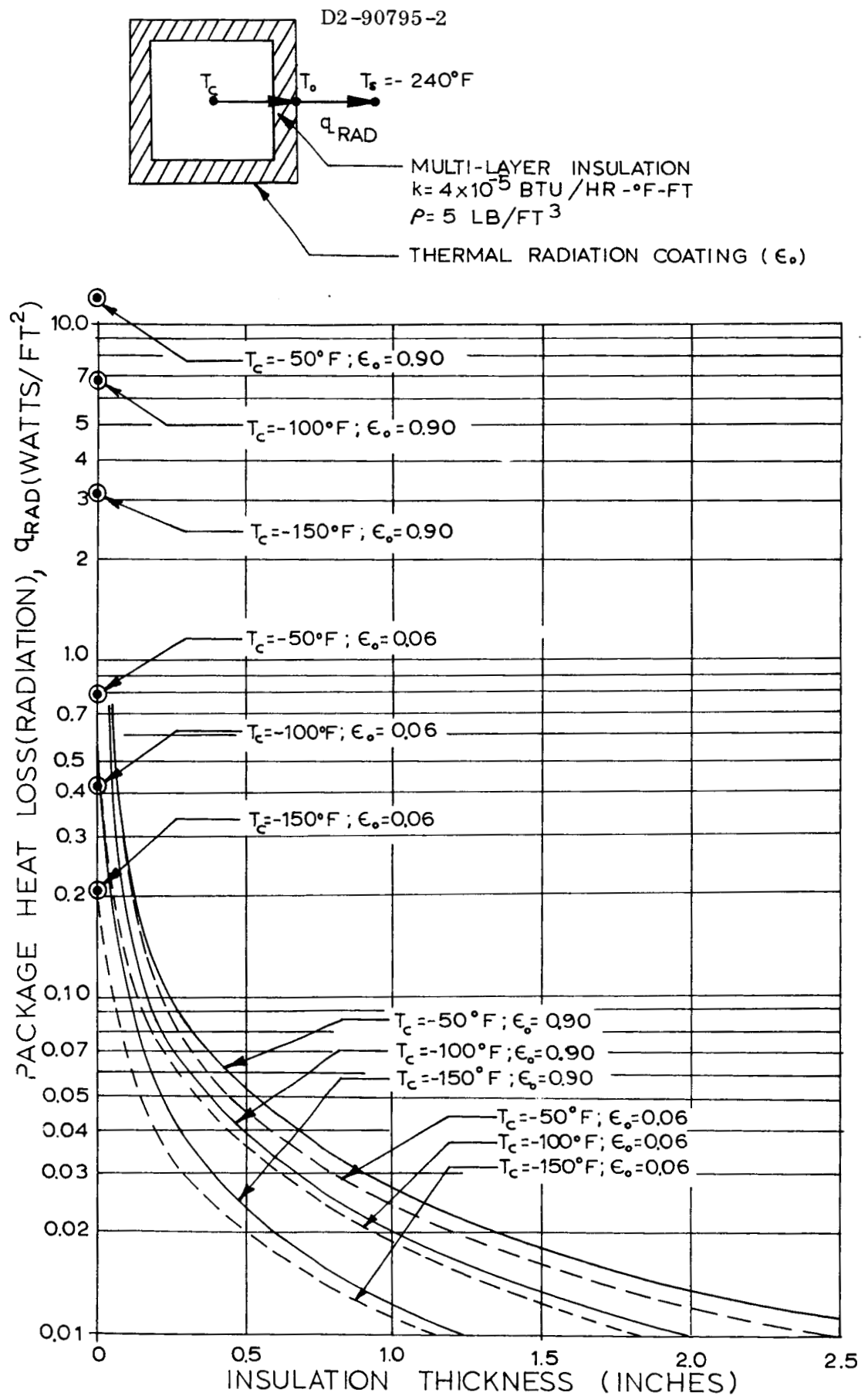


Figure 20: Radiation Heat Loss Multilayer Insulation

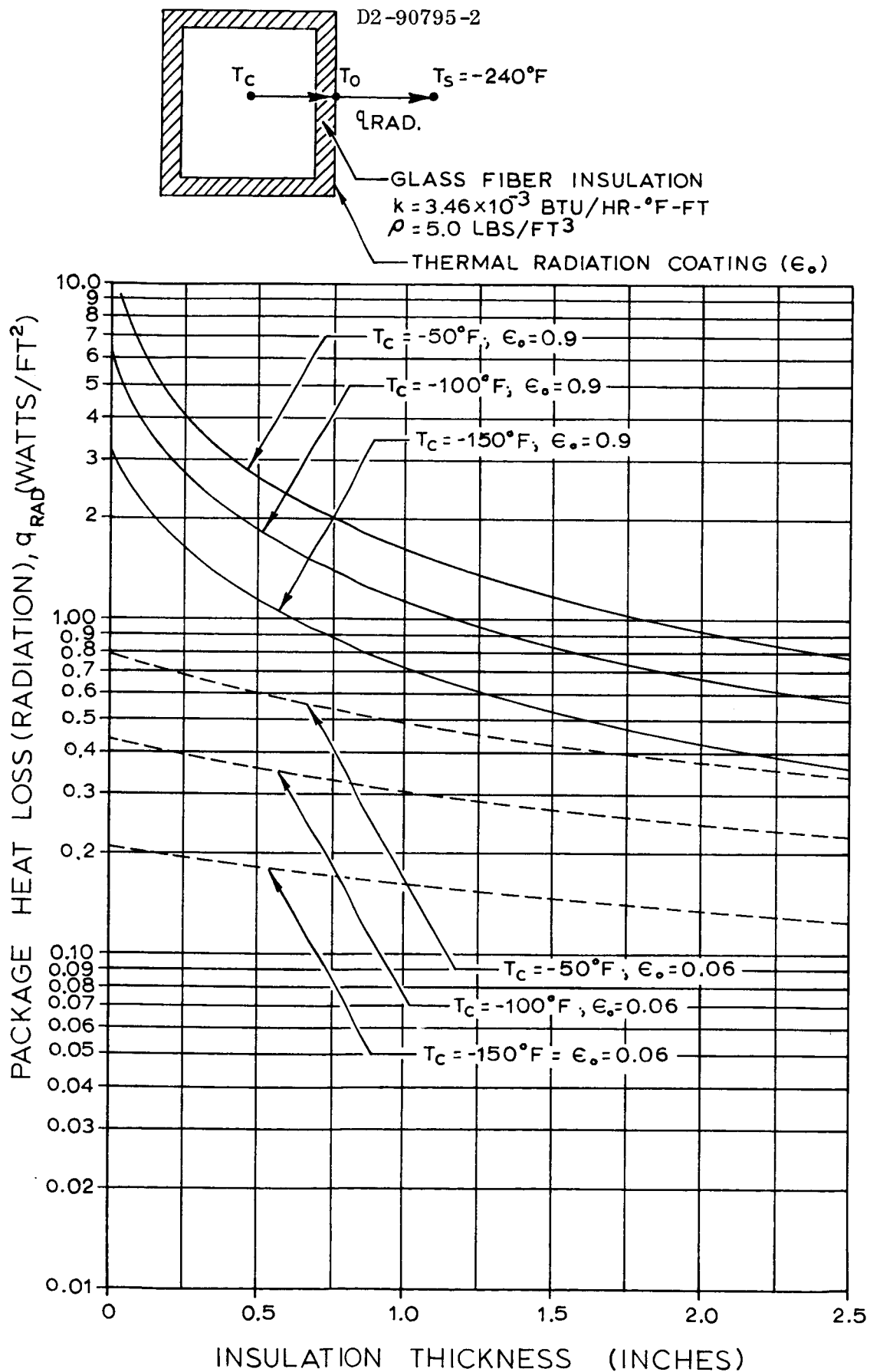


Figure 21: Radiation Heat Loss — Glass Fiber Insulation

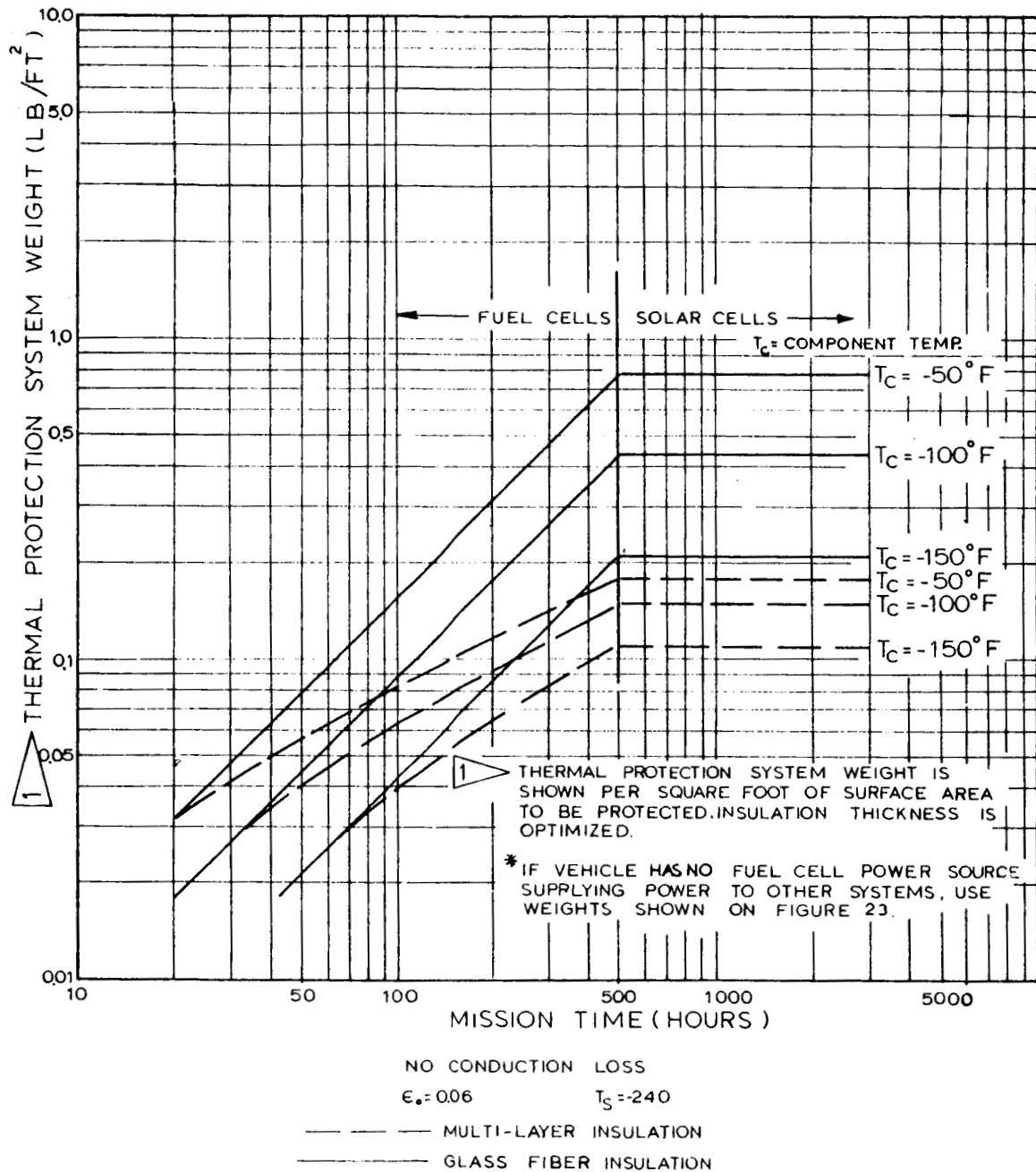


Figure 22: Thermal Protection System Weight For Vehicles With Fuel Cell Power Source *

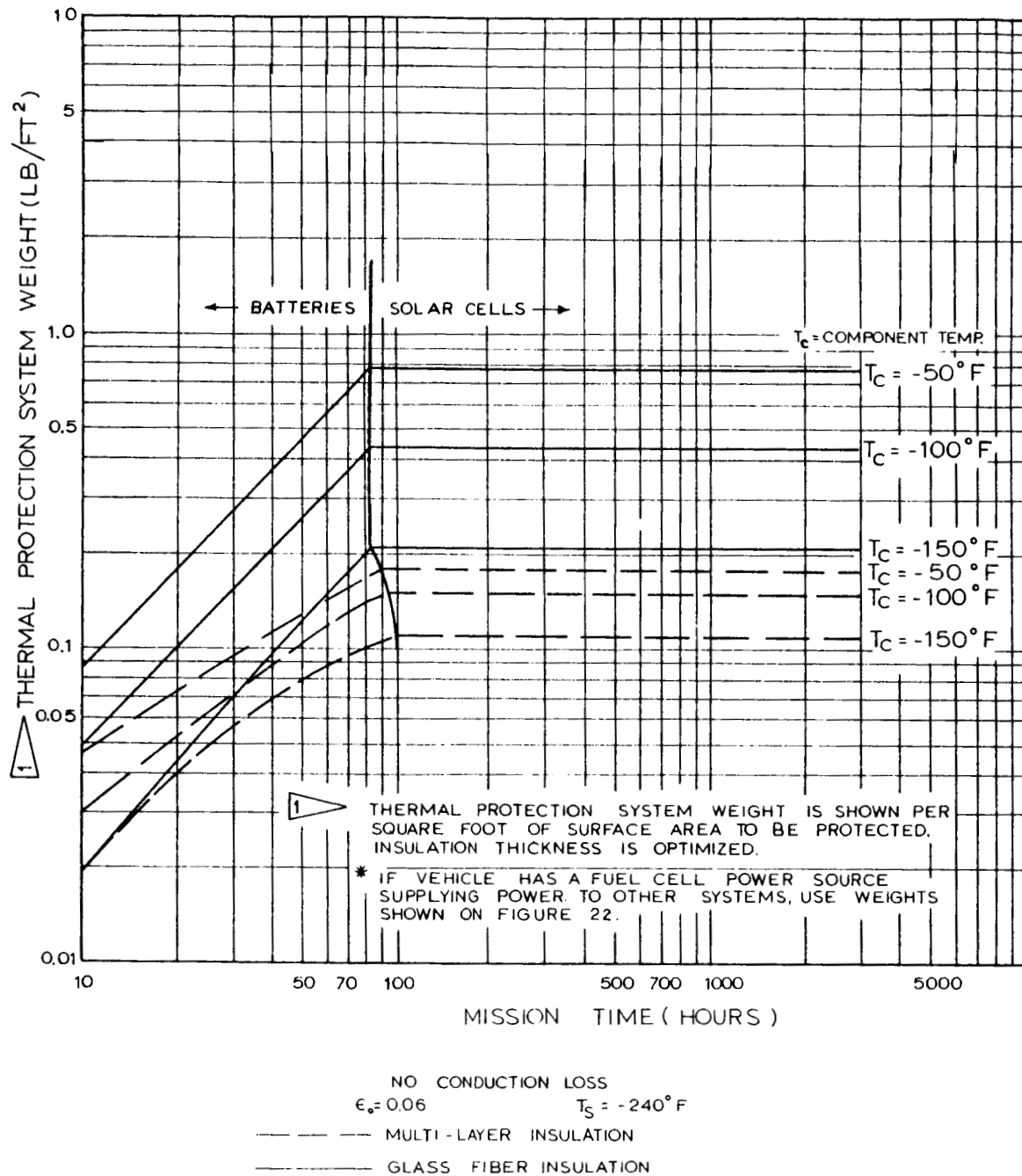


Figure 23: Thermal Protection System Weight For Vehicles
Without Fuel Cell Power Source *

of the total number of square feet of actuation system package area and the conduction loss. The advantage of the multilayer insulation is again apparent in Figures 22 and 23.

The conduction heat loss from a component is from the supports of the pumps, motors, reservoirs, etc., and the actuator bearings. The loss through supports can be reduced by such techniques as insulating spacers and increased contact resistance from multiple spacers. Actuator bearings present a unique problem since the addition of insulators or increased contact resistance will tend to reduce the actuation-system response. Figure 24 shows the estimated magnitude of the actuator end-bearing conduction loss. Depending on the "fit," the heat loss from a bearing at -100°F to a mounting shaft at -240°F can be 5 watts or even much greater. The effect of adding a nylon fiber bushing to the bearing is also shown.

A 10-watt conduction loss (for two bearings) compares with the heat loss by radiation (Figure 20), which can be reduced to less than 0.1 watt per square foot with a small amount of insulation. The controlling heat-transfer mechanism can be conduction unless this loss is significantly reduced. Developmental work is required to determine the thermal conductance of present supports and bearings. If these losses are excessive, low-heat-loss components should be developed that also have acceptable system-response characteristics. A design goal would be to reduce the bearing conduction loss to approximately 2 watts.

Figures 25 through 28 show the resulting thermal-protection-system weight for equipment in a -240°F temperature environment. Figures 25 and 26 are for a vehicle with a fuel cell installed to provide power for other systems. Figure 25 is for the components maintained at -100°F , and Figure 26 is for the components maintained at -150°F . Figures 27 and 28 are for a vehicle that does not have a fuel-cell power source. Figures 27 and 28 are for component temperatures of -100 and -150°F , respectively.

For batteries, solar-cell, or fuel-cell power sources, the total surface area and conduction loss was used to determine the thermal-protection penalty for the system. For the isotope heat source, the penalty for each package that requires an isotope capsule was calculated separately and the total weight was then determined.

The heater and temperature switch weights must be added to the weights shown in Figures 25 through 28. The heaters weigh 0.4 pound for each square foot of heater area. Heaters on one or possibly two of the inside surfaces are sufficient for each package, so the heater area is not the same as the total package surface area. The temperature switches weigh approximately 0.2 pound each. This weight assumes mechanical direct-acting switches. If conduction rods are required to conduct the isotope heat to the components, the rod weights must also be added to the weights shown in the figures.

The lower weight of the isotope system shown in Figures 25 through 28 for long missions and higher heater requirements indicates that the development required to provide isotope thermal protection systems should be initiated.

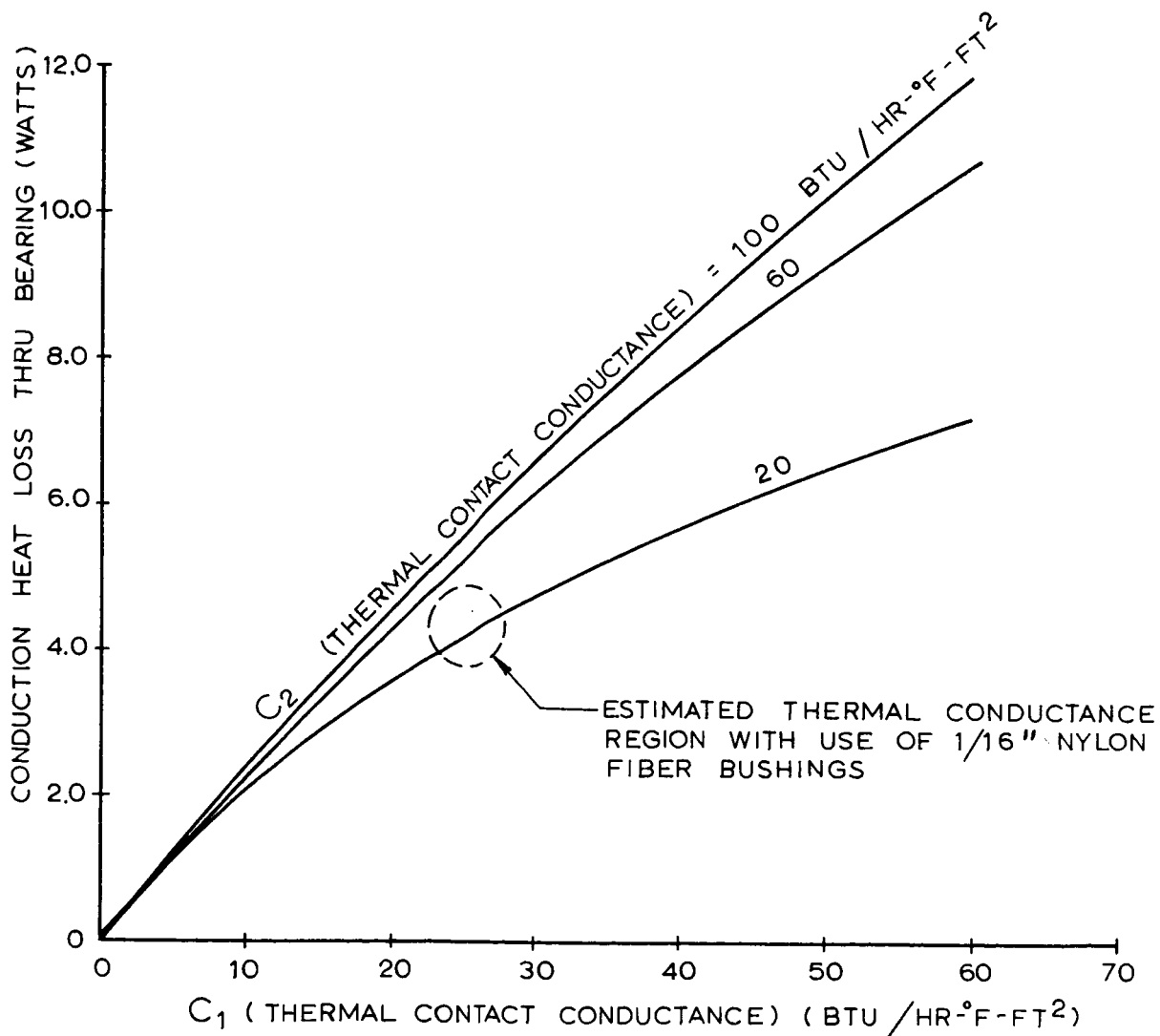
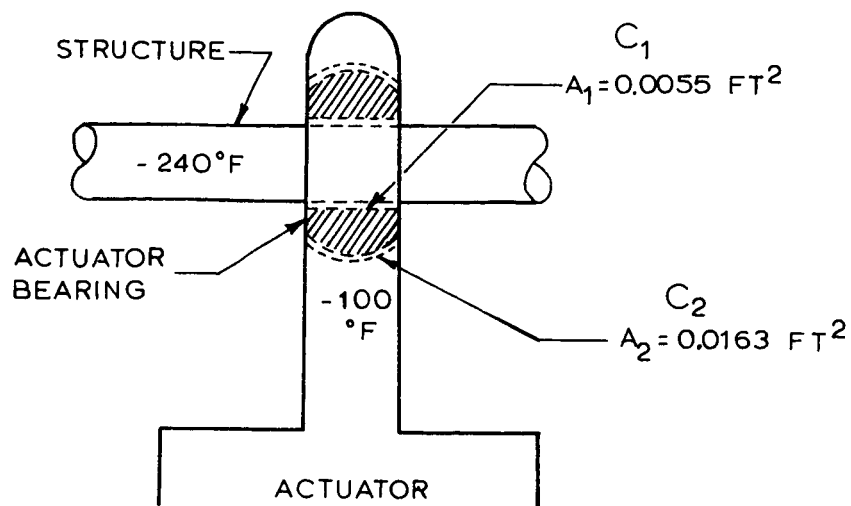


Figure 24: Conduction Heat Loss Through Actuator Bearing

MULTI-LAYER INSULATION $\epsilon_o = 0.06$

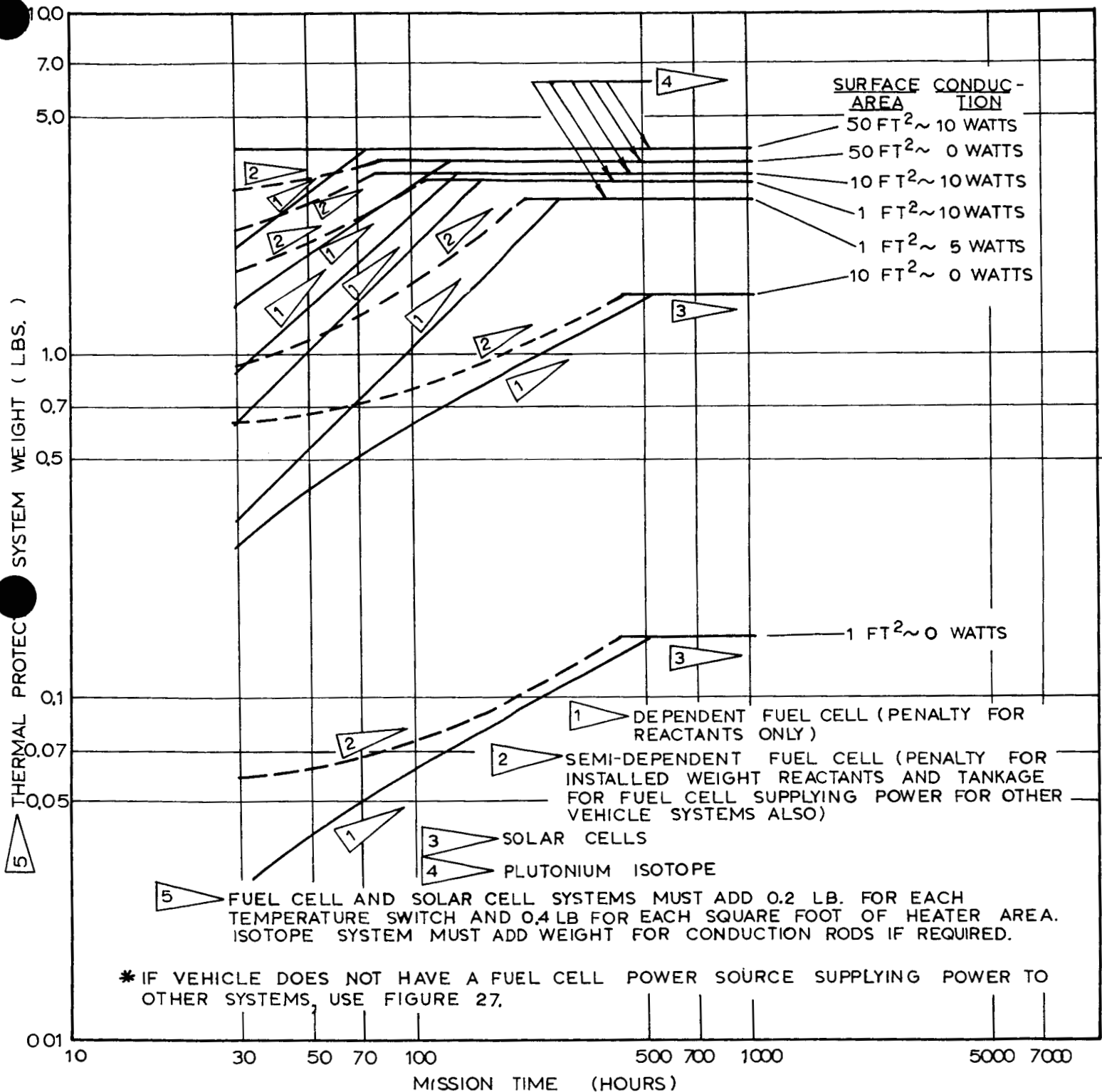
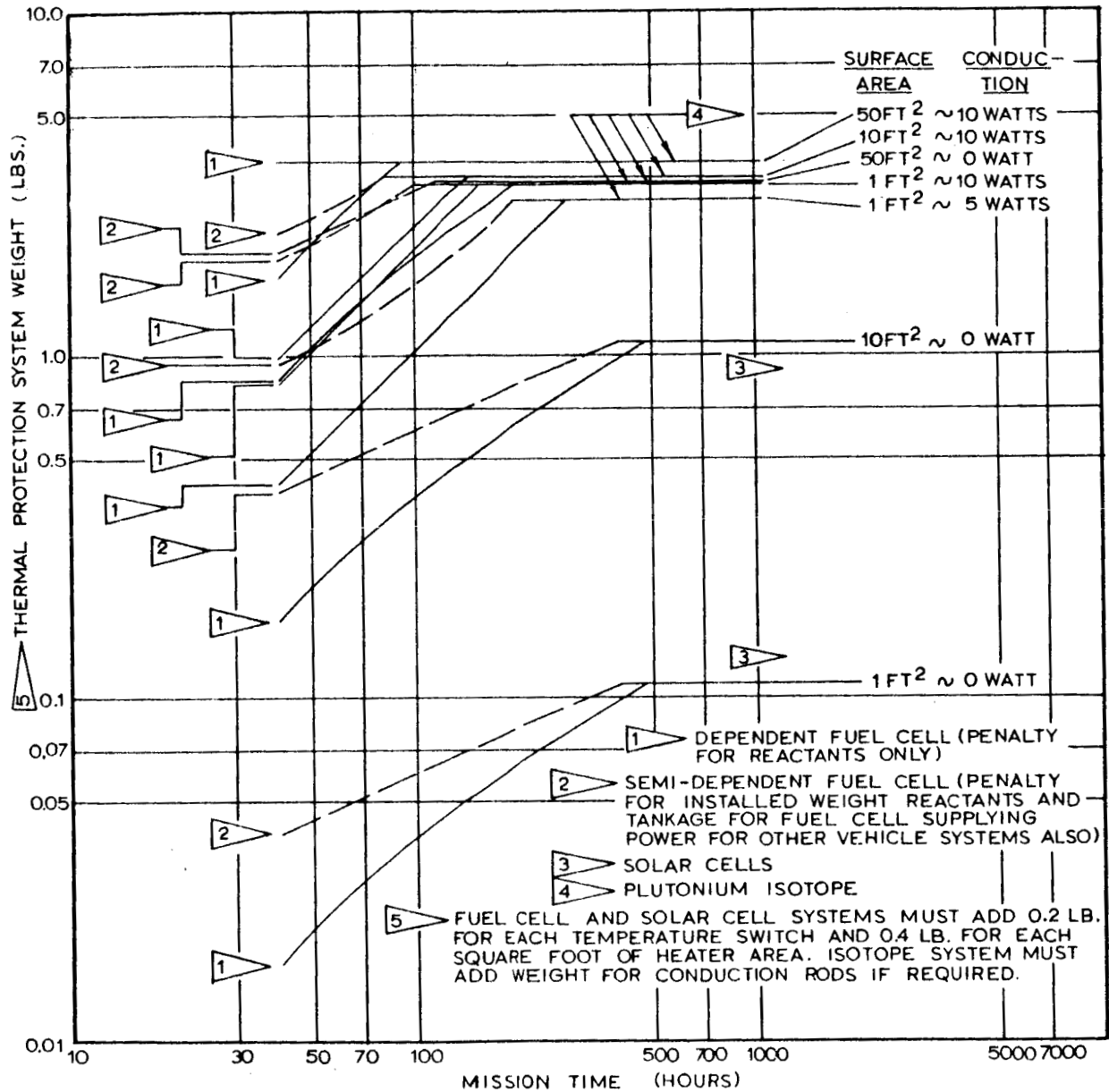


Figure 25: Thermal Protection System Weight Including Conduction Losses
For Vehicles With Fuel Cell Power Source * $T_c = -100^\circ\text{F}$ $T_s = -240^\circ\text{F}$

MULTI-LAYER INSULATION $\epsilon_0 = 0.06$



* IF VEHICLE DOES NOT HAVE A FUEL CELL POWER SOURCE SUPPLYING POWER TO OTHER SYSTEMS, USE FIGURE 28.

Figure 26: Thermal Protection System Weight Including Conduction Losses For Vehicles With Fuel Cell Power Source *

$$T_C = -150^{\circ}\text{F} \quad T_S = -240^{\circ}\text{F}$$

MULTI-LAYER INSULATION $\epsilon_o = 0.06$

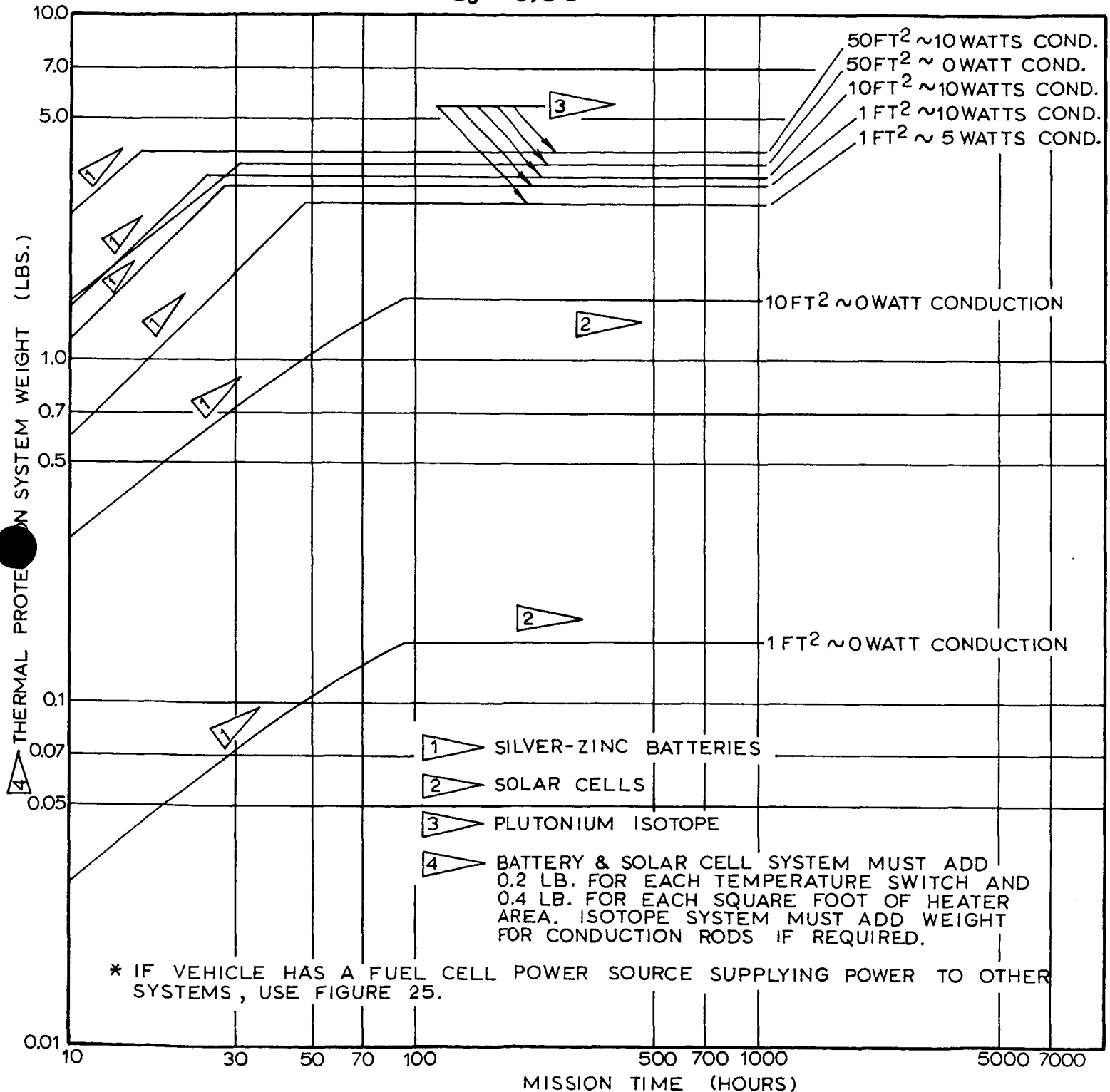


Figure 27: Thermal Protection System Weight Including Conduction Losses
For Vehicles Without Fuel Cell Power Source *

$$T_c = -100^{\circ}\text{F} \quad T_s = -240^{\circ}\text{F}$$

MULTI-LAYER INSULATION

$\epsilon_0 = 0.06$

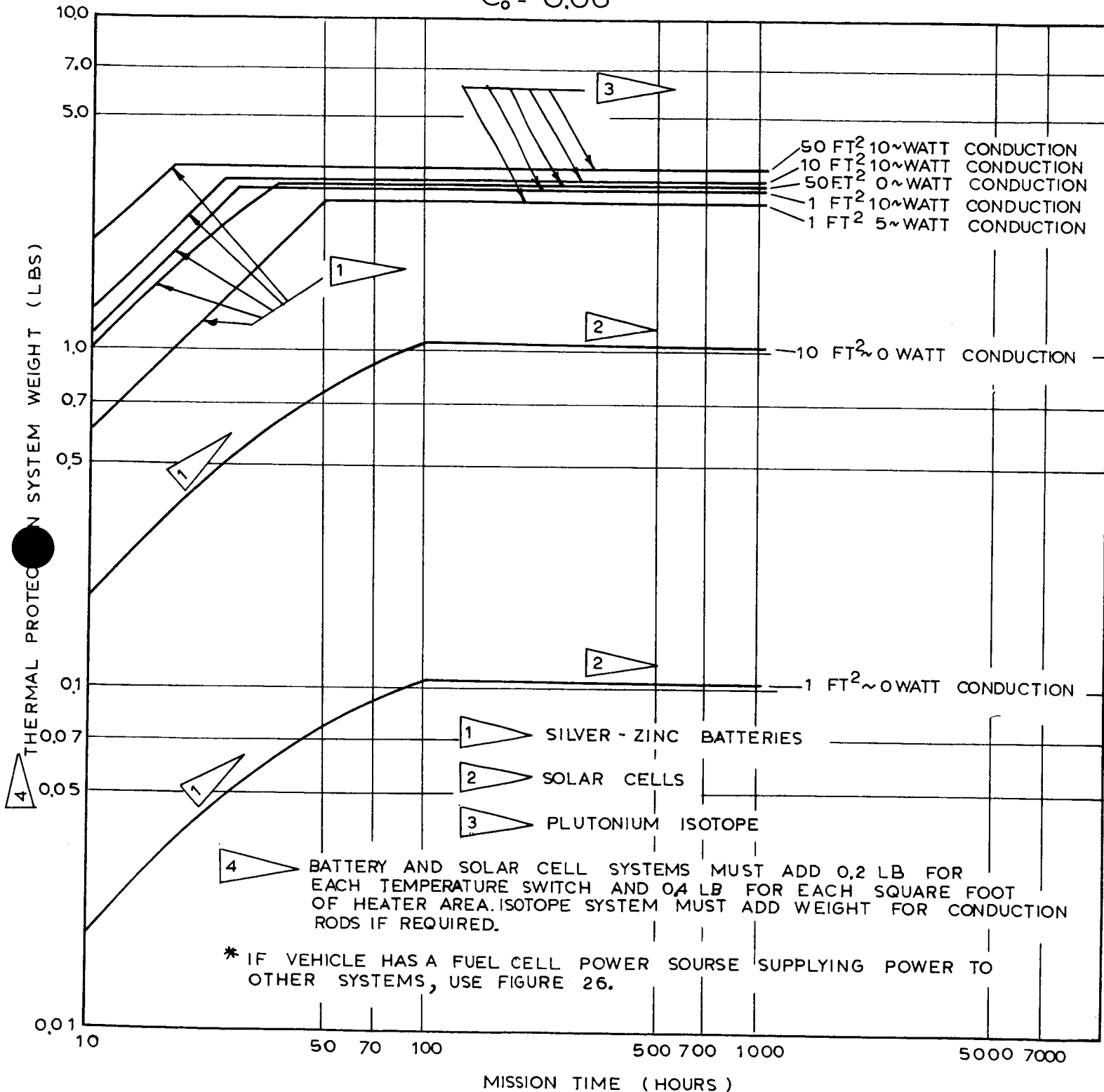


Figure 28: Thermal Protection System Weight Including Conduction Losses For Vehicles Without Fuel Cell Power Source *

$$T_c = -150^{\circ}\text{F} \quad T_s = -240^{\circ}\text{F}$$

4.0 TEST SYSTEM DESIGN

The space actuation task selected for simulation in the test program was the thrust vector control gimbaling of an RL-10 propulsion engine on a typical lunar landing vehicle. This task is one of the four tasks evaluated in the trade study portion of the contract reported in Volume I. The thrust vector control task was selected for the test system for the following reasons.

- 1) The task was easily adaptable to hydraulic actuation but had requirements that could be satisfied by other types of actuation systems.
- 2) Information from which gimbaling requirements could be calculated was presently available.
- 3) Equipment requirements were of a size that were within the scope of the test program.
- 4) Analysis of this task deserved consideration at this time because the application was comparable to a present hardware development program.

4.1 APPLICATION REQUIREMENTS

The test system was designed to simulate the type of motion and response demanded of a hydraulic system during lunar landing vehicles flight maneuvers under simulated environmental conditions. The control requirements were defined in the application description, which follows, with a more detailed analysis given in the load and system analysis sections.

4.1.1 APPLICATION DESCRIPTION

Thrust vector control (TVC) of a space propulsion engine such as the RL-10 will be one actuation task of many to be performed on a lunar landing vehicle. TVC will be confined to periods of main engine firing, which include braking into equiperiod lunar orbit, descent braking, hover, and landing. The engine thrust level will be controllable for hovering while selecting a landing site; fast response will be required for rapid maneuvering just before touchdown.

TVC requirements are ± 7.5 degrees motion of the RL-10 engine in a square pattern at a maximum rate of 20 degrees per second and an acceleration of 250 degrees per second per second. A total of 8 times of operation will be required and the servosystem break frequency desired is 3.2 cycles per second. These requirements were based on Reference 9, which incorporates a piloted analog simulation of the lunar landing mission, and on Reference 10, the engine specification.

Thrust vector control components will be exposed to space environments throughout the lunar flight. Before propulsion engine ignition, the engine flight attitude will be away from the Sun to minimize boiloff of cryogenic propellants. In this vehicle attitude, the gimbal actuation equipment is expected to reach a temperature of -240°F . The equipment must be warmed before use because of the limitations of existing hydraulic fluids

and seals. During use, the fluid temperature is not expected to exceed 100°F from heat caused by throttling.

A shaft power source for the hydraulic system will provide a maximum of 2.5 horsepower from an engine turbopump pad at an insignificant penalty to the engine (see Reference 10).

4.1.2 LOAD ANALYSIS

The load to be actuated will be a single Pratt & Whitney RL-10-A3 engine with a 60:1 expansion ratio with regeneratively cooled skirt. The engine will not be canted and the vehicle will have an assumed acceleration of 0.8-g Earth gravity during periods requiring thrust vector control. The wet engine weighs 372 pounds including 35 pounds for the skirt extension that increases the expansion ratio from 40:1 to 60:1. The engine center of gravity is 30.5 inches aft of the gimbal, 4.42 inches from the horizontal centerline, and 1.28 inches from the vertical centerline. The actuator attachment points to the engine establish the actuator centerlines as always parallel to the engine horizontal and vertical axis. With the engine in the neutral position, one actuator attachment point will have a 9.62-inch lever arm about the horizontal axis and the other a 9.06-inch lever arm about the vertical axis. The engine moment of inertias are 10.6 slug-feet² about the engine centerline, 83.1 slug-feet² about the horizontal centerline, and 81.4 slug-feet² about the vertical centerline.

Engine dimensions used in the load analysis for the 60:1-expansion-ratio engine are 46.3 inches for the exit diameter, 86 inches for the engine length, 62 inches from the throat to the exit plane, and 30.5 inches from the gimbal to the center of gravity.

Significant hinge moment components result from vehicle longitudinal acceleration, coriolis damping caused by flow through the nozzle, rotational inertia of the engine, and gimbal friction. The first three components were calculated; the value for gimbal friction torque of 200 foot-pounds was derived from Reference 10. The results of the hinge moment calculations are as follows for various value of gimbal deflection.

Actuation Hinge Moments for RL-10-A3 Engine Gimbaling

	<u>Gimbal Deflection (degrees)</u>				
	<u>0.5</u>	<u>1</u>	<u>2</u>	<u>4</u>	<u>8</u>
Hinge Moment Component					
Longitudinal Acceleration (in. -lb)	80	158	316	635	1260
Coriolis Damping (in. -lb)	120	120	120	120	120
Rotational Inertia (in. -lb)	135	135	135	135	135
Gimbal Friction (in. -lb)	<u>2400</u>	<u>2400</u>	<u>2400</u>	<u>2400</u>	<u>2400</u>
Total Actuation Torque (in. -lb)	2735	2813	2971	3290	3915

The maximum design torque of 3915 inch-pounds occurs at maximum deflection and was used as the design hinge moment in all following calculations. Actuator loading was determined by dividing the hinge moment by the actuator lever arm about the engine gimbal point. The lever arm can be selected, within certain limitations, by selecting the placement of the actuator stationary end attachment point. The following paragraphs describe and explain the effects of selecting the actuator stationary end mounting position.

Figure 29 shows the fixed relationship between the engine gimbal point and the actuator attachment point to the engine when the engine is centered and when it is at maximum positive and negative deflections. Overall actuator lengths from 10 inches minimum to 28 inches maximum were considered. Actuator mounting angles from a parallel to the engine centerline were considered at 15-degree increments up to 90 degrees.

An increase in mounting angle provides an increased actuator lever arm, thereby reducing the actuator force requirement. A penalty for increasing the mounting angle is the accompanying increase in actuator stroke as the angle from a parallel to the engine to centerline increased. This stroke increase is proportional to increasing angle up the point of tangency to the path of motion of the actuator attachment point to the engine. This is shown in Figure 29 and in tabular form in Figure 30. The increase in actuator stroke is accompanied by an increase in required piston velocity to maintain the frequency response requirements. Increased piston velocity requires higher flow rates and, therefore, increased power and system weight.

A minimum critical actuator length exists below which a linear actuator of particular effective area cannot be fabricated practically. For this study application, the critical length was defined as 10 inches or 2.5 times the actuator stroke, whichever was larger. The critical-length actuator has a minimum lever arm at some deflected position of the actuator. This is shown for a typical installation in Figure 29; values are tabulated in Figure 30.

The minimum lever arm was used to determine the maximum instantaneous actuation force that must be provided by the critical-length actuator. These forces, shown in the right-hand column of Figure 30, are the design loads for further calculations.

The mounting angle of 11.5 degrees was selected to provide the best conditions for obtaining and reducing performance data from the test program. The choice was based on the desire to obtain the following characteristics:

- 1) An actuator stroke large enough to provide adequate position transducer output at all tested frequencies yet keeping within the envelope requirement established by the environmental chamber used in testing;
- 2) As low an actuator piston velocity (flow rate) as practical, thus allowing as long a time as possible to perform frequency scan during the test;
- 3) An actuator force requirement high enough to require a differential piston area that is practical to fabricate.

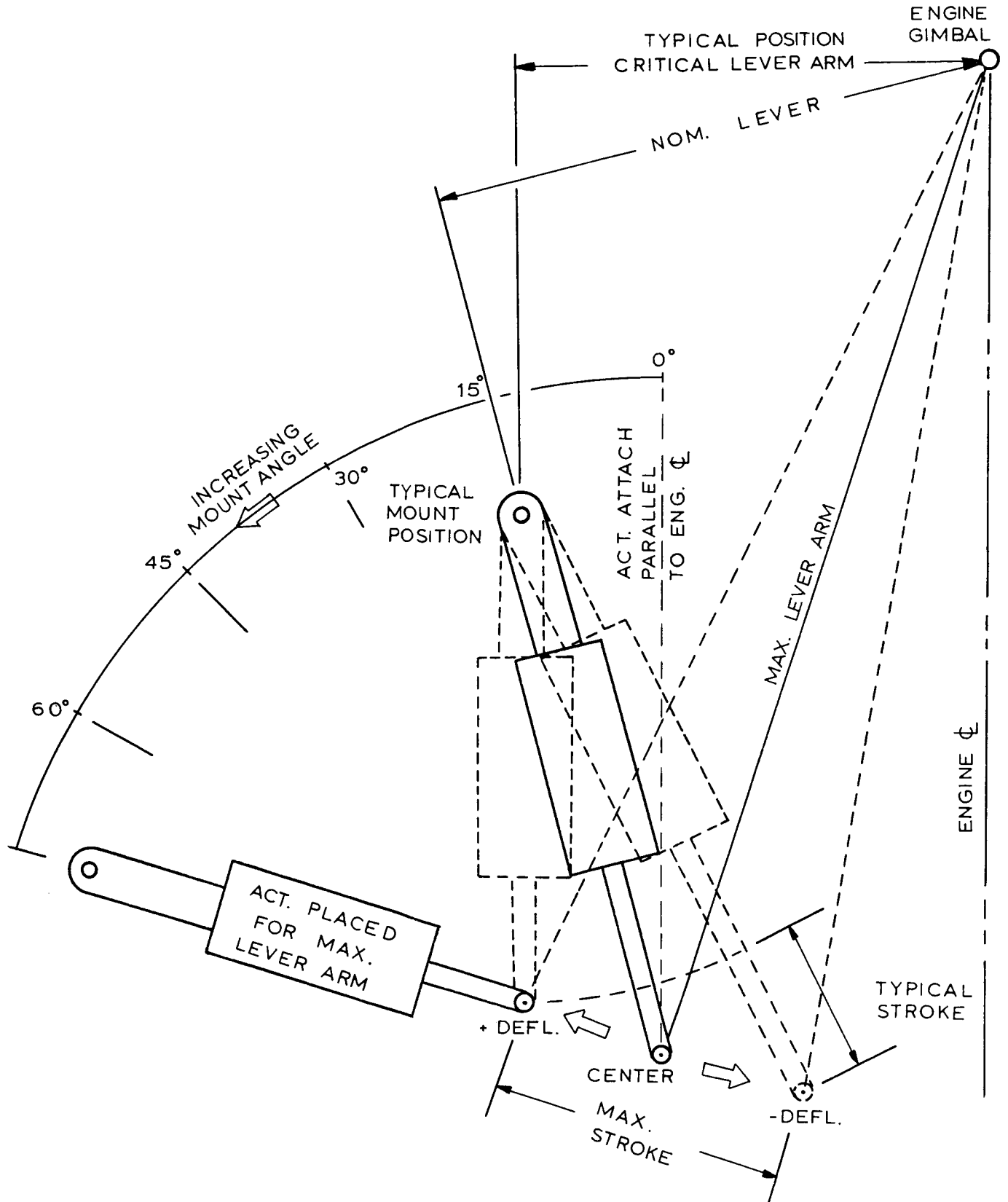


Figure 29: Actuator Position Selection

Angle Position of Actuator Centerline	Average Actuator Stroke	Piston Velocity	Lever Arm From Nominal Actuator Centerline	Actuator Force at Center Position	Critical Actuator Length*	Critical Lever Arm at Worst Deflection Position	Maximum Actuator Force
(degrees)	(inches)	(in/sec)	(inches)	(pounds)	(inches)	(inches)	(pounds)
0	2.5	3.5	9.1	430	10	0.07	55900
11.5	4.0	5.8	14.5	270	10	7.0	559
15	4.5	6.5	16.3	240	12	11.0	356
30	6.2	8.9	22.2	176	16	20.8	188
45	7.4	10.6	26.4	148	18	26.8	146
60	8.1	11.6	29.1	135	20	28.4	138
75	8.3	11.9	29.6	132	20	29.0	135
90	7.9	11.4	28.3	138	20	25.3	155

* Critical actuator length = 10 inches or 2.5 times stroke, whichever is greater.

Figure 30: ACTUATION REQUIREMENT VARIATION WITH ACTUATOR POSITION

4.1.3 SYSTEM ANALYSIS

The 4.0-inch actuator stroke resulting from the selection of the 11.5-degree mounting angle was used as the actuation design point for the test system. Use of this design point results in ± 0.90 inch at the frequency of 6.0 cps when a servosystem having a 3.0-cps break frequency is a design criterion. The use of 6 cps as a maximum frequency provides simulation of a minimum propulsion-engine deflection of ± 0.5 degree of motion. This deflection value is 6 percent of the required maximum engine travel and was determined to be adequate for the application. The 6-cps frequency is also the frequency beyond which the slope of the db-frequency curve is constant for a first-order servosystem designed with a 3-cps break frequency. For this frequency and all higher frequencies, the system requires maximum flow.

The maximum force requirement of 559 pounds for the selected task required a piston area of 0.279 square inch when using supply fluid at 3000 psig and a two-thirds pressure drop at the load and one-third pressure drop across the servovalve.

The original requirement for a 4000-psig system was modified to 3000 psig in the initial phases of the test program. This modification was allowed to simplify the design so that current-technology pressure vessels and support equipment could be used. In addition, pressures optimize at values considerably lower than 4000 psi for the majority of space applications because force requirements are small when aerodynamic loads are not encountered. Use of pressures above optimum under these conditions results in an impractical actuator design because extremely small piston areas are required. It is possible that pressures less than 3000 psig would be recommended for an optimized design.

It was determined that a problem might be encountered in duplicating the design load accurately at all temperatures during testing because of the variation in coefficient of friction between parts of the loading device with temperature and vacuum. Reference 11 describes work accomplished to understand friction in high vacuum. To ensure actuation performance at all temperatures, the force capability of the test actuator was increased to 780 pounds by using a piston area of 0.39 square inch. This increase in force capability provides a factor of 1.4 in the design.

The piston velocity of 6 inches per second, which accompanies the 4.0-inch stroke for the selected task, required fluid flow of 0.435 gallon per minute to satisfy the actuation task in the flight application. To explore the actuation frequency range of 0.5 to 6 cps during test system operation, fluid flow between 0.39 and 2.2 gpm is required using an actuator with a 0.39-square-inch piston area.

The system tested is a single-pass or blowdown system. Such a system for the lunar landing vehicle flight application requires a reservoir containing 3.48 gallons of fluid (average flow of 0.435 gallon per minute for 8.0-minute total intermittent operation). The volume of fluid used to explore the frequency range of 0.5 to 6.0 cycles per second using the 0.39-square-inch test actuator and 2.25-minute test run was determined as follows:

<u>Freq Range</u> <u>(cps)</u>	<u>Mean Freq</u> <u>(cps)</u>	<u>Percentage</u> <u>of Stroke</u>	<u>Avg Act.</u> <u>Stroke (in.)</u>	<u>Avg Flow</u> <u>(gpm)</u>	<u>Percentage</u> <u>of Duration</u>	<u>Volume of</u> <u>Fluid (gal.)</u>
0.5 to 1	0.75	92	±1.84	0.56	28	0.353
1 to 2	1.50	85	±1.70	1.03	28	0.652
2 to 4	3.00	71	±1.42	1.73	28	1.09
4 to 6	5.00	56	±1.12	2.27	16	<u>0.82</u> 2.915

Dry-run tests with the servoanalyzer and an electrical load simulation indicated that 2.25 minutes are adequate for the 0.5-cps to 6.0-cps frequency scan without exceeding the maximum speed allowable for functioning of the analyzer.

A design factor of 1.2 for ullage was applied to the above volume requirement to prevent complete blowdown of the system reservoir during an operational test. Figure 31 is a summary of design data for the practical alternates to developing a test system based on the rigid requirements of the selected application. The requirements for the selected application are shown in Column 1 with three alternatives in the remaining columns. Column 2 summarizes the design for an actuation system satisfying the selected application and using the oversize actuator. Column 3 contains data for a system using the application size actuator, but fluid volume sufficient only for the frequency scan test. Column 4 contains data for the system recommended for the test program. This system uses an oversize acutator and only sufficient volume for the frequency scan test.

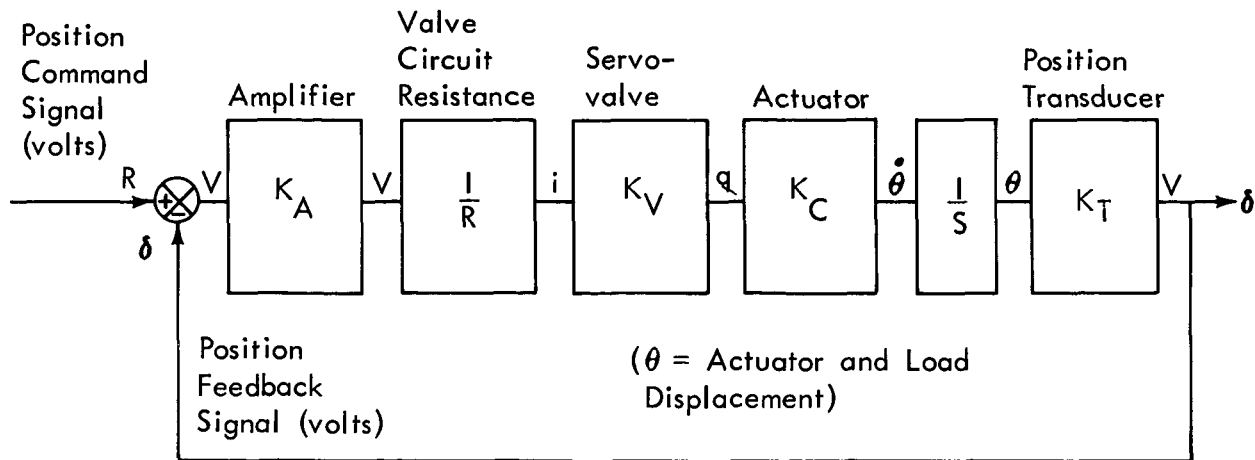
The RL-10 engine vectoring application described in Section 4.1.1 requires a 3.2-cps break frequency for the actuation system design. To satisfy this requirement in the test system, the hydraulic servoactuator was incorporated in a servocontrol loop with an operational amplifier and a position feedback transducer. This control loop was analyzed as a first-order system because the hydraulic system response tests were at low frequencies (6 cps maximum). The analysis approximation as a first-order system was used and proved satisfactory for previous testing reported in Reference 1. The block diagram below represents the analysis for a system break frequency of 3 cps; this frequency was used in the test system as a close approximation to the application requirement.

The closed-loop gain $\left(\frac{\delta}{R}\right) = \frac{1}{TS + 1}$ where $T = \frac{R}{K_A K_V K_C K_T}$.

Here $\frac{1}{T}$ is defined as the system break frequency = 3 cps = 18.8 rad/sec; therefore, the term $\frac{K_A K_V K_C K_T}{R} = 18.8 \text{ sec}^{-1}$.

Alternate	1	2	3	4
Requirement	Rigid Flight Application	Flight Application with Oversize Actuator	Frequency Scan with Application-Size Actuator	Frequency Scan with Oversize Actuator
Frequency Range (cps)	0.4 to 6.0	0.5 to 6.0	0.5 to 6.0	0.5 to 6.0
Act. Stroke at 0.5 cps (inches)	±2.00	±2.00	±2.00	±2.00
Act. Stroke at 6.0 cps (inches)	±0.90	±0.90	±0.90	±0.90
Servo Break Frequency (cps)	3.2	3.0	3.0	3.0
Actuator Force (pounds)	559	780	559	780
Act. Piston Area (square inches)	0.279	0.39	0.279	0.39
Maximum Flow Rate (gpm)	0.435	0.608	1.57	2.2
Operation Time per Test (min)	8.0	8.0	2.25	2.25
Fluid Volume per Test (gal.)	3.56	4.86	2.08	2.91

Figure 31: TEST SYSTEM DESIGN ALTERNATES



The gain factors for several of the elements are known: K_C , the reciprocal of the net actuation piston area, is equal to $1/0.39 = 2.56 \text{ in}^{-2}$; the servovalve circuit resistance (R) consists of the torque motor coil resistance of 420 ohms, with the coils connected in series at $+75^\circ\text{F}$, plus 1000 ohms in series with the coils to implement the recording of valve current; thus, 1420 ohms is the total circuit resistance (R).

The position transducer sensitivity (K_T) is 3.20 volts per inch. This value was based on the wattage rating of the transducer and the operational requirements of the frequency response analyzer because the position signal was used in the analyzer circuit as well as in the system servoloop. In consideration of the actuator stroke used, the position transducer sensitivity was selected so that the analyzer did not require a change of decibel range during a system operational test between 0.5 and 6 cps because of attenuation of the position signal. Because the transducer was to be used in vacuum testing, an extra factor on the wattage rating was applied because convective cooling would not be available.

The three servovalves selected for use in the test program had no-load flow gains of 8 gpm at 10 ma or 3.08 cubic inches per second per milliampere, measured using MIL-H-5606A fluid at 3000 psi. The following equation was used to determine the flow gain of these valves using the higher-density E-3 fluid and assuming a constant actuator differential pressure of 1400 psi caused by the inertia and friction load.

Flow gain = $K_V = K \sqrt{\Delta P/\rho}$, where K is a valve constant assumed not to change with the change in fluid.

$$K_V (\text{E-3}) = K_V (5606) \sqrt{\frac{\Delta P/\rho (\text{E-3})}{\Delta P/\rho (5606)}} = 1.56 \text{ cu in./sec/ma}$$

The above analysis showed that the servovalve no-load flow with E-3 fluid would be half that with MIL-H-5606A, which was adequate for the 2.2-gpm test requirement.

The operational amplifier gain was calculated, using the gains discussed above, as follows:

$$K_A = \frac{18.8 R}{K_V K_C K_T} = 2.08 \text{ volts/volt.}$$

4.2 SYSTEM DESIGN

Special considerations were required in the design of a hydraulic breadboard system for operational evaluation in space environments. The design had to provide access to equipment that might require servicing. The primary design considerations were minimizing fluid leakage from dynamic seals, eliminating leakage from all static seals and couplings, providing methods to easily obtain measurements of operational performance, and providing a system having the best potential for incorporation of improvements.

4.2.1 SINGLE-PASS-SYSTEM DESCRIPTION

A basic schematic diagram of the single-pass hydraulic system used in the test program is shown in Figure 32. The spherical reservoir contained the E-3 hydraulic fluid during exposure of the system to test environments. System operational sequences were initiated by pressurizing the fluid in the reservoir using 6000-psig bottled nitrogen regulated to 3000 psig. A nominal 10-micron-rated micron filter was placed downstream of the reservoir to protect the servovalve orifices from contamination.

Fluid flowed through the actuator in response to servovalve commands to move the inertia and friction load that simulated the operational requirements for gimbaling an RL-10 propulsion engine on a lunar landing vehicle. All this equipment was in the test chamber that maintained environmental control of the actuation equipment. The actuator, reservoir, and servovalve designs are discussed separately in Sections 4.2.2, 4.2.3, and 4.2.4.

The single-pass system in the flight application has no provisions for capture of the fluid after it passes through the actuation system. The test system must have such provisions because the fluid must be reused in many consecutive blowdown tests. Hydraulic equipment to capture the fluid and return it to the test system high-pressure reservoir was in a hydraulic cart outside the test chamber (refer to Figures 32 and 33). The various manual valves shown provide versatility in the cart for use during fill, run, and emergency dump operations. The valves most important to system operation were Valve A, which controls high-pressure nitrogen to the test system reservoir, and Valve C, which was used during refilling of the test reservoir. Further details of the use of the hydraulic cart are discussed in Section 5.1.2.

4.2.2 ACTUATOR DESIGN

The hydraulic test system actuator was designed to satisfy the load requirements established in Section 4.1. The major parts of the actuator were the housing, piston, and two

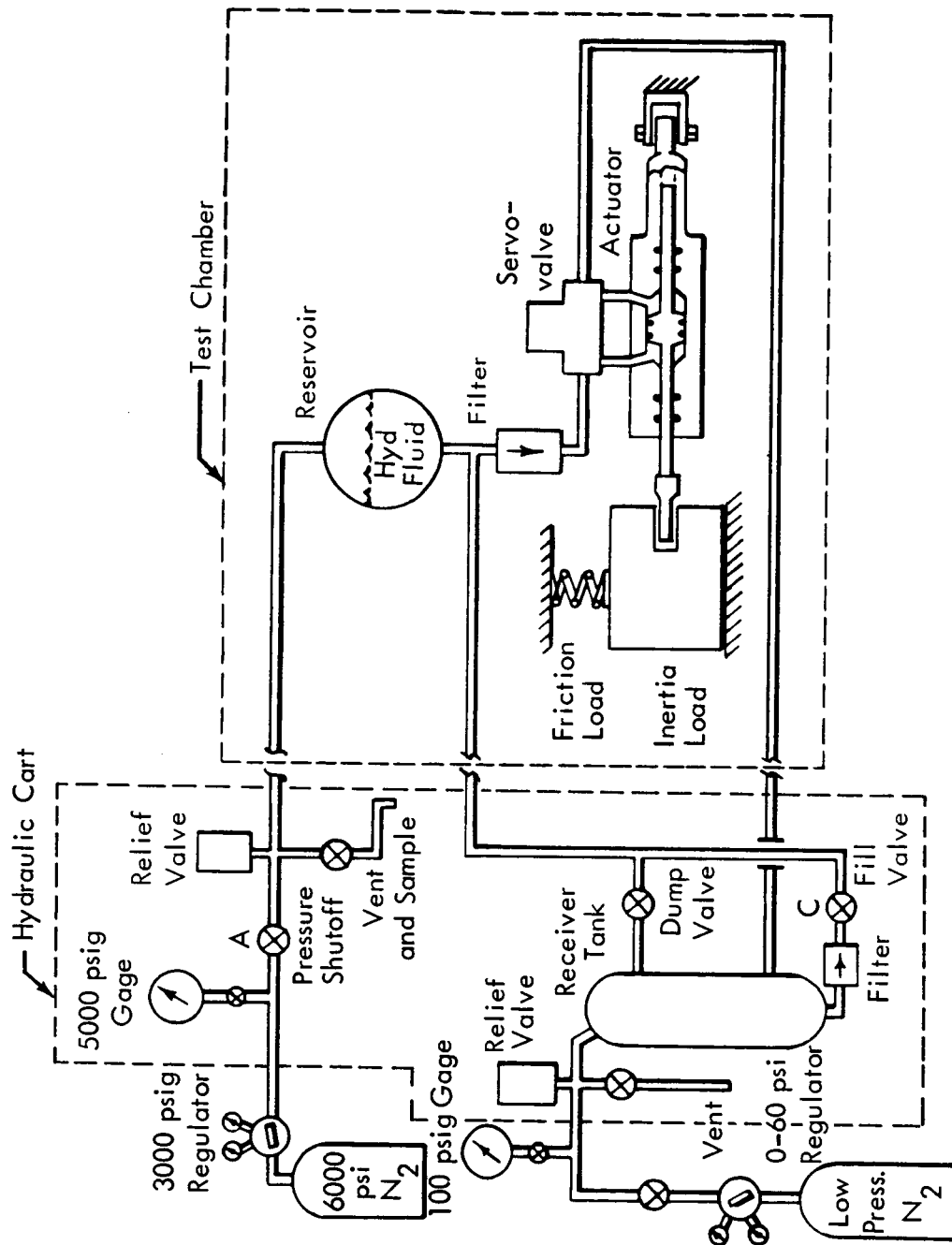


Figure 32: Basic Test-System Schematic

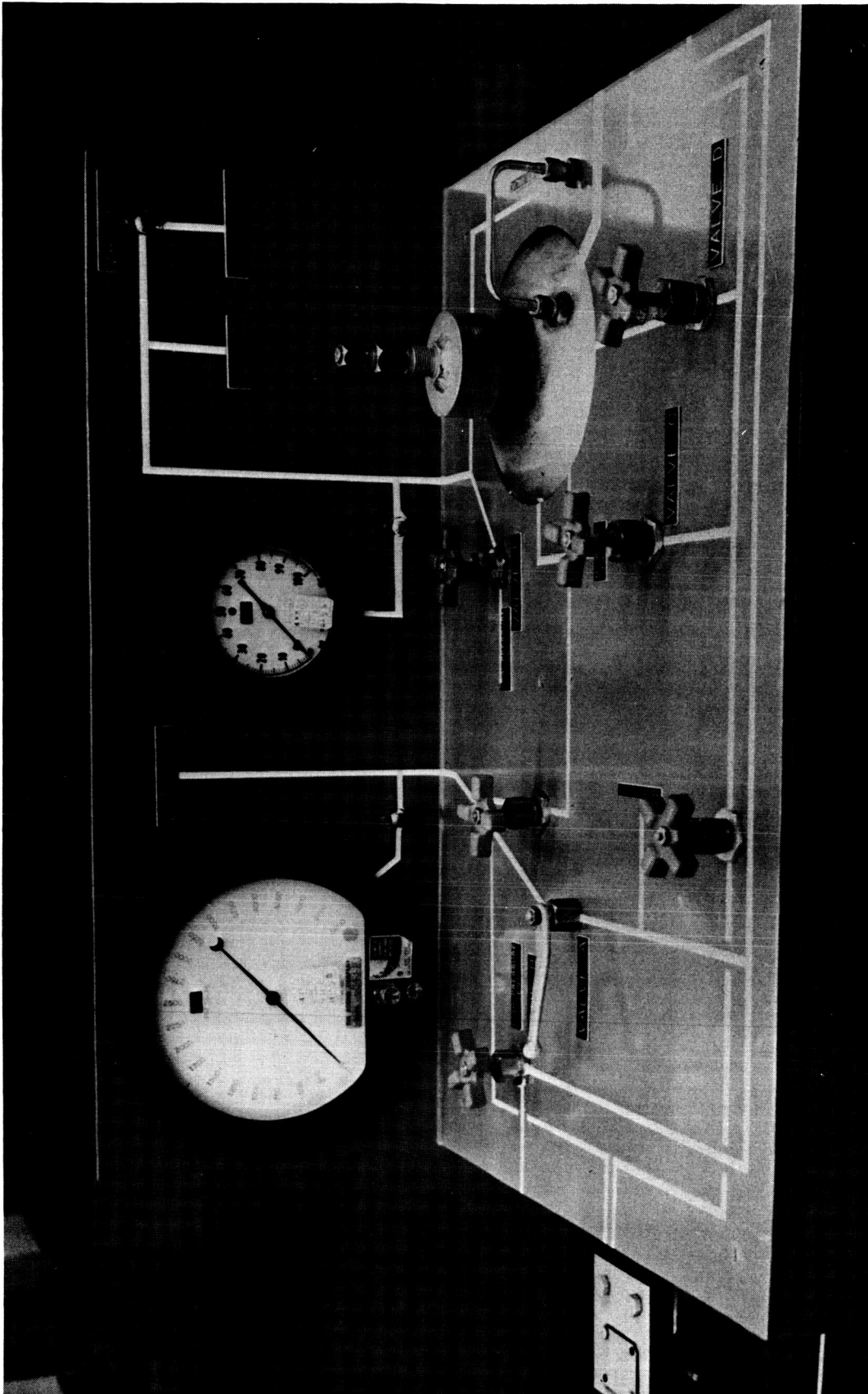


Figure 33: Hydraulic Cart

seal glands shown in a disassembled layout in Figure 34. In addition to these parts, the complete actuator incorporated an adjustable rod end bearing and a head end cap with bearing. These parts provided the means for attaching the actuator to the inertia load and the load fixture structure. All parts of the actuator were machined from 304LC stainless steel in accordance with the material selection reported in Section 3.2.1. The assembly drawing for the actuator is Reference 12.

An important feature of the actuator was the removable seal gland that provided easy seal configuration changes. A second design feature was the use of redundant seal installations on the piston and in the seal glands. Grooves for two seal configurations were placed on the piston to provide additional sealing if the single elastomeric O-ring allowed an undesirable amount of leakage. Dynamic primary and backup rod seal grooves were provided for the same reason and to implement measurement of leakage passing the primary seal.

4.2.2.1 Housing

The actuator housing was made from 304LC stainless steel bar with the grain parallel to actuator motion. The cylinder bore was plated with a nominal 0.014-inch thickness of electroless nickel deposition of 0.005 to 0.007 inch in a single plate. Four control ports were provided at the interface between the housing and the servovalve to be attached. Ports 1 and 2, passing to opposite sides of the piston, were tapped for pressure measurements. Transducers were installed directly at the connections on the housing. System pressure and return ports were located in the housing to provide the shortest path between the ports and the servovalve.

4.2.2.2 Piston

The actuator piston and rod were made to provide equal piston area exposure to supply pressure for both directions of piston motion. The rod diameter was nominally 0.867 inch for adequate stiffness under the loading conditions of the application. The piston was nominally 1.106 inches in diameter. Chrome plating was added to provide an additional 0.006 inch on the diameter for both the piston and rod. The exposed end of the rod was threaded to accommodate the adjustable rod end; the adjustment was used to center the actuator with the center of the position-measuring transducer. The exposed end of the piston rod was also machined for attaching a bellows assembly to be used only if exposure to vacuum environment produced effects requiring isolation of dynamic gland seals. The opposite end of the rod was manufactured with wrench flats to be used when tightening the rod end.

Three seal grooves were machined on the piston. The center groove was for installation of an elastomeric O-ring with a nominal squeeze of 20 percent. The squeeze was designed higher than the normal 8 to 13 percent used in groove dimension recommended by seal suppliers to compensate for the expected dimensional changes at the extreme low temperatures. The two outside seal grooves were machined for "omniseal" installations, as discussed in Section 3.1.4. These grooves were only to be used if the elastomeric seal squeeze was insufficient to prevent leakage across the piston at low temperature.

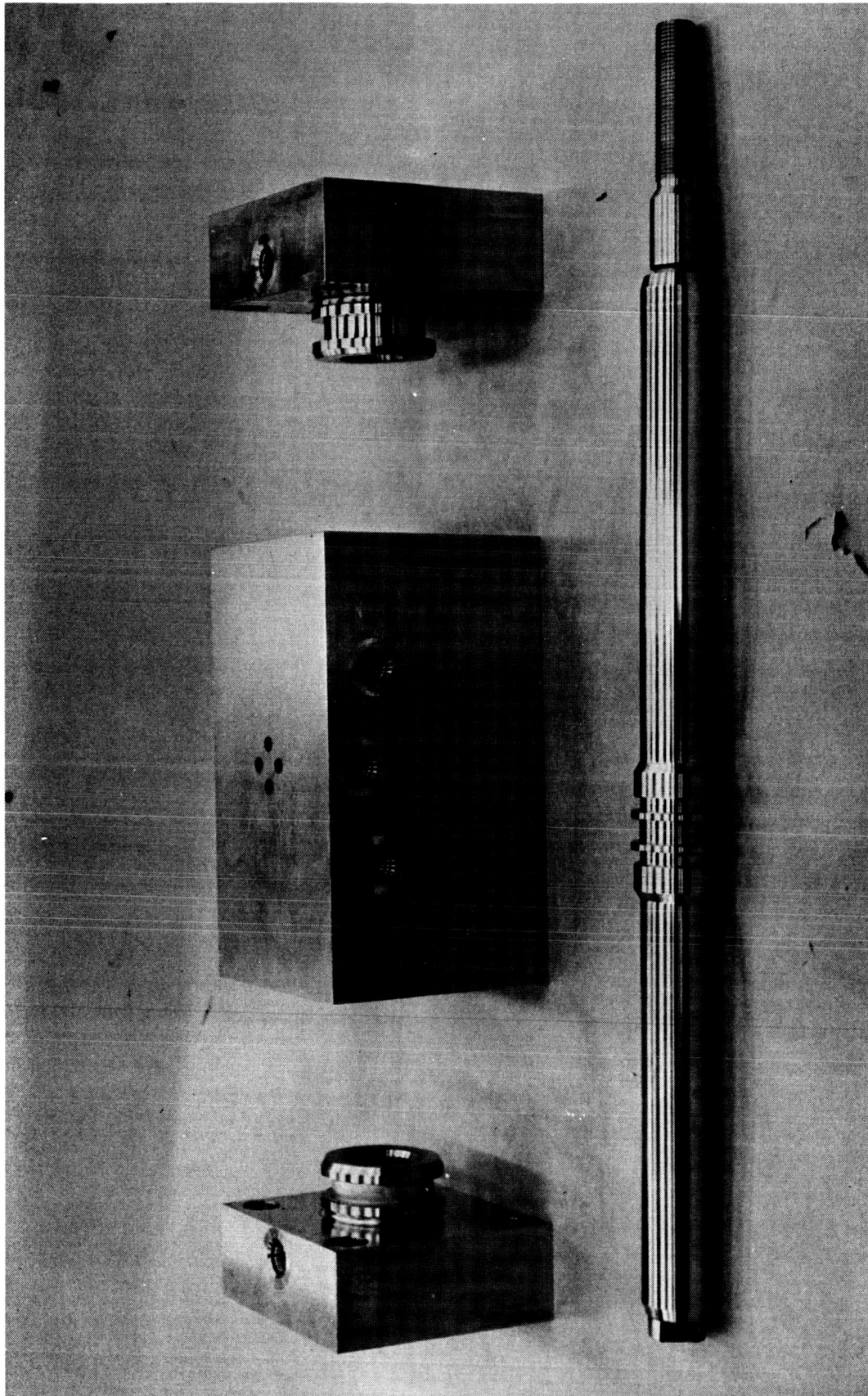


Figure 34: Test Actuator Parts

Installation of the "omniseals" required stretching of the seals by sliding over the 30-degree ramp between the rod and the piston shown in Figure 34. In 24 hours, the "omniseals" recovered almost all of the dimensional change caused by stretching. The seal manufacturer recommended a 15-degree ramp, but this shallow a slope was difficult to incorporate in an actuator design. Care was required, even with the 30-degree slope, not to damage the piston stop. To prevent such damage, the full stop-to-stop stroke of 4.0 inches was not used during operational tests.

4.2.2.3 Glands

Each seal gland was manufactured with two external static seal grooves and three internal dynamic seal grooves. A single static elastomeric seal was incorporated to seal each gland to the housing with a redundant metal seal as a backup for the elastomeric installation. The three dynamic seals were provided in a similar arrangement to those on the piston with the cavity between the center elastomeric seal and the outside "omniseal" vented to a leakage measurement port. The inside "omniseal" was to be used only if leakage past the elastomeric seal was considered objectionable.

The elastomeric seal grooves were designed with a nominal 20-percent squeeze in all installations. The metallic seal was an Aerospace Component Corporation product with a modified U-shaped cross section. The seal was made of Inconel X with soft nickel plating that would deform to the roughness of the sealing faces.

The installation of the "omniseal" in the internal grooves in the gland required deformation of the teflon during installation. After partial installation, the deformation could be worked out by applying finger pressure. An installation tool resembling the end of the piston rod was also used to help reform the seal to its original shape.

Each gland was attached to the housing with four bolts that could be removed easily for actuator internal inspection or gland interchange. These four bolts at the head end of the actuator were also used to attach the end cap to the assembly.

4.2.2.4 Attachment Ends

The rod end and head end cap were used primarily as bearing retainers through which the attachment of the actuator to the inertia load and stationary structure was made. The bearings were Shafer spherical, self-aligning, teflon-lined bearings capable of operation at low temperature. The rod end, in addition to being a bearing retainer, was adjustable on the piston rod to center the actuator with the position transducer.

4.2.2.5 Plating

Difficulty was encountered in obtaining acceptable plating on the actuator parts. Pitting and chipping as shown in Figures 35 and 36 were evidenced as plating problems. Most problems were attributed to lack of proper cleaning. Replating of some parts was required to obtain tolerances in the plating that were acceptable. With improved cleaning methods and more experience in plating stainless steel, these problems should not occur.

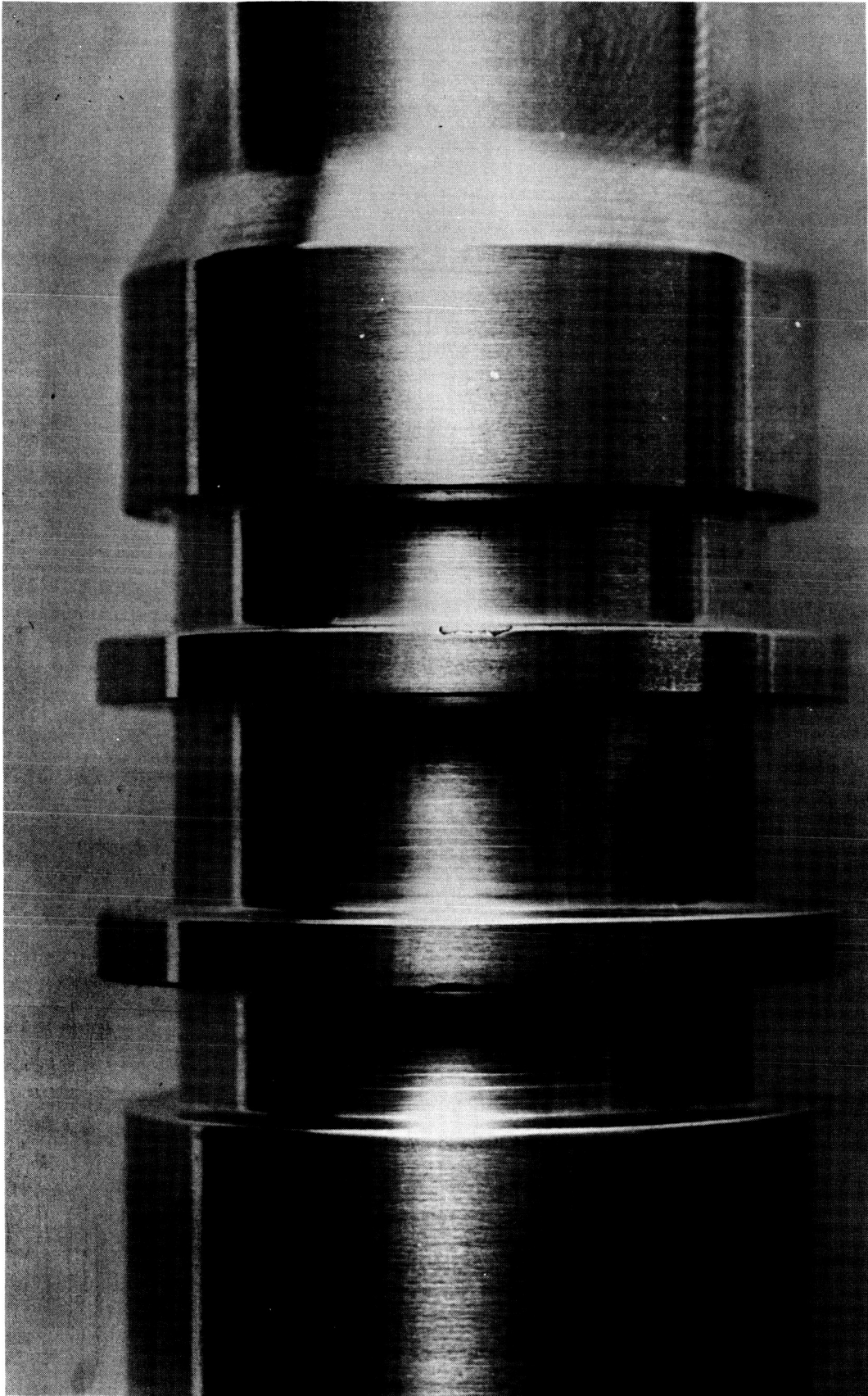


Figure 35: Chipped Plating Example



Figure 36: Pitted Plating Example

4.2.3 RESERVOIR

The design requirements for the high-pressure reservoir were based on the ASME pressure vessel code of Reference 13. These requirements were forwarded to potential suppliers in the form of a procurement specification. The more important requirements are shown below.

The hydraulic reservoir external pressures vary between 10^{-8} torr and 14.7 psia and internal and external storage temperatures between -300°F and 275°F . The high-pressure operational temperature is between -155°F and 275°F . Internal design pressures are 3000 psig (working), 6000 psig (proof), and 12,000 psig (burst). The reservoir is either cylindrical or spherical in shape with a volume of 850 ± 50 cubic inches. If a cylindrical shape is recommended, the inside diameter is 8.0 inches or greater. No weight limit is specified for the reservoir; however, sound design practices shall be followed. The reservoir is equipped with two male flared-tube connections, per MS 33656G4, welded on directly opposing surfaces of the vessel.

The vessel to the above specification, supplied by Airtek Dynamics Incorporated, was a modified helium storage bottle for the S-IVB propulsion stage. The vessel was spherical and made of titanium 6Al-4V with a nominal thickness of 0.318 inch. An analysis was made to determine the adequacy of the titanium 6Al-4V for the high-pressure reservoir. The minimum requirements for strength of this material are 170 ksi ultimate and 150 ksi yield. At a 12,000-psig burst pressure, the typical uniform stress given by PR/2t was 148 ksi, indicating a satisfactory choice of material.

4.2.4 SERVOVALVES

The three servovalves used in this program were modified Moog Series-32 valves. These valves, modified for use at temperatures below -65°F , were used because new valves for this temperature range could not be supplied in time to meet the contract schedule.

The modification consisted of changing seals as shown in the following table.

O-Ring Location	Qty per Valve	O-Ring Size (in.)	Original (Moog) O-Ring	New (Parker) O-Ring
Spool stop	2	ID 0.114 ± 0.005 CS 0.070 ± 0.003	080-04273-2	2-6-S424-7
Filter plug	2	ID 0.114 ± 0.005 CS 0.070 ± 0.003	080-04273-2	2-6-S424-7
Bushing	2	ID 0.489 ± 0.005 CS 0.070 ± 0.003	080-04273-4	2-14-S424-7
Connector	1	ID 0.489 ± 0.005 CS 0.070 ± 0.003	080-04273-4	2-14-S424-7
Interface	4	ID 0.301 ± 0.005 CS 0.070 ± 0.003	080-04273-12	2-11-S424-7
Motor Cap	1	ID 1.365 ± 0.006 CS 0.040 ± 0.002	080-04273-44	---
Flexure sleeve	1	ID 0.180 ± 0.005 CS 0.040 ± 0.002	080-04273-51	---

The new seals were made from Parker S-424-7 compound which was compatible with DuPont E-3 fluid and provided adequate performance at low temperatures. Because the motor-cap and flexure-sleeve seals were not available in Parker sizes, special substitutions were made for these applications. The motor-cap seal was especially molded and another Parker seal that was not identical in dimensions but was within tolerances for the flexure-sleeve seal, was used.

Valve characteristics prior to the above seal changes are shown in the following table.

<u>Model</u>	<u>Serial No.</u>	<u>Flow (gpm)</u>	<u>Null</u>	<u>Hysteresis/Null</u>	<u>Remarks</u>
32-103	3	8.3 - 8.7	0.3 ma	0.1 ma	Use in vacuum storage assembly
32-103A	4	7.2 - 7.7	0.2 ma	0.5 ma off center	Use as backup valve
32-103A	5	7.5	0.06 ma	0.12 ma	Use in operational test assembly

Following the seal changes, the valves were recentered using the E-3 blowdown system and the pressure-gain characteristic was determined for each valve as a measure of the accuracy of adjusting the valve during reassembly. Flow-gain characteristics were not determined due to the limited fluid capacity of the E-3 blowdown system.

The modified valves required an adapter between the valve and actuator housing. Four additional interface seals were required with the adapter. Seal squeeze between the valve and adapter was controlled by the groove dimensions in the valve. The minimum 20-percent squeeze on the seals between the adapter and housing was controlled by the adapter dimensions.

4.3 TEST FACILITY EQUIPMENT

The test facility included equipment necessary to maintain test environments or apply simulated loading.

4.3.1 VACUUM CONTAINER

The requirement to store a hydraulic servoactuator in a hard-vacuum environment for 5 months and, subsequently, operate it as part of a system without removing the vacuum environment imposed special conditions for the storage container. A cutaway sketch of the container designed for this application is shown in Figure 37. The container was an 8-inch-diameter cylinder with one sealed end and long enough to contain the test servoactuator in the retracted position. A 6-inch-diameter vacuum-pump outlet port with a connecting flange was centrally positioned on the cylinder with the flange facing downward. Other container penetrations included two 0.25-inch hydraulic fittings welded in place, two (redundant) vacuum-gage connections, and an electrical connector for servovalve control wiring.

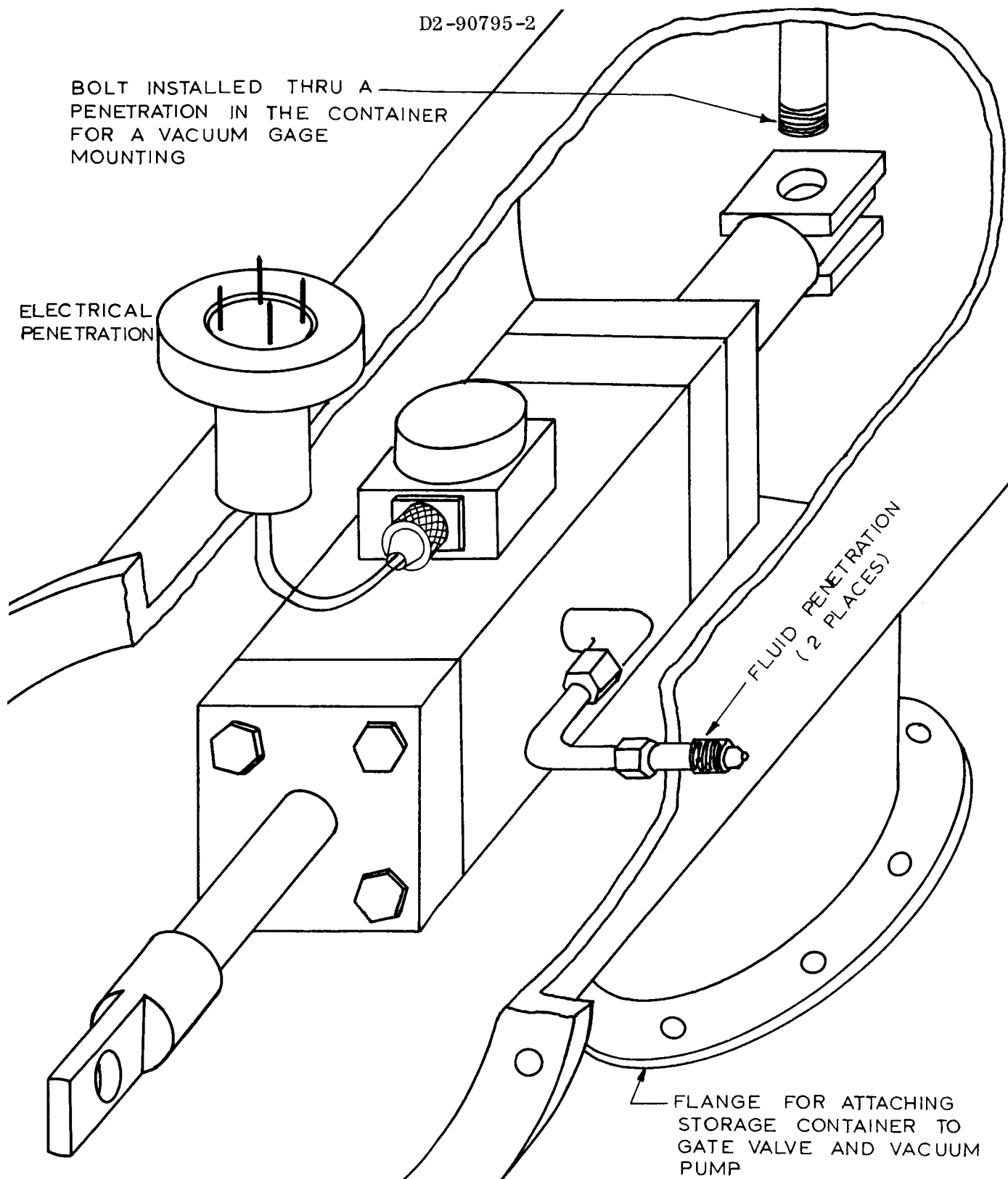


Figure 37: Actuator Installation In Vacuum Container

The removable end of the container was sealed by an 11-inch-diameter O-ring and held in place by 12 bolts. A clevis was welded internally at the sealed end of the container to accept the actuator-head end connection. The bolt that holds the actuator in the clevis was installed through one of the penetrations for a vacuum-gage, prior to gage installation. The clevis for the actuator rod end was welded to the inside of the removable lid of the container. External clevises on the container were spaced to match attachment points on the load apparatus discussed in the next section.

This container design enabled easy installation at a storage station and allowed tests for long periods at hard vacuum to be conducted without need for a large vacuum pumping facility. With a gate valve installed at the pump attachment flange, the container could be sealed at hard vacuum, transferred to a major test facility, and installed in the test-system load apparatus. All necessary servoactuator connections could be made without breaking the vacuum seal. After pressurizing the servoactuator to maintain a retracted position, the flange bolts could be removed and the major facility pumped down to hard vacuum. Subsequent operation of the system could be performed in hard vacuum, and the removable end of the container would move with the inertia load during operation.

4.3.2 LOAD APPARATUS

The actuation requirements in Section 4.1.2 for simulation during the testing portion of the contract included a hinge moment of 3915 inch-pounds and a minimum lever arm of 7 inches. Using these requirements, a maximum actuator load of 560 pounds was determined. The component parts of the hinge moment and the actuator load established by that part of the hinge moment are shown below.

<u>Hinge Moment Component</u>	<u>Torque (in.-lb)</u>	<u>Load (lb)</u>
Longitudinal acceleration	1260	180
Coriolis damping	120	17
Rotational inertia	135	19
Gimbal friction	2400	<u>344</u>
	Total	560

The rotational inertia load was represented during the test by the inertia of a sliding block. The weight required for this block was calculated as $W = Fg/a$ where a , the load acceleration was taken from the requirements of the actuation task and was 250 degrees per second per second. Since 4 inches of actuator movement was equivalent to 16 degrees of propulsion-engine deflection, the acceleration was expressed as 63 inches per second per second and

$$W = (19) (386.5)/63 = 117 \text{ pounds.}$$

The length of the sliding block was limited to 12 inches (including the clevis) for actuator attachment. This restriction was determined by the in-line equipment lengths placed in the load apparatus and the available length for test-chamber installation. A 6- by 6- by

12-inch mild-steel block, with approximately 19 cubic inches removed for a slot through which the actuator rod end was inserted, weighs 116.5 pounds, which was considered satisfactory for the 117-pound requirement.

The remainder of the application load, 541 pounds, was simulated with a friction loading device. For a constant load to be provided to the actuator, the static and sliding friction of the contacting materials of the friction device should be equivalent. This friction condition was obtained by using mild steel on lead. This material combination provided a friction factor of 0.95 (see Reference 14) resulting in a friction load requirement of $541/0.95 = 569$ pounds. The friction load was applied to the sides of the mild-steel inertia load by the spring-loaded mechanism shown in Figure 38. A single spring directly loaded one of two lead pads against the inertia load. A second pad was rigidly installed on the opposite side of the load in line with the spring. The pad alignment was maintained by a supporting structure of corrosion-resistant steel. Tie bolts across the structure at the top and bottom of the inertia load were provided as an extra precaution to keep the structure from spreading.

The spring that provided the friction load was made from 0.3625-inch-diameter, 302 corrosion-resistant steel wire. The spring had 12 active coils, a free length of 6.5 inches, and a deflection of 1.0 inch per 285 pounds of load. The load at solid height was 406 pounds with an accompanying stress of 51,475 psi. The spring was compressed by tightening the nuts on two 3/8-16NC threaded rods. Evenness of the tightening was checked with a torque wrench.

A test analysis was conducted to determine the repeatability and retention of a load condition within the test temperature range. The analysis showed that loading was not repeatable from test to test due to thermal effects on the different materials in the load apparatus. A load calibration was required just before use of the test system in an operational sequence test. A motor-driven gearbox mechanism was added to provide remote turning of the load adjusting nuts. This remote adjustment was necessary because manual adjustment was not possible at extreme low temperatures or at hard vacuum. Resistance heating coils around this adjustment motor were required for use at temperatures below -65°F . Similarly, the grease in the gearbox was replaced with dry lubricant for low-temperature operation.

Structural members provided both support for the inertia load block and an attachment point for the friction spring-loading mechanism. This structure was in the shape of a modified U-section. The inertia load translated within the U, but was offset from direct contact with the structure by teflon guides that offer insignificant resistance to motion. Holes in the sides of the U-section allowed the lead pads to protrude and contact the load-block surfaces.

Extensions from the structural members held the servoactuator in correct alignment with the inertia load and carried the weight of the reservoir and filter in the operational test system. Only the sides of the U section were extended. The space between the U-section and the extended sides was wider than at the inertia-load support section so that the vacuum container could be installed for operational testing of the vacuum-stored servo-actuator.

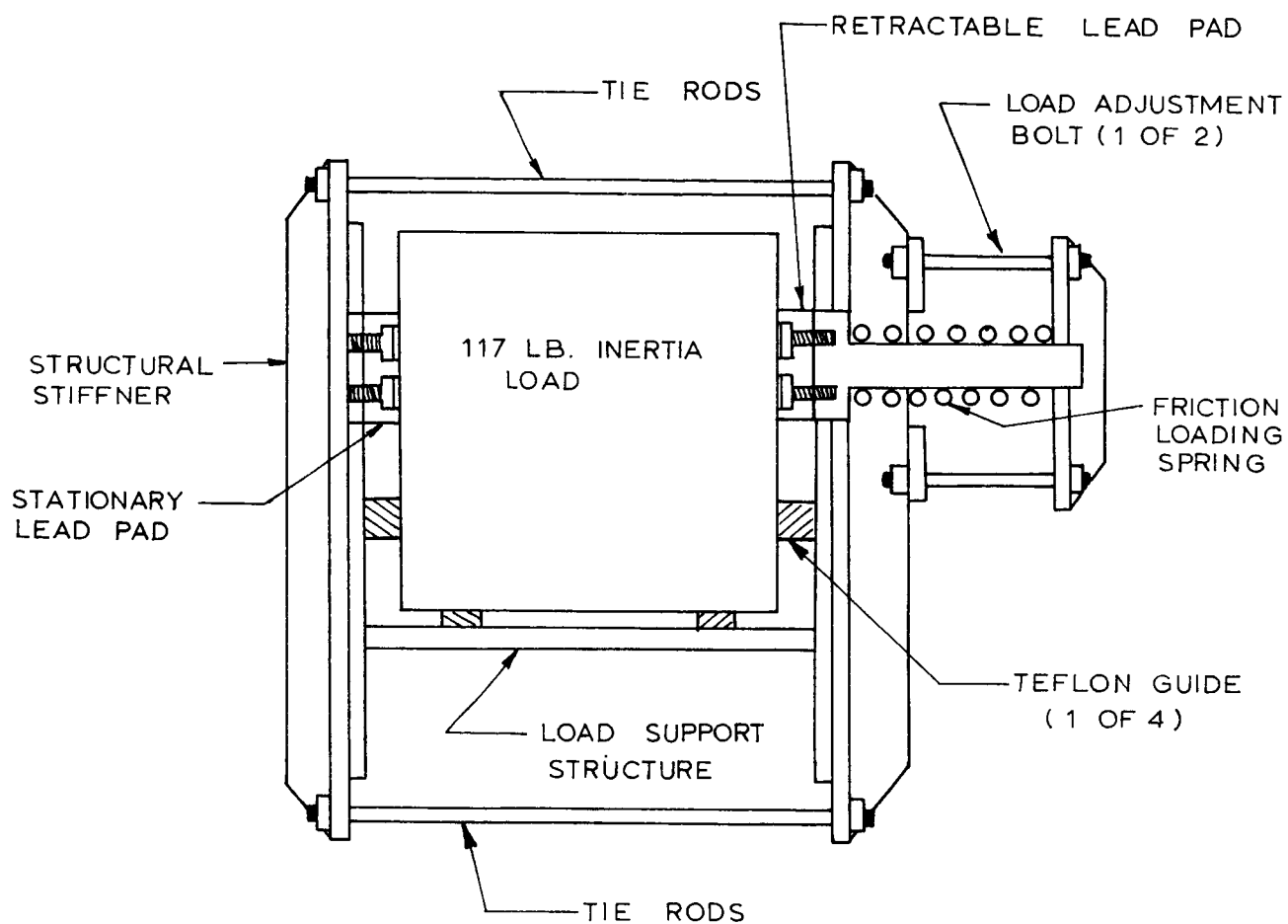


Figure 38: Loading Device Cross Section

The load-structure ends were provided with fittings for attachment of the entire structure in the test chambers. These attachments made the installation rigid during operational testing (see Figure 39).

4.3.3 COOLING CONTAINER

Low-temperature soaks required throughout the program were accomplished by using liquid nitrogen to cool the test system. A cooling container isolated the test system and load apparatus within the temperature environment controlled by the container. The container was particularly important when a hard vacuum environment, in addition to low temperature, was desired, and radiation was the only means of thermal control. The copper cold plates that formed the walls of the container (shown in Figure 39) enclosed the test system and load apparatus and fit in the test chambers. The front and part of the bottom of the container were removable as a single piece to provide access to the test-system components and load apparatus. Coiled copper tubing (0.5-inch diameter) was soldered to the external surfaces of the container so that 4 to 6 inches of spacing was provided between adjacent passes of tubing. The tubing was designated in relation to four zones, each being capable of individual control. Zone 1 was the removable section of the box, Zone 2 was the left side and left one-half of the back and top, Zone 3 was the right side and right one-half of the back and top, and Zone 4 was the bottom of the container. Liquid-nitrogen inlet connections were at the bottom of Zone 1, top of Zones 2 and 3, and front of Zone 4 (Figure 39).

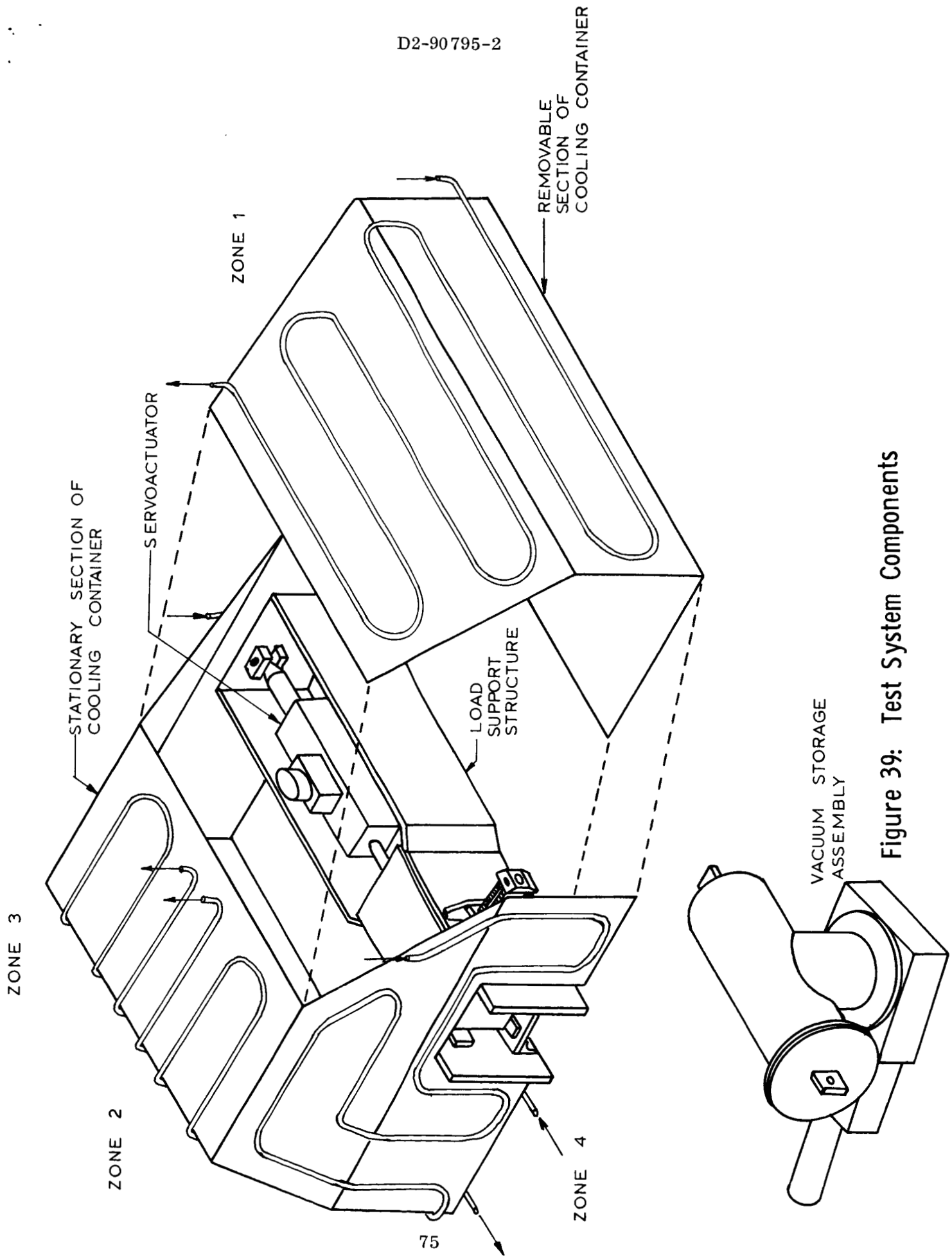


Figure 39: Test System Components

5.0 TEST PROGRAM

The purpose of performing a space-oriented test program for hydraulic system evaluation was to establish the suitability of hydraulics for operation in low-temperature and vacuum environments to be encountered in space. The pioneering effort of the test program was also a means of determining the need for or extent of the future development to provide flight-quality hydraulic actuation systems. Secondary objectives of the program were to investigate the ability of a system to be used at the high temperatures encountered in space and to withstand nonoperational thermal cycling between high and low temperatures.

5.1 TEST PLAN

The chronology of testing done during the program is shown in Figure 40, which outlines the basic tests, test environment, test duration, and system operational sequences performed during the tests. Each of these tests is described with the results of testing in Sections 5.2 through 5.5.

5.1.1 DATA ACQUISITION

Basic instrumentation was common for all of the tests performed and was used either to control the operation of the test system or to measure the operational characteristics or environment of the test system.

Control of the test system was provided through the circuitry associated with the servo-loop operational amplifier and the frequency-response analyzer. The amplifier (discussed in Section 4.1.3) established the gain for the system. Thus, the amplifier provided the command input to the test system when combined with the sinusoidal signal generated by the analyzer, the load position feedback signal indicating actuator position, and a dither signal for improved servovalve performance.

In addition to supplying a portion of the command signal, the frequency-response analyzer was the primary instrument used to measure system response. The command signal and the load position signal were connected to the e_1 and e_2 terminals of the Industrial Measurements Corporation Model 100 frequency-response analyzer, which computed the amplitude ratio and phase angle between the two signals. The analyzer displayed the compared signals by meter readouts of input frequency in cps, amplitude ratio in decibels, and phase angle in degrees. The analyzer also provided analog voltages for remote recording of log frequency, decibels, and phase angle. The advantage of remote recording was utilized to obtain X-Y plots of closed-loop system response data for each operational sequence.

The analyzer was connected to the actuation system through the test selector switch, so that when the actuation system is not being operated the analyzer can be switched to an R-C test circuit. This is desirable because the analyzer requires sinusoidal signals at the e_1 and e_2 terminals at all times when it is energized. The test circuit,

Test	Temperature Environment (°F)	Pressure Environment	Test Duration	Actuation Duration (minutes)	Number Test Runs	Fluid Pressure (psi)	Actuation Frequency (cps)	Fluid Temperature (°F)
<u>Low-Temp Perf</u> Servoactuator perf	75 to minimum fluid temp	Atm	2.5 min	2.5	10	3000	0.5-6	75 to minimum operable
<u>Hard-Vacuum Effects</u> Storage	75	Less than 10^{-6} torr	5 mo. max	None	1	20-0	---	75
Servoactuator perf	75	Less than 10^{-6} torr	2.5 min	2.5	1	3000	0.5-6	75
<u>Combined Environ Perf</u> Simulated flight	Min fluid operation	Near 10^{-8} Torr	6 days	2 @ 2.5	1	10 Store 3000 act.	0.5-6	Minimum operable
High-temp test	275	Atm	2.5 min	2.5	1	3000	0.5-6	275
<u>Thermal Cycling</u>	-240 to 275	Atm	100 hrs	None	1	10	---	-240 to 275

Figure 40: Test Program Outline

which has a 3-cps break frequency, is used to calibrate the X-Y recorders — these recorders being adjusted to the amplitude ratio and phase angle indicated on the analyzer readout meters.

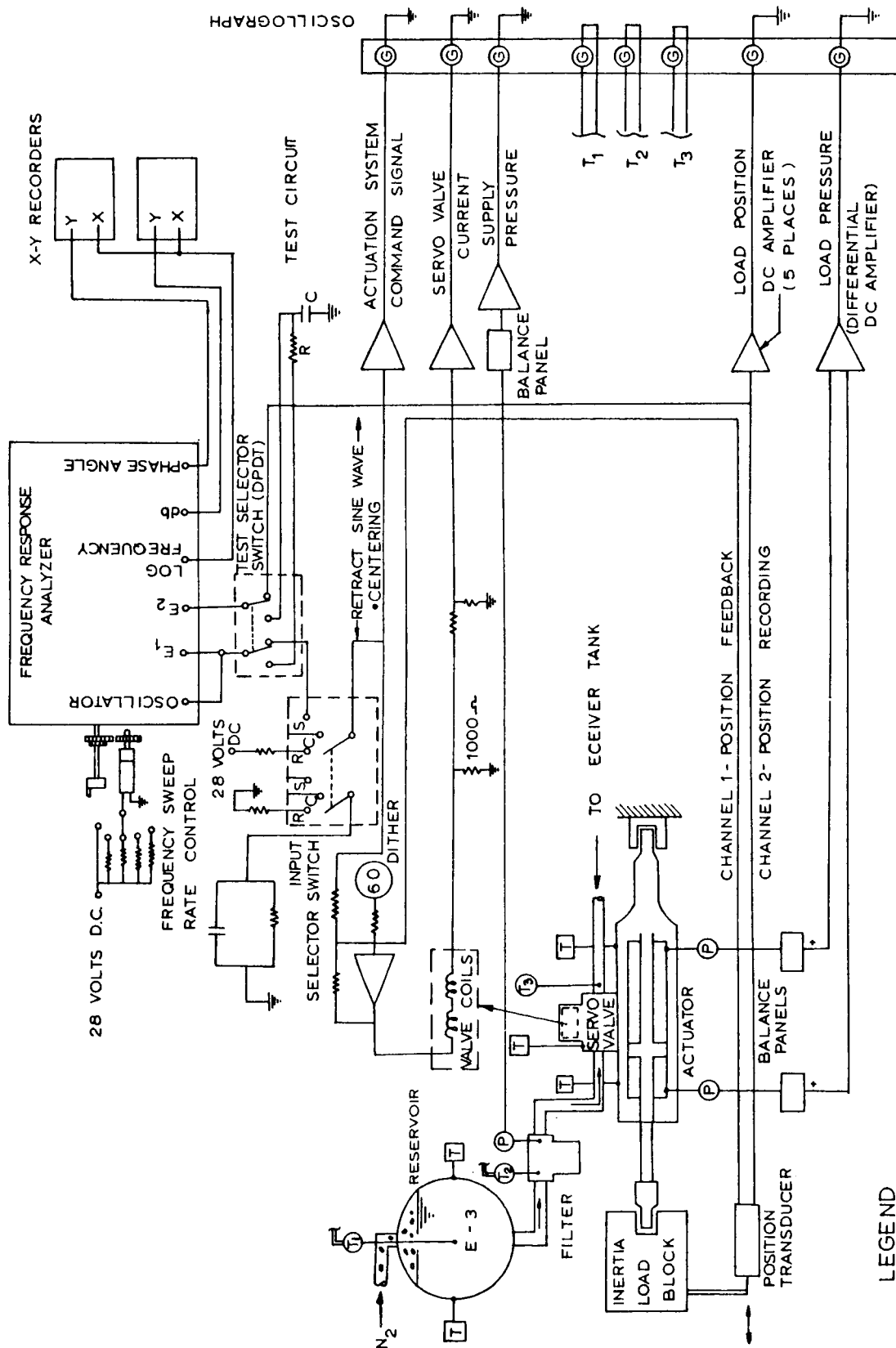
The frequency control on the analyzer was driven by an electric motor and a gear train to provide a frequency sweep during system response tests. Because large time constants in the analyzer circuits exist at low frequencies, a single-speed continuous frequency sweep results in errors in the analyzer output. These errors increase in proportion to the sweep rate. Because system test run time was limited to less than 3 minutes by the design capacity of the hydraulic reservoir, the speed of the motorized drive was adjusted to sweep the frequency from 0.5 to 6 cps in approximately 2.75 minutes, with the speed of the drive varied by switching various resistances in series with the direct-current motor during the sweep to compensate for nonlinearities in the analyzer frequency control. The 3-cps test circuit was used to determine the optimum sweep rates at various frequencies that would minimize the error in the analyzer data. The sweep rate control adapted kept errors within 0.2 db in amplitude ratio and 2 degrees in phase lag.

Since the hydraulic actuator loop was designed with a break frequency of 3 cps, a maximum test frequency of 6 cps was considered sufficient. At 6 cps the slope of the amplitude ratio curve became constant at 6 db per octave for all higher frequencies. The fluid-flow rate also reached a maximum at 6 cps and remained constant at higher frequencies. Testing beyond 6 cps would not provide data for system operational characteristics different than those obtained at 6 cps.

An oscillograph was used as a backup instrument for the measurement of system response. The command signal and the load position were recorded on this instrument to check the data from the frequency-response analyzer. The amplitude ratio was determined by comparing the peak-to-peak deflection of the command and load position traces. The phase angle was determined by locating the center of a given frequency wave on each of the above sinusoidal traces and measuring the time lag between the two. The open-loop amplitude ratio was determined by comparing the load position and value current traces on the oscillograph chart.

Before each test run, the command signal, load position, and current recording channels were calibrated by applying a known voltage from a regulated direct-current supply, measured with a digital voltmeter, to the input of each direct-current amplifier. The amplifier gain was adjusted to give the proper galvanometer deflection, resulting in an accurate calibration from the signal pickoff points through the amplifiers and galvanometers to the traces on the oscillograph chart. Figure 41 shows the locations of the signal pickoffs for these recording channels. The load position transducer excitation was supplied by regulated direct-control power supplies, and the excitation voltage was checked with the digital voltmeter before each test run.

The position transducer was a plastic-film potentiometer containing two separate resistive elements and brushes. It was wired so that one channel provides a signal in phase with the command signal, for use in the frequency response analyzer, and a



— T — SURFACE TEMPERATURE THERMOCOUPLE - RECORDED ON STAMPING RECORDER
 — T — FLUID TEMPERATURE THERMOCOUPLE - RECORDED ON STAMPING RECORDER OR
 OSCILLOGRAPH (SEE INSTRUMENT LIST)
 — P — PRESSURE TRANSDUCER

LEGEND

Figure 41: Data Acquisition Schematic

second channel provides an out-of-phase position signal for use as position feedback to the operational amplifier.

In addition to the sinusoidal signals within the servoloop, the system supply pressure and the differential pressure across the actuator piston were also recorded on the oscillograph. The supply pressure was sensed by an unbonded strain-gage pressure transducer, Statham Model P24, 0 to 3000 psi. Location of this gage in the system is shown in Figure 42. This transducer does not have a low-temperature capability; therefore, resistive heating wire was wound on the transducer and used to warm the transducer prior to low-temperature test runs. Power to the heater was turned off during test runs to avoid signal interference. Two low-temperature pressure transducers, CEC Type 4-354, were used to measure the differential pressure across the actuator piston. The two transducers measure the pressure on each side of the piston, with the bridge circuit outputs of the transducers connected differentially to obtain a voltage signal proportional to the differential load on the piston. Installation of these transducers is described in Section 4.2.2. Figure 41 also shows the placement of the copper-constantan thermocouples that measure fluid and component temperatures. Component temperatures were measured with thermocouples bonded to the surface of the components while fluid temperatures were measured with immersion thermocouples. The temperatures were recorded on a Minneapolis-Honeywell (Brown Instruments Division) multiple-point stamping temperature recorder. The multiple-point stamping recorder provides a repeat measurement of each temperature monitored every 20 seconds. The thermocouples measuring the temperature of the fluid in the reservoir, pressure line, and return line were wired through switches so that these temperatures could be monitored on the stamping recorder during environmental temperature stabilization of the actuation system and then switched for continuous recording on the oscillograph during a system dynamic test run. The switching circuits included $+32^{\circ}\text{F}$ reference junctions used when the thermocouple voltages were being recorded on the oscillograph. The measurement of fluid leakage was obtained manually and by visual observation. Leakage past all external seals was measured visually and the amount was estimated. Fluid that leaked past the primary gland seals and was trapped in the leakage collection ports was measured in a graduate after each dynamic run of the test system. Leakage of fluid during the vacuum storage test was measured by marking the level of fluid in the sight gage provided for this purpose.

Environmental pressure was monitored using the Alphatron Model 530 vacuum gage in the 1000 to 10^{-4} torr range. Below 10^{-4} torr, the Varian hot-cathode ionization gage was used. During the vacuum tests, the chamber pressure was maintained within the range of the hot-cathode ionization gage, and the Alphatron vacuum gage was used only during pumping down to simulation pressures. Figure 43 shows a simplified schematic diagram of the hot-cathode ionization tube similar to a triode electron tube without a glass envelope. Electrons are emitted from the hot filament and are attracted toward the positively charged grid colliding with any gas molecules that might be present. The gas molecules are ionized, attracted toward the negatively charged anode, and produce a circuit current proportional to the number of gas molecules present.

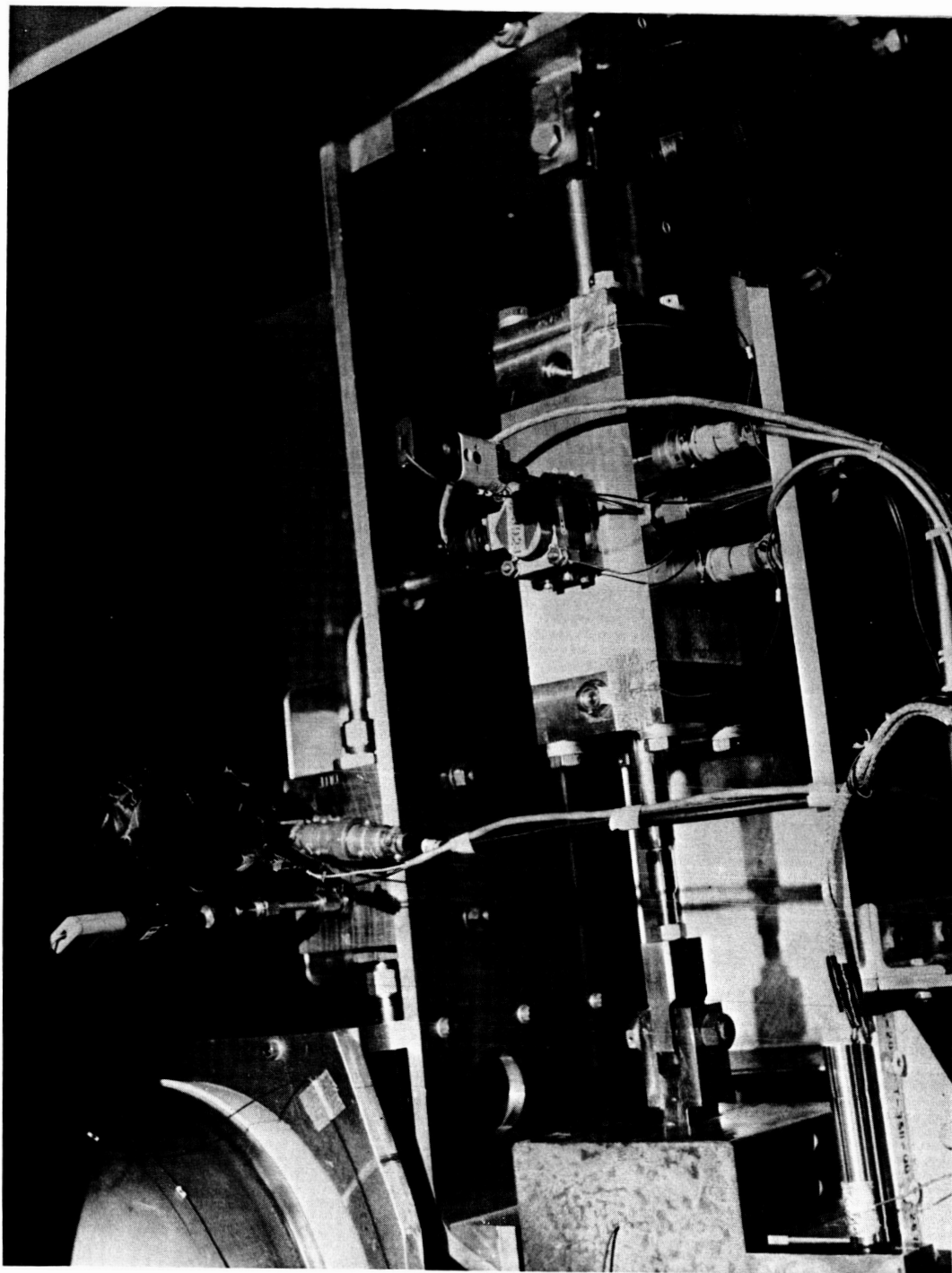


Figure 42: Operational Test System

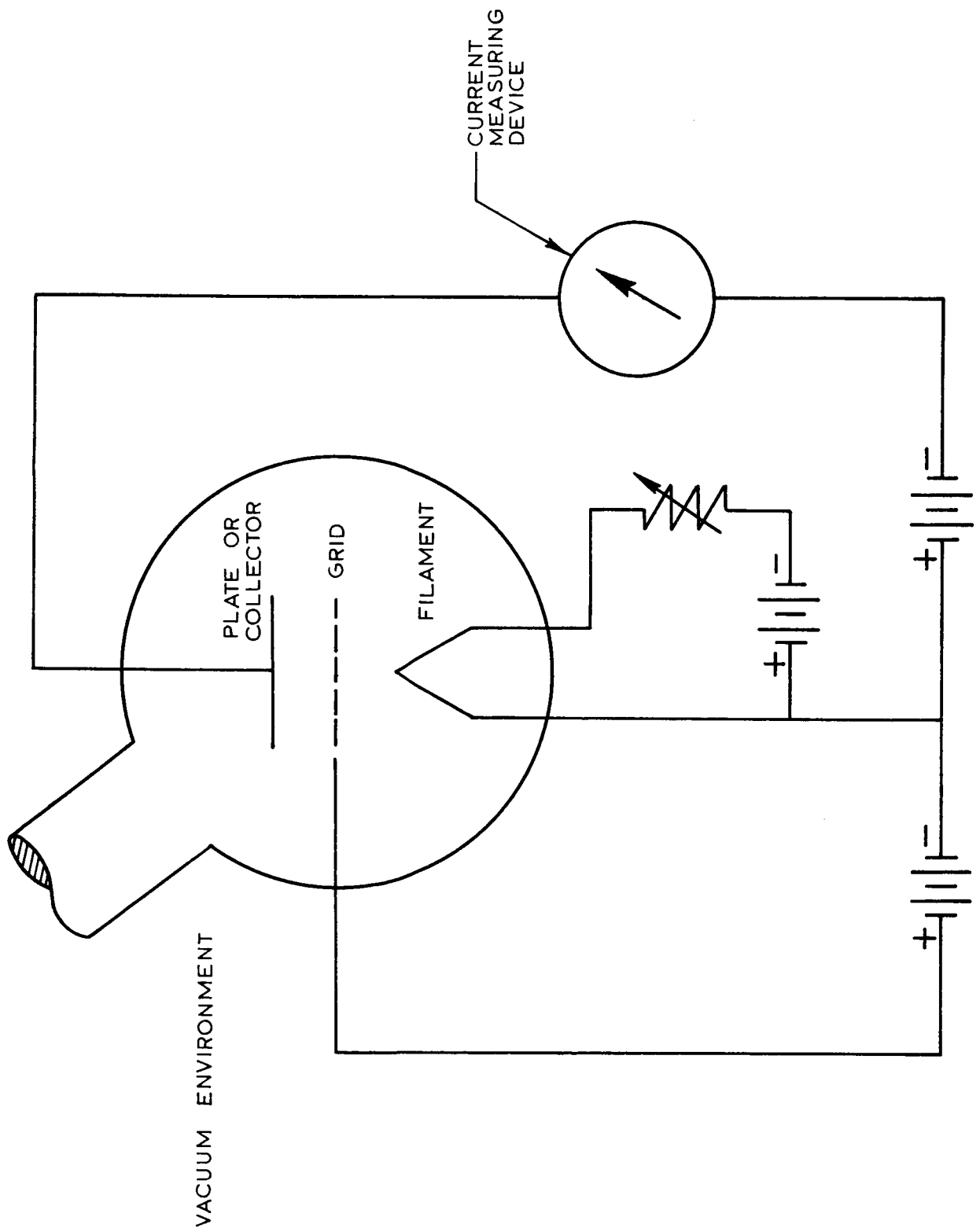


Figure 43: Hot Cathode Ionization Vacuum Gauge

Useful range of this vacuum measuring device is from 10^{-3} to 10^{-9} torr with an accuracy of ± 4 percent in the 1×10^{-3} to 2×10^{-6} torr range and an accuracy of ± 6 percent in the 2×10^{-6} to 10^{-7} torr range.

5.1.2 TEST SYSTEM ASSEMBLY

The test system previously described in Section 4.2.1 was assembled with the test facility equipment described in Section 4.3 to provide an operational test system and a vacuum storage assembly that could be moved from one test station to another without disassembly. Assembly of two servoactuators was a prerequisite to the above items, one actuator being used in each. Hydraulic support equipment was attached to and used with the operational test system to provide the necessary equipment for transfer and pressurization of fluid for operational tests. (Refer to Figure 44 for the complete system schematic.)

5.1.2.1 Servoactuator Assembly

Each of the two test actuators whose design has been described in Section 4.2.2 was assembled with phenyl silicone seals of Parker S-424-7 compound. The actuators were assembled with only the elastomeric seal on the pistons. For the dynamic rod seals, an elastomeric seal and single turn backup were installed in an internal groove in each seal gland. An "omniseal" was installed in the adjacent groove within each gland so that the two seals, O-ring and "omniseal," were on opposite sides of a seal collection port. The external static elastomeric seal and static metal seal were installed on each gland. The end cap and head-end seal gland for each actuator were attached to the housings with sets of four stainless steel bolts. The rod-end seal glands were similarly attached to the housings. A safety-wired locknut was used to prevent motion of the rod end of each actuator when the rod ends were properly adjusted.

The Serial Number 5 servovalve was attached to the Number 1 actuator to be used initially in the operational test system. The Serial Number 3 servovalve was attached to the Number 2 actuator for use in the vacuum storage assembly. These servovalves were attached with the adapters described in Section 4.2.4 and required four interface seals between the servovalve and adapter and four seals between the adapter and actuator housing.

Assembly of the Serial Number 1 actuator was completed by installing the pressure pickups for differential pressure measurement across the piston and leakage collection tubes to hold leakage past the elastomeric dynamic seal in each seal gland. The ports for these installations on the Serial Number 2 actuator to be used for vacuum storage were plugged.

5.1.2.2 Operational Test System

The operational test system as described below is used in all tests except the operational sequence performed with the vacuum stored servoactuator. During this test the Number 1 servoactuator is replaced with the vacuum storage assembly.

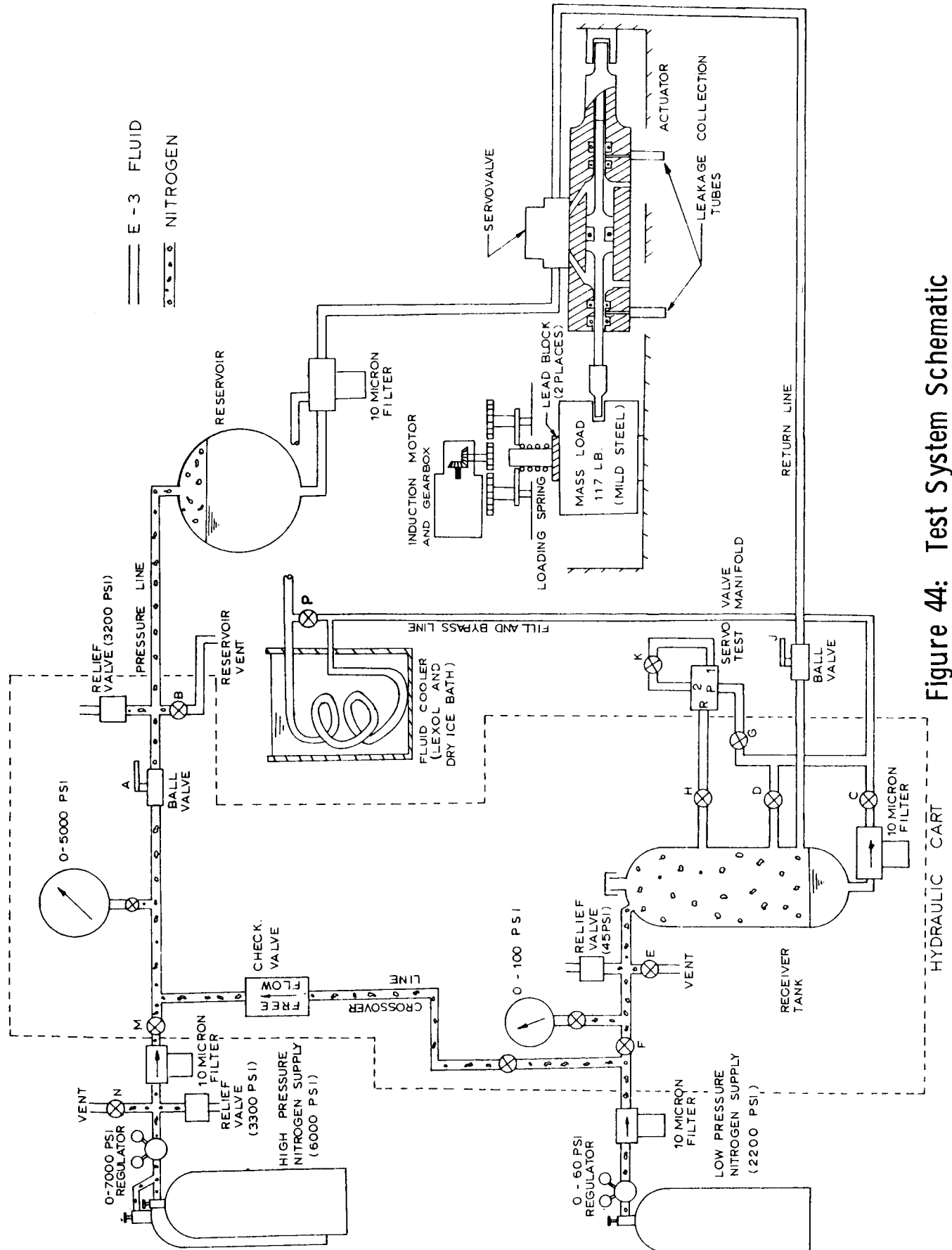


Figure 44: Test System Schematic

The cooling container and load apparatus described in Section 4.3 were assembled to form the rigid structure of the operational test system. The test system reservoir, filter, and Number 1 servoactuator were attached to the load structure within this system assembly. Tubing was added between the reservoir and filter, as were actuator supply and return lines, to complete the installation shown in Figure 42. The servoactuator was installed for ease of complete removal from the assembly. Actuator removal was required between major portions of the test program for refurbishment. Ease of removal was also desired in case of seal or valve failure during an environmental soak or an operational sequence.

The immersion thermocouples discussed in Section 5.1.1 were installed through fittings at hydraulic components as shown in Figure 41. Surface thermocouples were bonded to components of the test system using aluminum-backed tape and to facility-item structure by staking.

The fixed end of the actuator-position-measuring transducer was secured to the structure of the load apparatus with the movable end attached to the inertial load. This assembly procedure was chosen to eliminate the expensive and less maintainable installation of the transducer within the actuator body. This method of mounting is not recommended for flight applications, but was suitable for initial evaluation testing of a breadboard system designed to investigate operational problems.

5.1.2.3 Vacuum Storage Assembly

The vacuum storage assembly is used to isolate the Number 2 servoactuator in a hard-vacuum environment for an extended storage test. The assembly is constructed to be transferrable for installation within the operational test system for performance evaluation after the storage period.

The Number 2 servoactuator was installed in the vacuum container described in Section 4.3.1 by bolting the actuator head end to the stationary part of the container and the rod end to the removable container lid. Tubing and electrical connections were made inside the container to allow all necessary connections for operation of the servoactuator to be made at the external side of the container penetrations. The installation was conducted in clean-room conditions since any contamination within the container would reduce the vacuum pumping capability.

Two ion gages were installed in the vacuum container for environmental pressure measurement. A description of the gage operation is provided in Section 5.1.1. The second gage was installed because the expected life of a single gage was not sufficient to last the test storage period.

The fluid pressure fitting on the container was fitted with a standpipe to be used to determine the amount of fluid leakage during storage. A 20-psig regulated air supply was used to pressurize the standpipe. The fluid return fitting on the container was fitted with a 0- to 50-psi gage to monitor the applied pressure.

The vacuum storage assembly was completed by installing a Stokes 6-ST-3 high-vacuum-pressure gate valve at the 6-inch vacuum pump port. The electrical-solenoid-controlled, pneumatically operated gate valve provides the capability to seal the storage container at hard vacuum in preparation for transfer to the large environmental chamber and installation in the operational test system. The gate valve also provides a safety mechanism in that the valve closes automatically in case of power failure to the vacuum pumps.

5.1.2.4 Hydraulic Support Assembly

The hydraulic support assembly consists of the high-pressure nitrogen supply for pressurizing the reservoir, the low-pressure nitrogen supply for refilling the reservoir, and the hydraulic cart containing the receiver tank and manual control valves for fluid transfer control. Two 6000-psi dry-nitrogen pressure bottles were manifolded together for the high-pressure nitrogen supply. The bottles were manifolded to prevent excessive restriction of gas flow by the small openings in the shutoff valves on the bottles. A 0- to 7000-psi gas regulator was used to regulate the nitrogen pressure to 3000 psi. A relief valve, set at 3300 psi, was installed downstream of the pressure regulator. A nominal 10-micron filter was also installed to prevent contamination of the test system from scale that might be present within the nitrogen bottles. The low-pressure nitrogen supply consisted of a single 2200-psi nitrogen bottle, a low-pressure regulator, and a nominal 10-micron filter. The nitrogen supply systems are connected to the hydraulic cart and are shown schematically in Figure 44.

The hydraulic cart was assembled to contain the equipment for pressurization control and transfer of hydraulic fluid to and from the operational test system. The functions controlled with the hydraulic cart, using the nomenclature in Figure 44, are as follows. Valves M and A were installed to control 3000-psi pressurization of the E-3 fluid reservoir in the test system. Valve M allows complete disconnection of the high-pressure nitrogen supply without altering the stabilized pressure condition of the system. Valve A is a 90-degree quick-acting valve for pressure emergency shutoff. Valve J was installed to control pressurized fluid flow and was added to the system to prevent valve leakage flow from reducing the reservoir capacity. Valve D was provided as an emergency dump to deplete the reservoir in case of a serious malfunction of the system during operation. During pressurized blowdown of the reservoir, Valve E (the receiver vent) must be open.

The refilling function of the hydraulic cart requires a different set of valving. Valve F was provided to allow pressurization of the receiver tank, keeping Valve E closed. Valve C was provided to control the flow to the reservoir, keeping Valve B open to vent the reservoir during fill. At low temperature, it is advantageous to precool the fluid during the filling operation. The fluid cooler containing the Lexsol/dry-ice bath was installed for this purpose, with 40 feet of fluid line immersed in the bath. Valve P was kept closed to pass fluid through the cooler.

A fluid flow path for servovalve checkout using E-3 fluid was installed as part of the hydraulic cart. Valves G, H, and K control the use of this checkout block. Reservoir blowdown was used to provide high-pressure fluid to the checkout block through the bypass line.

5.1.3 OPERATIONAL SEQUENCE

The same operational sequence was followed during all of the dynamic tests of the actuation system. This procedure was followed to ensure that test results would be comparable from one test to another.

5.1.3.1 Test Preliminaries

Prior to the performance of each operational sequence with the test system, the hydraulic reservoir was filled with E-3 fluid and environmental stabilization in the test chamber was obtained as determined by monitoring temperature and environmental pressure. The oscillograph and the X-Y recorders were calibrated before each test and the high-pressure nitrogen supply was regulated to 3000 psig. Nitrogen bottles were replaced at intervals to ensure that continuous 3000-psi supply would be available throughout the test sequence.

5.1.3.2 Test Operation

The following sequence was followed in chronological order during each system operational test performed in the program. Refer to Figure 44 and Section 5.1.2.4 for a description of the function of the manually operated valves defined by letter designations in the following description.

Prerun Calibration —

- 1) The reservoir was pressurized to 3000 psi by opening Valve A and the system was observed for fluid leakage.
- 2) Keeping the input selector switch in the retract position, the return line shutoff, Valve J, was opened.
- 3) The input selector was switched to the centering position, causing the actuator piston to move from the retracted position to a center stroke position.
- 4) The input selector was then switched to provide a 0.5-cps sine-wave command from the frequency response analyzer to the servoactuator. During the ensuing few cycles of 0.5-cps motion, the differential pressure across the actuator piston was recorded on the oscillograph and the readings compared to the 1400-psi desired pressure.
- 5) The input selector was switched to the retract position, causing the actuator to return to its retracted position.
- 6) The load-adjusting motor was operated to correct the load to provide 1400-psi differential pressure across the actuator piston. The applied correction was 22 seconds per 100-psi correction required. The procedure of Steps 3 through 5 were repeated as necessary to obtain the desired load.

Operational Sequence —

- 1) The operational sequence was initiated by starting the oscillograph chart drive and switching the input selector to the centering position. The oscillograph data recording during centering provided information for calculating system step response.
- 2) The input selector was switched to provide the frequency response analyzer output command to the servoactuator. Time was allowed for switching transients to dampen, and then the X-Y recorders were started.
- 3) The frequency-sweep-rate control was moved to its first position to begin the 0.5- to 6-cps frequency sweep. The control was switched to the second position at 1 cps, the third position at 1.3 cps, the fourth position at 1.7 cps, and the fifth position at 2.5 cps.
- 4) At completion of the sweep, 6 cps, the X-Y recorders were turned off, the input selector switch returned to the retract position, and the oscillograph chart drive turned off.
- 5) The reservoir was depressurized by closing Valve A and venting the remaining gas by opening Valve B.

Postoperational Inspection — The seal leakage collection tubes on the servoactuator were inspected and drained of any leakage after the test chamber was restored to room temperature and environmental pressure. The amount of leakage from each tube was measured and recorded in the test log along with the results of an in-place inspection of the system for leaks, evidence of seal deterioration, or unusual wear.

5.2 LOW-TEMPERATURE TESTS

The low-temperature series of tests were the first system tests performed with the DuPont E-3 fluid and the single-pass blowdown hydraulic system.

5.2.1 TEST OBJECTIVES

The low-temperature tests were conducted to evaluate the design of the single-pass hydraulic actuation system, described in Section 4.2, in low-temperature environments. A second objective was to continue the evaluation of the advanced hydraulic fluid selected in Section 3.1.2 at temperatures below -100°F and determine the minimum temperature at which this fluid could be used in a hydraulic actuation system. Another test objective was to establish the compatibility of the hydraulic fluid, the elastomeric seals, and the actuation design under conditions of dynamic operation at low temperature and high pressure.

5.2.2 FACILITIES

The low-temperature tests were conducted in the Boeing strato chamber shown in Figure 45. This chamber is 7 feet in diameter by 12 feet long with a vertical section 5 feet in diameter extending 4.5 feet above the roof of the horizontal section of the chamber.



Figure 45: Low Temperature Test Facilities & Instrumentation

The entrance door in the chamber is 5 feet in diameter. The chamber has a low-temperature capability of -105°F , which is obtained by circulating chamber air through refrigeration coils. Temperature control within the chamber is provided automatically using set temperature controllers to turn on and shut off airflow through the refrigeration coils as needed. The refrigeration system consists of four stationary compressors having a total output capacity of 11.4 tons of refrigeration using Freon 12. Figure 46 shows the low-temperature hydraulic system installed in the strato chamber, with the refrigeration coils and air blower in the background.

The hydraulic blowdown system to be tested was installed within the load fixture and cooling container as described in Section 5.1.2. This assembly was securely bolted to the structure of the strato chamber to prevent movement of the installation in reaction to the load inertia forces during dynamic testing. Figure 46 shows a view of the hydraulic system assembly.

The hydraulic cart, described in Section 5.1.2, was located outside the strato chamber. Fluid connections between the hydraulic cart and the test system were made using tubing routed through penetrations in the strato chamber walls. The nitrogen pressurization assemblies were attached to the hydraulic cart (see Figure 44). The liquid cooling bath was placed adjacent to the hydraulic cart outside the test chamber and completed the installation of the hydraulic support equipment. The installation is shown in Figure 45.

As part of the installation procedure, the hydraulic system and hydraulic cart were flushed with isopropyl alcohol and then purged with dry gaseous nitrogen. A leak check was performed with nitrogen prior to filling the system with clean E-3 fluid. Samples of isopropyl alcohol and the E-3 fluid were taken from the system and analyzed for contamination according to the procedure in Reference 15 to verify the cleanliness of the system before and after filling with E-3. Results of these analyses showed the contamination level of the alcohol to be 0.2 mg per 100 ml of fluid and the contamination level of the E-3 fluid to be 0.1 mg per 100 ml.

An investigation was conducted during installation procedure to determine the amount of hysteresis in the adjustment of the inertia/friction load described in Section 4.3.1. It was determined during operation of the actuation system while measuring differential actuator piston pressure that acceptable repeatability in the inertia/friction load was not attainable without a short calibration check prior to each dynamic run. Because it was not medically safe to perform manual adjustments of the loading apparatus at temperatures below -65°F , a motorized remote adjusting mechanism was added to the load apparatus. Use of this mechanism has been explained in Section 5.1.

Figure 45 shows the instrumentation and system control electronics installed in equipment racks near the test chamber. The instrumentation and its use is described in Section 5.1.1. The gain of the control electronics was reduced to provide a system break frequency of 3 cps. Actuator cycling tests were performed during the installation sequence to adjust the servoamplifier gain to provide this break frequency for the system. The cooling container described in Section 4.3.3 was required as part of the facility because the strato chamber as a low-temperature test facility was limited to

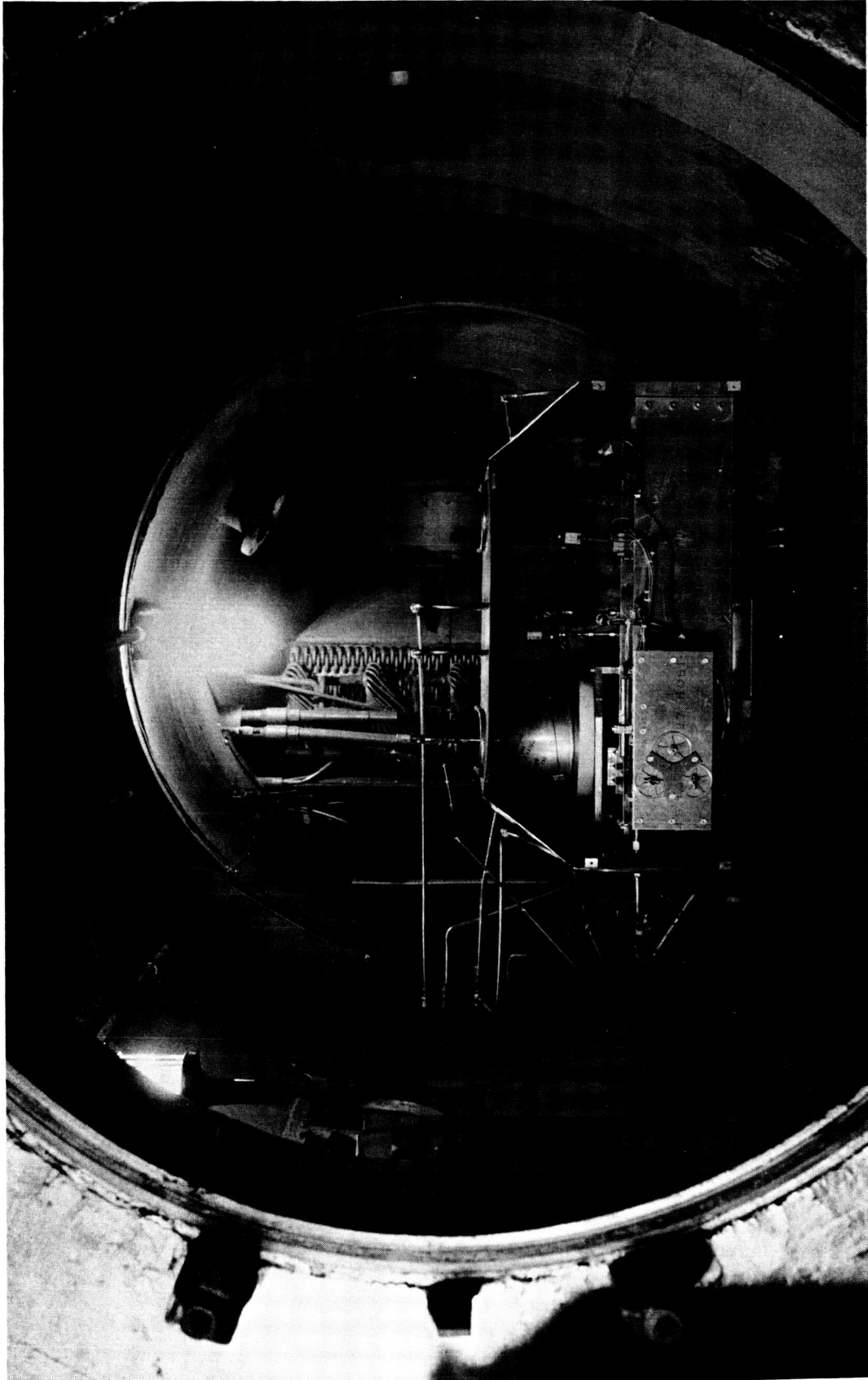


Figure 46: Test System Installation-Low Temperature Tests

-105°F using the Freon-12 cooling system. The copper coils forming the four cooling zones on the cooling container were extended through penetrations in the test chamber walls to manual control valves located outside the test chamber for each zone. Portable liquid-nitrogen dewars were connected to the common inlet to these manual valves when needed for cooling below -100°F. The front panel of the cooling container was not installed until test temperatures below the capability of the strato chamber were reached.

5.2.3 TEST PROCEDURE

Evaluation of the operational characteristics of the previously described single-pass blowdown hydraulic system at low temperature was conducted by performing a series of tests at successively decreasing levels of stabilized system temperature. Tests were performed at +75, 0, and -50°F, and subsequently at 25°F increments of decreasing temperature to determine the change in characteristics with temperature and the minimum practical operating temperature for the system. Room-temperature tests, referred to as baselines, were performed at intervals during the low-temperature series to evaluate any permanent changes in the system as a result of low-temperature exposure.

Before each system operational test run, the high-pressure nitrogen supply was checked to ensure that sufficient nitrogen was available to complete the test run at a pressure of 3000 psi. In general, two 6000-psi bottles containing 494 cubic feet of nitrogen at standard conditions provided sufficient pressurization for two test runs and the checks and calibrations of the system prior to these runs. An undetected gas leak or extra system checkout sometimes made it necessary to change bottles more frequently.

Cooling of the test system to each of the desired stabilized temperatures was accomplished using the facilities described in Sections 4.3.3 and 5.2.2. Filling of fluid reservoir with E-3 was delayed until the system was cooled to approximately -50°F. The reservoir was then filled, passing the fluid through the cooling bath of Lexsol and dry ice. The cooled fluid entered the reservoir at -65°F, thus providing quicker cooling than could be accomplished if the reservoir had been filled initially. As the system temperature was further reduced, the fluid in the reservoir cooled more slowly than the actuator, servovalve, and filter; therefore, the reservoir fluid temperature was monitored to determine when the system had stabilized at the desired temperature.

Prior to the operational sequence test at each stabilized low temperature, the important fluid temperature measurements were switched from recording on the multiple-point stamping recorders to the oscillograph for continuous data during the operational sequence. The multiple-point stamping recorder was used to record measurements where only small temperature changes occurred in the hydraulic system during the operational tests.

Instrumentation used during the test is described in Section 5.1.1. During the operational sequence tests, dynamic recordings of the actuation-system input command signal and the resulting load position signal were recorded on the oscillograph to

duplicate the data from the frequency response analyzer and to monitor the waveform of the position signal. This backup data was necessary since the frequency-sweep generator in the analyzer introduced recording errors into the X-Y plots due to the large time constants in the amplitude ratio and phase circuits. The need for backup data was further emphasized by the magnitude of the instrumentation transients when shifting decibel ranges on the analyzer. These errors increased during some low-temperature testing when response was significantly different from that at room temperature.

The operational sequence tests were performed as outlined in Section 5.1.3. After completion of each test, the hydraulic fluid in the actuator-rod-seal leakage collection tubes was measured, and the system was visually inspected for leakage. Inspection was not advisable prior to warming the test chamber, because opening the chamber while still cold produced a heavy frost condensation from the room-temperature air that entered the chamber. This frost made it impossible to detect anything but a very large leak. Difficulty was also experienced if the chamber was kept closed and warmed to room temperature before inspection. This procedure allowed fluid leakage to evaporate prior to opening the chamber. The procedure adopted was to open the chamber for inspection after partial warming for a preliminary inspection; a more complete inspection followed at room temperature. The oscillograph data was reduced after each test run to check the accuracy of the frequency response analyzer data, to verify that system pressure and load pressure had been correct, and to evaluate other low-temperature effects on actuation-system operational characteristics.

Subsequent to the discovery of some contamination in the system, which is discussed in Section 5.2.4.2, the micronic filter in the first stage of the servovalve was inspected after each operational test sequence.

5.2.4 TEST RESULTS

The first three low-temperature test runs (75, 0, and -50°F) were performed with Number 5 servovalve installed on Number 1 actuator. Malfunction of the servovalve (described below in the discussion of fluid contamination) necessitated replacement of the servovalve with the backup valve (see Section 4.2.4 for description of Number 4 backup valve). Subsequent low-temperature test runs using this backup valve were performed at -75, -100, -125, and -140°F. A load check at -155°F resulted in such low-amplitude actuator motion that a test run was not made at this temperature because the amplitude data could not be analyzed. Limited operation of the actuator was achieved at -165°F — the actuator slowly extended and retracted in response to centering- and retract-command signals, but would not respond to the programmed sinusoidal command signals. The test results are described more fully below.

5.2.4.1 Fluid and Seal Performance

The low-temperature test results show that the DuPont Freon E-3 fluid flowed at temperatures as low as -165°F under high pressure, although there was a marked change in fluid performance at temperatures below -100°F. A curve illustrating the effect of

temperature on fluid performance was developed from the dynamic test data (Figure 47). Because flow, pressure, fluid density, and other characteristics varied between tests, the following equation describing flow through a servocontrolled hydraulic system was used to correlate the dynamic data available from test runs at various temperatures.

$$Q = K I \sqrt{\frac{P_s - P_L}{\rho}}$$

where: Q = volumetric flow rate through the valve control ports;

K = the valve flow coefficient, dependent on control orifice geometry, discharge coefficient, valve first-stage gain, feedback-spring stiffness;

I = current through the valve torque-motor coils;

P_s = supply pressure;

P_L = load pressure (differential pressure across the actuator piston);

ρ = fluid density.

Rewritten,

$$K = \frac{Q}{I \sqrt{\frac{P_s - P_L}{\rho}}}.$$

The flow coefficient (K) was computed from the test data recorded on the oscillograph. The flow rate (Q) was computed from the oscillograph traces of the sinusoidal actuator motion as follows:

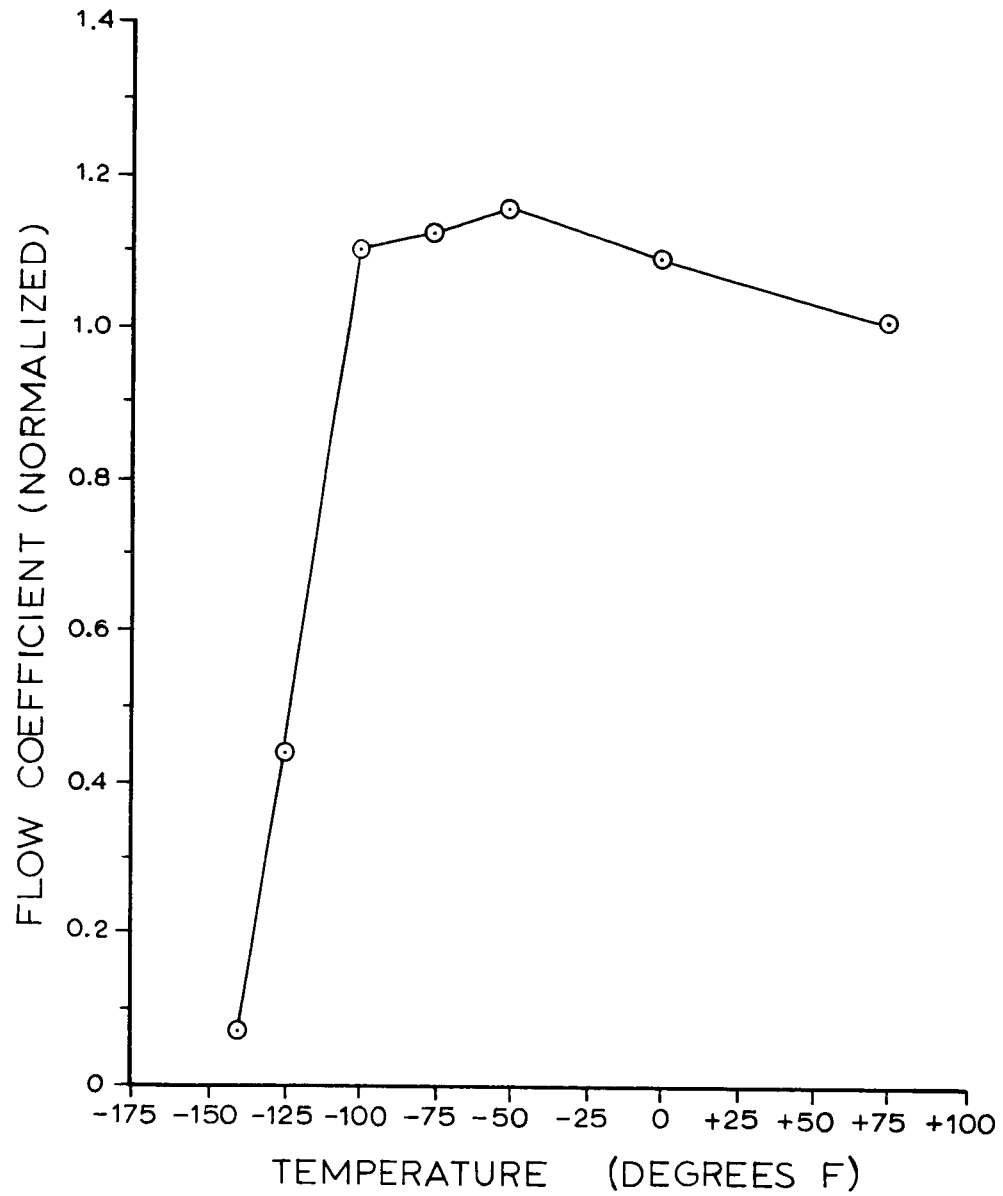
- 1) Actuator piston position = $A (\sin \omega t)$;
- 2) Actuator piston velocity = $(A) (\omega) (\cos \omega t)$;
- 3) Peak velocity = $(A)(\omega)$;
- 4) Peak flow rate = $(A\omega)(\text{piston area})$.

The known values of A , ω , and piston area were then used to calculate the peak flow rate (Q) used in the equation. Fluid density (ρ) is given in Reference 16.

Peak current (I) and the supply and load pressures (P_s and P_L) were measured from the oscillograph traces.

Data points were computed for test runs at +75, 0, and -50°F (using Servovalve Number 5) and for the lower-temperature test runs and some baseline runs (using Servovalve Number 4).

The two valves (4 and 5) had different values of K at +75°F, and the data from both valves were normalized so that K at +75°F was unity. Figure 47 shows that as the fluid temperature is decreased, the flow coefficient becomes larger than the value at +75°F until the temperature reaches a value below -100°F where the flow coefficient decreases very rapidly. This variation in K is also seen in the test-system closed-loop frequency response data discussed in Section 5.2.4.3. The sudden break in the



$$\text{FLOW COEFFICIENT} = K = \frac{Q}{I \sqrt{\frac{p_s - p_L}{\rho}}}$$

Figure 47: Flow Coefficient Vs Temperature

plot of K versus temperature is attributed to fluid viscosity, which increases rapidly as the temperature decreases.

Although the curve of Figure 47 contains the best available test data on the performance of DuPont Freon E-3 fluid at low temperatures, it cannot be determined to what extent the data describes flow through second-stage metering orifices of the servovalves or performance of the first stage of the valve. Studies of temperature effects in the first and second stage of the valves were beyond the scope of this contract. The sudden performance degradation, presumed due to high fluid viscosity, indicates a need to further evaluate the effects of fluid viscosity on valve performance.

The actuator-rod seals performed satisfactorily throughout the low-temperature test sequence. No seal leakage was observed at temperatures above -75°F . The actuator-rod-seal leakage collected during test runs at -100°F and below is as follows:

<u>Test Temperature</u>	<u>Leakage</u>
-100°F	A few drops from each rod seal.
-125 and -140°F (both test runs during the same cold soak)	1 cubic centimeter from each rod seal.
-155 and -165°F (same cold soak)	None.

No leakage was measured at -155 and -165°F because the actuator was cycled only a few times at these temperatures, and the amount of fluid that the rod pumped through the seals was too small to detect.

Inspection of rod seals at the conclusion of the low-temperature tests revealed abrasion and nibbling of the seal material as shown in Figure 48. Fluid contamination is considered partly responsible for this wear. The piston seal, also shown in Figure 48, was discolored by a black substance that was ground into the seal material. A similar substance was discovered on a seal in the vacuum-storage actuator (see Section 5.5). Emission spectral analysis showed that this material contains chromium and nickel, but there was not enough material to perform a more thorough analysis. The actuator piston and rod are plated with chromium, and the rod seal glands and the cylinder bore are plated with nickel. The black material may have been a fluid contaminant mixed with fine particles of chromium and nickel that had been abraded from the metal surfaces.

After the test run at -100°F , hydraulic fluid was found on the top surface of the actuator. This fluid could have leaked from the servovalve mounting seals, the face seals between the valve adapter plate and the actuator, or from the servovalve end-cap seals. It was not possible to determine which seal had leaked since the DuPont Freon E-3 fluid is colorless and leaves no stain. The servovalve mounting and end-cap seals did not have a squeeze greater than that normally used on these components. No evidence of a repeat of this leakage condition occurred in the remainder of the test program.

A serious leak developed in the micronic filter at a test-run temperature of -75°F . This leak occurred past the seal between the filter bowl and body. The original seal

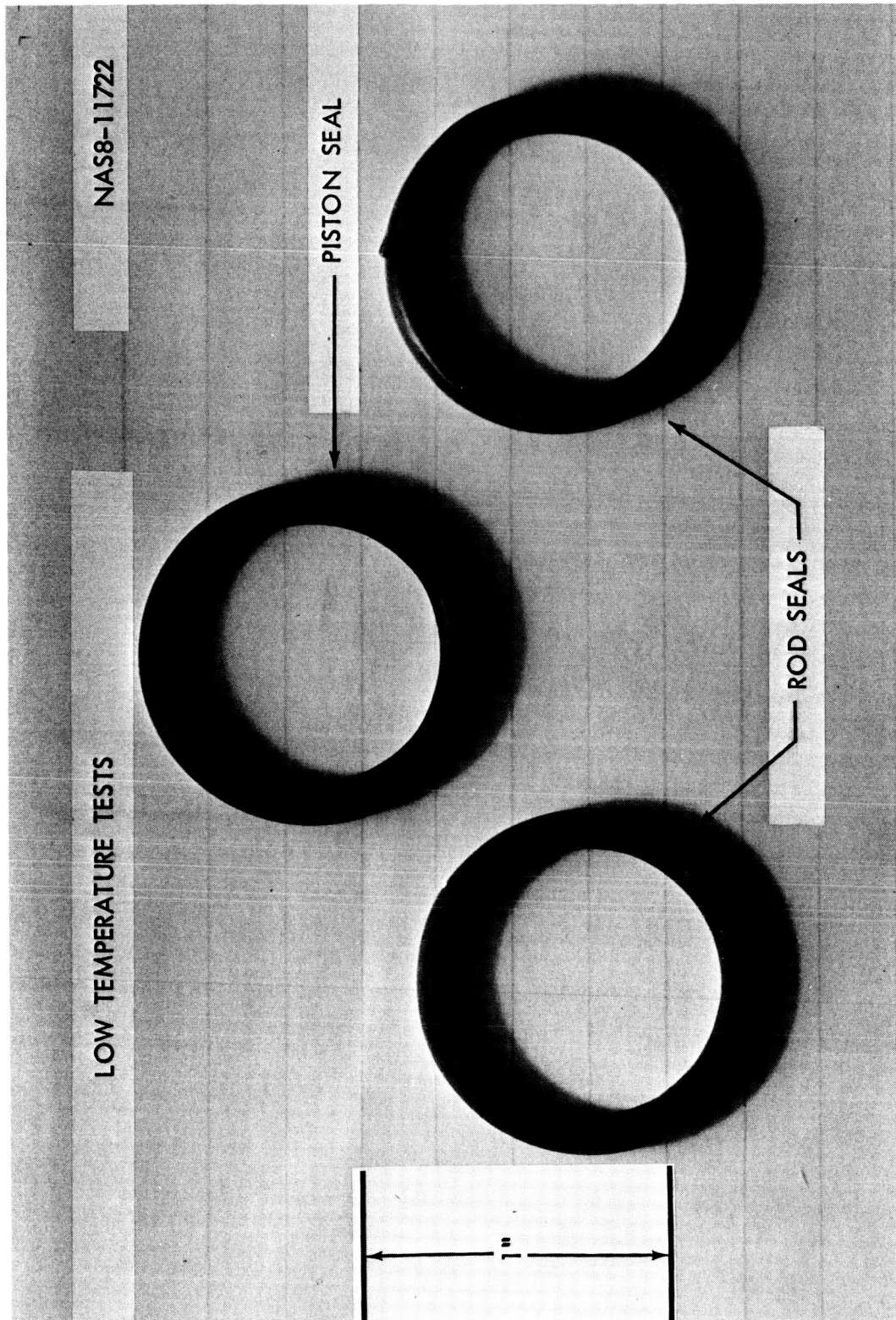


Figure 48: Low-Temperature Actuator Dynamic Seal Wear

sharp edges. It is believed that the sand came from a system component manufactured by sand casting, or a component that had been sandblasted and not properly cleaned prior to installation in the test system. The main suspects are the high-pressure reservoir and the receiver tank in the hydraulic cart.

5.2.4.3 System Frequency Response Data

Because Servovalve Number 5 was replaced after the -50°F test run, the system frequency-response data with each servovalve is shown on a separate plot to facilitate comparison of low-temperature data with a baseline ($+75^{\circ}\text{F}$ test run) using the same valve. Figure 49 shows the system closed-loop frequency response data with Servovalve Number 5, and Figure 50 shows the closed-loop data using Servovalve Number 4 for tests at -100°F and above. The response data for all test runs at temperatures above -100°F is shown in Figure 51 with the envelope of the $+75^{\circ}\text{F}$ baseline data drawn in to avoid the confusion of plotting all five $+75^{\circ}\text{F}$ test runs separately. The closed-loop response data for all low-temperature and baseline tests is shown in Figure 52 with the data from $+75$ to -100°F shown as an envelope because the graphic scale used does not allow sufficient space to plot these curves individually.

The response data from $+75$ to -50°F (Figure 49) shows that the low-temperature test runs resulted in a slightly higher amplitude and less phase lag than the test run at $+75^{\circ}\text{F}$. This result correlates with the flow data discussed in Section 5.2.4.1 where the actuator flow coefficient was higher at 0°F and -50°F than at $+75^{\circ}\text{F}$. The response data has a lower amplitude at -50°F than at 0°F ; this can be attributed to differences in load pressure, current, and fluid density. These differences are compensated for in the plot of flow coefficients.

Figure 50 shows the system closed-loop response data with Servovalve Number 4 installed on the actuator. The data for test runs made below -100°F are not shown on this plot so that a larger scale can be used. As in the data described above, the response at low temperature shows a higher amplitude than at $+75^{\circ}\text{F}$.

It can be seen that the amplitude ratio at 0.5 cps is greater than 0 db on some of the test runs with Valve Number 4. The high amplitude is accompanied by high phase lag. This characteristic of the response data was noted on several test runs using Servovalve Number 4, but none with Valve Number 5. During the checkout of the valves prior to the beginning of the test program, it was noted that Servovalve Number 4 showed a great deal of hysteresis until it had been operated for a number of cycles. Because of this, it was kept as a spare while the best valve (Number 5) was installed on the low-temperature actuator. The only data taken on valve performance with E-3 fluid was in pressure-gain tests to check null current and hysteresis after the valves had been reassembled with the phenyl-silicone O-ring seals installed.

Further investigation of the system test data showed that the current to Servovalve Number 4 was very high at 0.5 cps. The open-loop frequency response of the system (the amplitude ratio of actuator position to servovalve current) was computed and the results showed that at 0.5 and 1 cps the open-loop amplitude response was much lower

D2-90795-2
FREQUENCY (CPS)

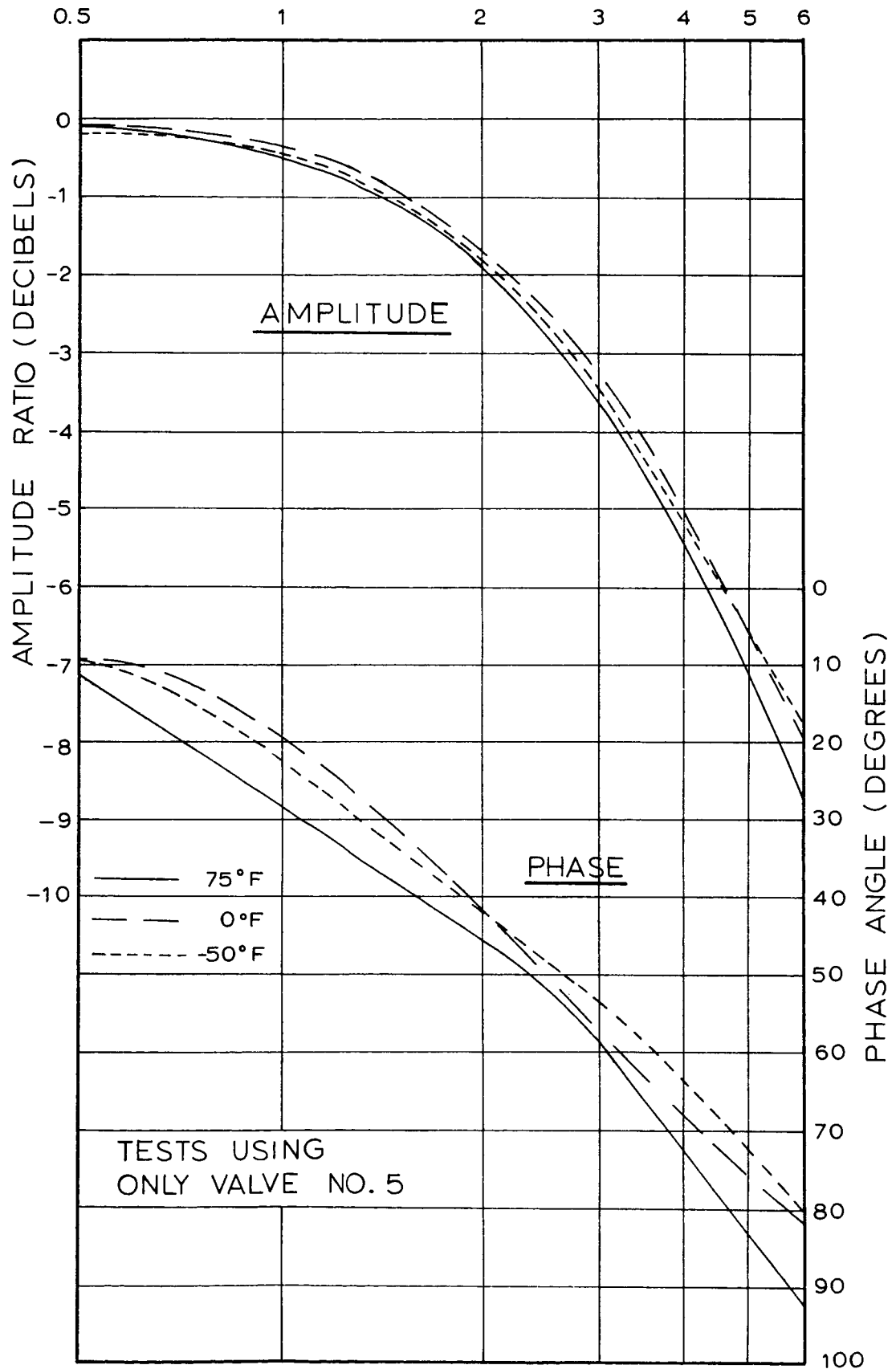


Figure 49: System Response, +75 To -50°F
100

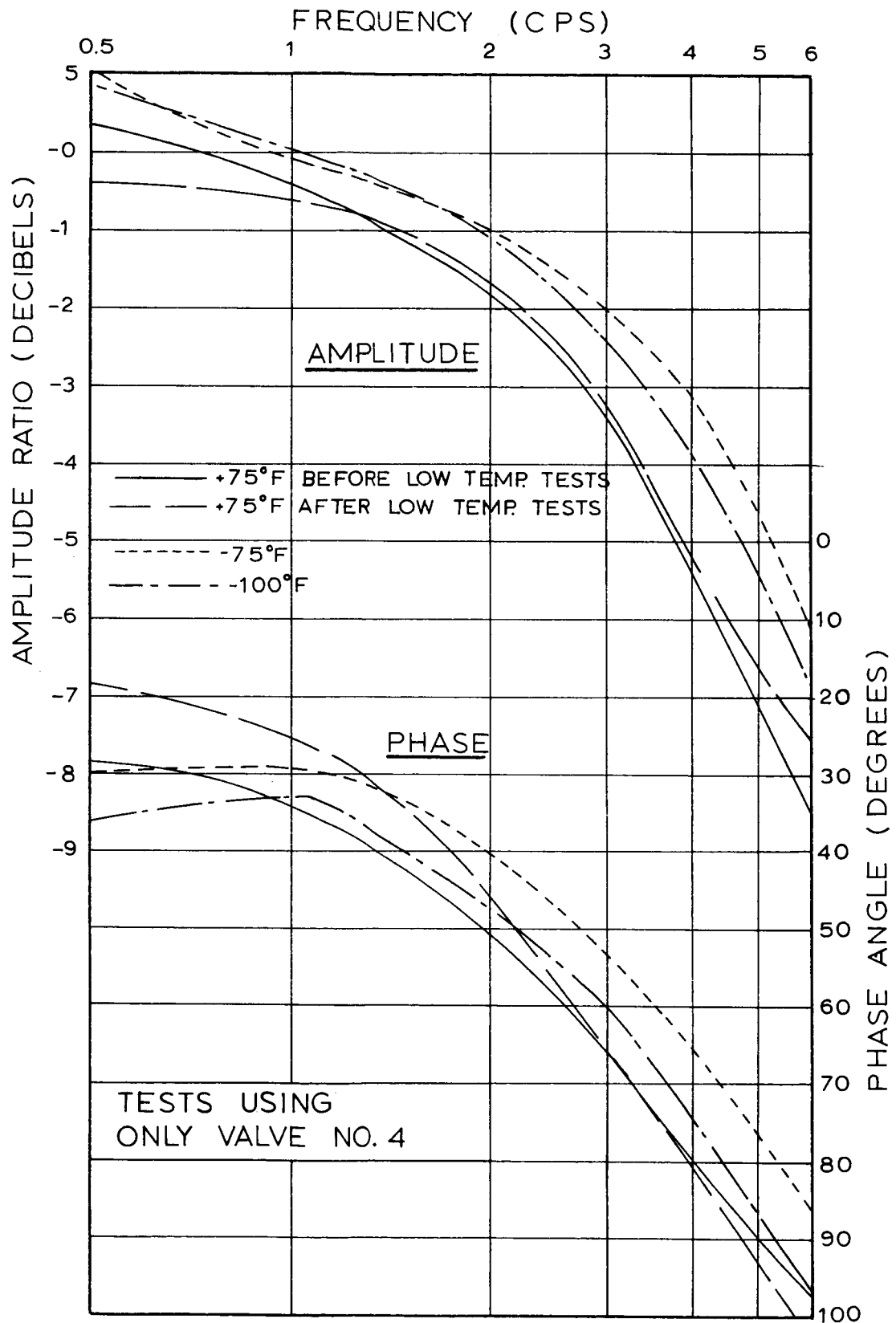


Figure 50: System Response, +75 To -100°F

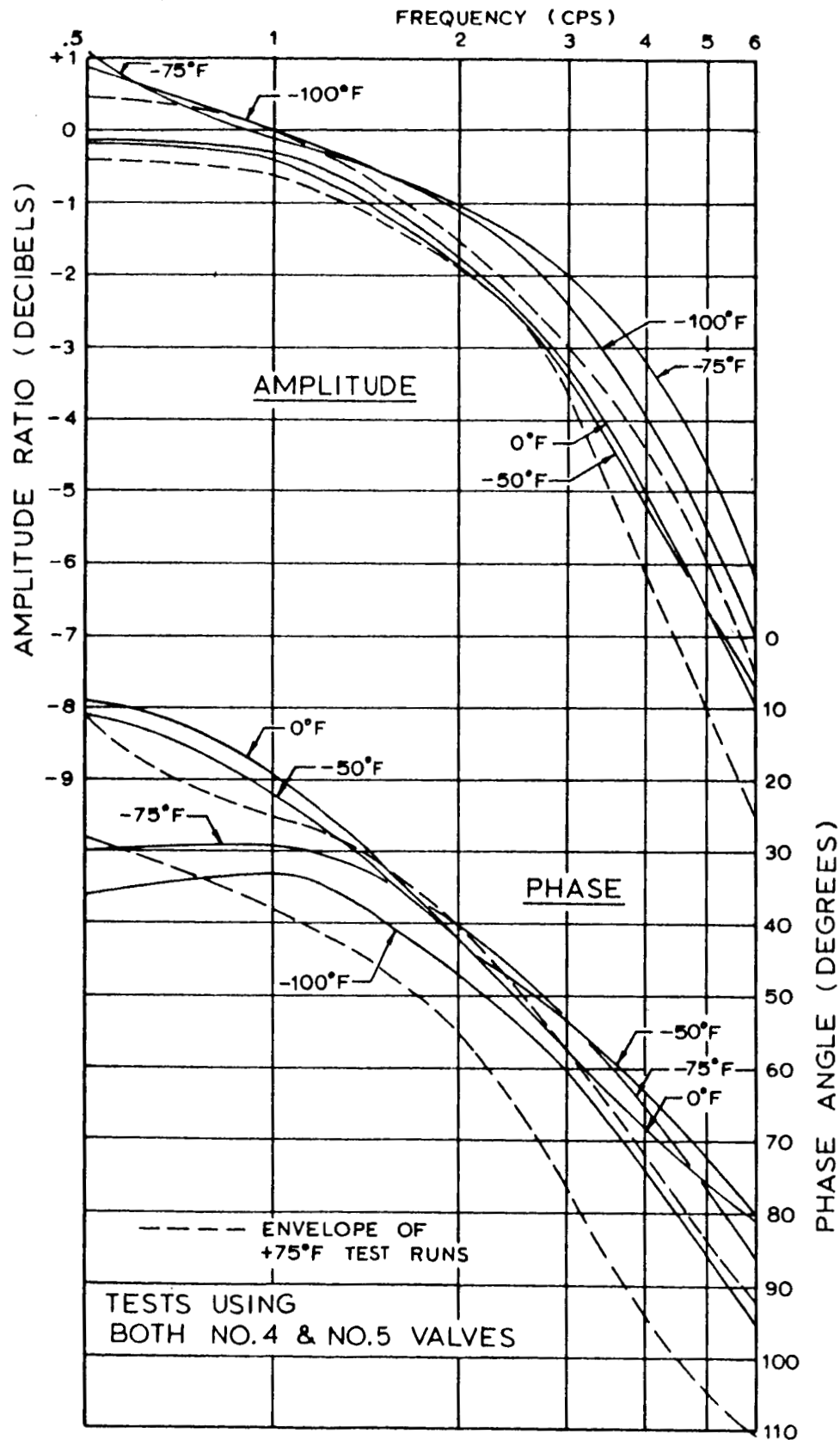


Figure 51: System Response, +75 To -100°F

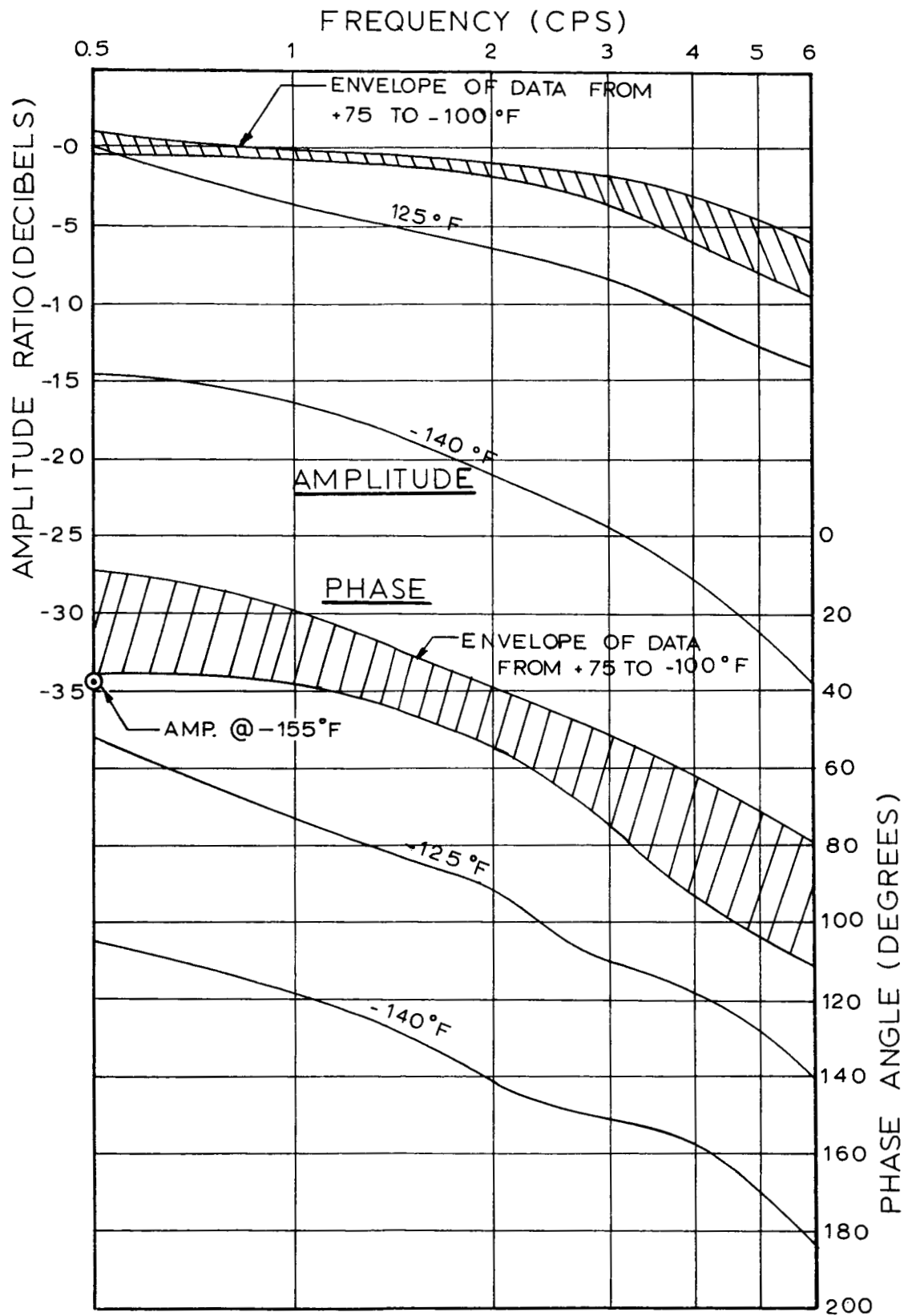


Figure 52: System Response, +75 To -140°F

than expected. Since the earlier checkout of the valve had shown that it had high hysteresis until it had been operated for a period of time, a test was performed in which the actuator was cycled at 0.5, 1, 2, 3, and 4 cps. The frequency was then decreased to 3, 2, 1, and 0.5 cps to see if operation would improve the actuator response at 0.5 cps. The resulting data, plotted in Figure 53, shows that the initial 0.5- and 1-cps data points diverge from the -6-decibel-per-octave line on which the other points fall, while the 0.5- and 1-cps points at the end of the test are at the proper locations on the plot.

The closed-loop phase angle, also plotted in Figure 53, was quite high at the beginning of this test and decreased to about one-half by the end of the cycling. The open-loop phase lag could not be measured with any accuracy because of the low amplitude and distorted waveform of the valve-current oscillograph traces at 0.5 cps.

The low open-loop amplitude response and high closed-loop phase lag exhibited in this and other tests are indicative of very high valve hysteresis, which disappears after the valve has been operated for a period of time. Excessive phase lag appears in the actuator position-feedback signal and, when summed with the sinusoidal command signal at the servoamplifier, the error signal (valve current) increases in proportion to the phase lag. This explains the closed-loop amplitude data that exceeds unity (0 db) and is contrary to theoretical predictions of the system response.

Since this hysteresis effect appeared in only one servovalve, it is felt that the effect is due to an unknown valve defect and is not caused by the hydraulic fluid, seals, or any other factor in the low-temperature test program.

Figure 51, containing all the closed-loop system response data from +75 to -100°F, allows comparison of the data obtained with both servovalves. As in the previous frequency-response plots, the amplitude response is seen to increase with decreasing temperature down to above -100°F. The envelope of +75°F baseline data is wider than indicated by baseline curves in the previous plots because some extra baseline data taken during the low-temperature tests has been included. Minor variations in supply pressure and load pressure account for the variations in the baseline data, and the initial and final baseline runs only are used for comparison in Figure 50.

The system closed-loop frequency-response data from +75 to -140°F, plotted in Figure 52, illustrates the rapid decrease in system response at temperatures below -100°F, as previously shown by the flow data of Figure 47. A single data point at 0.5 cps was obtained at -155°F and is plotted for comparison with other amplitude curves.

The open-loop frequency-response amplitude data from 75 to -140°F is plotted in Figure 54. This data, derived from the ratio of peak actuator position to peak servovalve current, has already been presented in a normalized form in Figure 47, and is shown here to illustrate once again the low-temperature effects on fluid performance.

The low open-loop response at 0.5 and 1 cps can be seen on the curves for all tests performed with Servovalve Number 4 installed on the actuator.

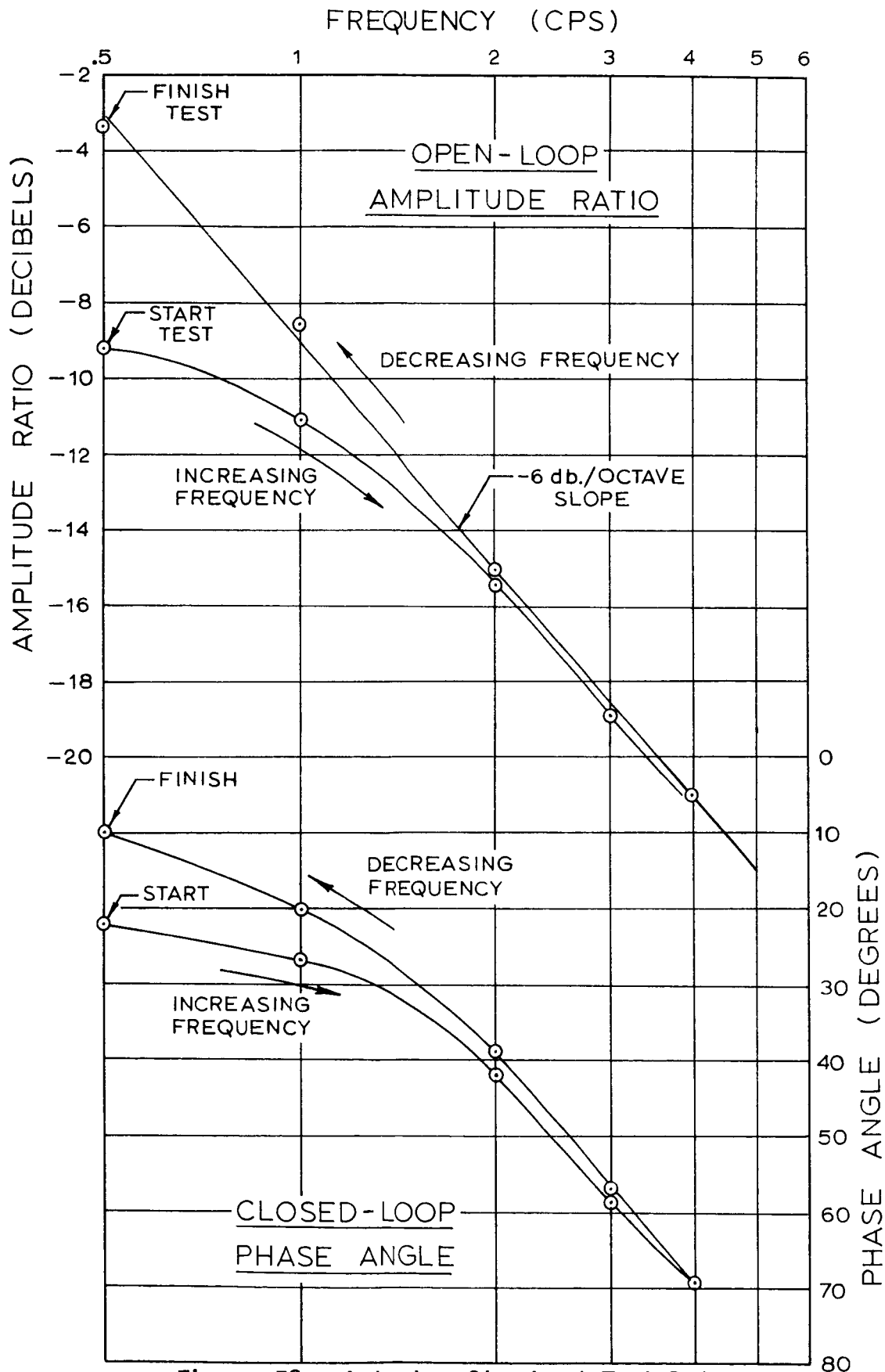


Figure 53: Actuator Checkout Test Data

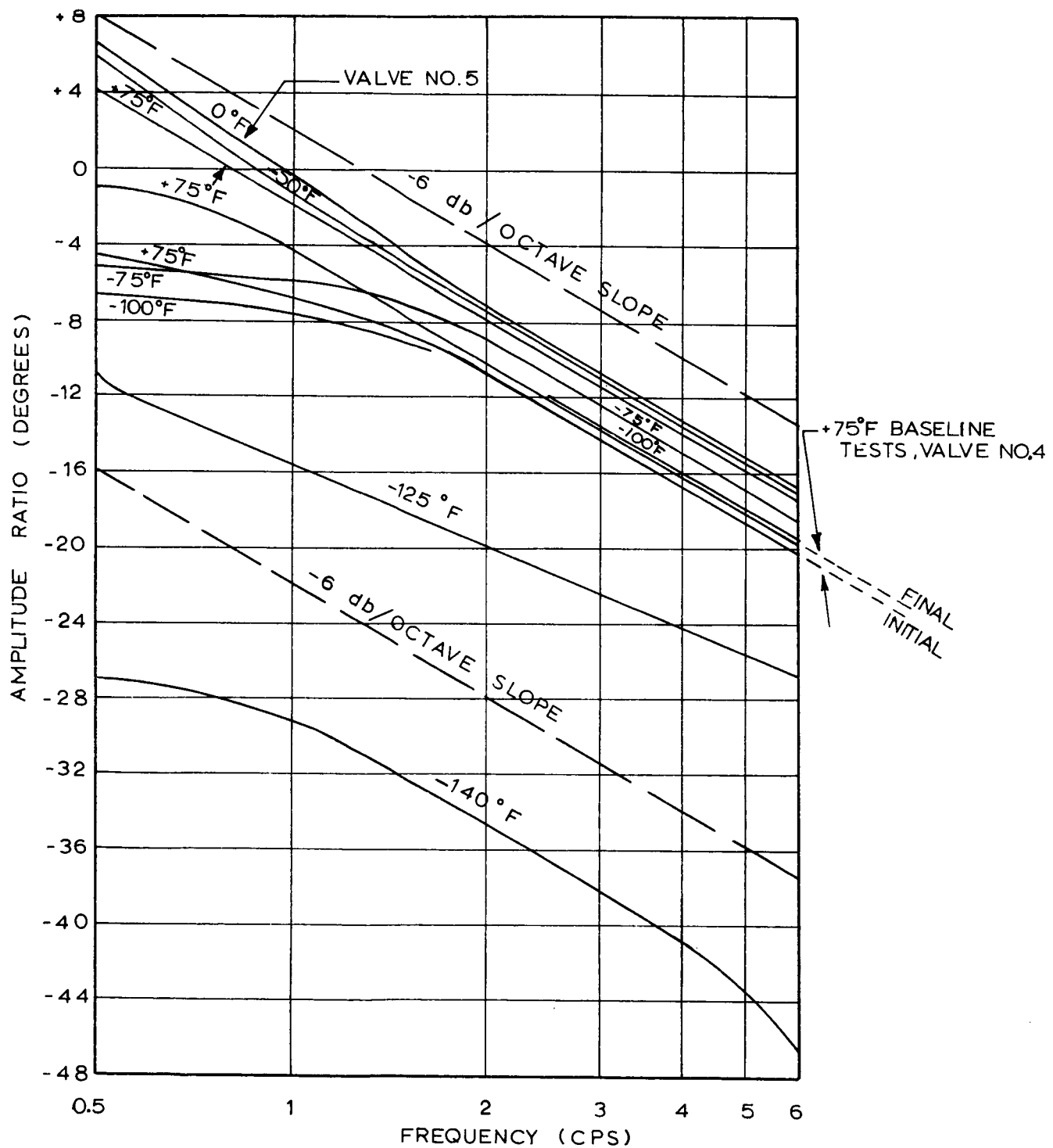


Figure 54: Open-Loop Frequency Response, +75
TO -140°F

The system step response at low temperature is shown in Figure 55. As in previous system-performance data, the response drops off very rapidly at temperatures below -100°F .

5.2.4.4 System Pressure and Temperature Control

Fluid throttling during the operational sequence tests produced very little temperature rise in the system. The fluid temperature in the reservoir rose somewhat when warm high-pressure nitrogen was used to blowdown the reservoir. The higher reservoir temperature did not produce a significant rise in the temperature of the fluid passing through the actuator.

System-fluid temperatures and supply pressure for a typical low-temperature test (-125°F) are shown in Figure 56. The data shows that the rise in temperature within the reservoir was not sensed at the inlet to the servoactuator. Measurement of reservoir fluid temperature after approximately 100 seconds was considered invalid because, at that time, the thermocouple was no longer immersed in oil. The effect of fluid throttling in the system is shown as the difference between the actuator inlet and return fluid temperatures and is negligible.

Temperature differences between the warmest and coolest points in the test system, exclusive of the reservoir fluid, are shown in Figure 57 for all operational sequence tests performed. These temperature differences varied from 2 to 15 degrees. The magnitude of the difference increased as the desired stabilized temperature approached the maximum cooling capacity of the Freon-12 cooling system, while the use of liquid nitrogen reduced the difference.

The variation in supply pressure during the typical operational sequence (Figure 56) is shown as a shaded band. A cyclic variation in the supply pressure was observed during all tests performed below -100°F . The pressure variations cycled at the same frequency as the actuator movement. Peak pressure coincided in time with the end of the actuator stroke where the velocity was zero. Low pressure occurred when the actuator velocity was maximum. The supply-pressure variation was caused by the pressure drop through the micronic filter located upstream of the supply-pressure transducer. Since the supply pressure did not show this effect at temperatures of -100°F and above, the fluid viscosity at low temperature is concluded to be the cause.

5.2.5 CONCLUSIONS

The low-temperature test results showed that a hydraulic system using DuPont E-3 fluid and phenyl-silicone seals will perform satisfactorily within the temperature range of $+75$ to -140°F . This temperature range thoroughly explored the low-temperature capability of the selected fluid in a blowdown system. Further research is required to determine the minimum operational temperature using the phenyl-silicone seals and the operational life of these seals at lower temperatures.

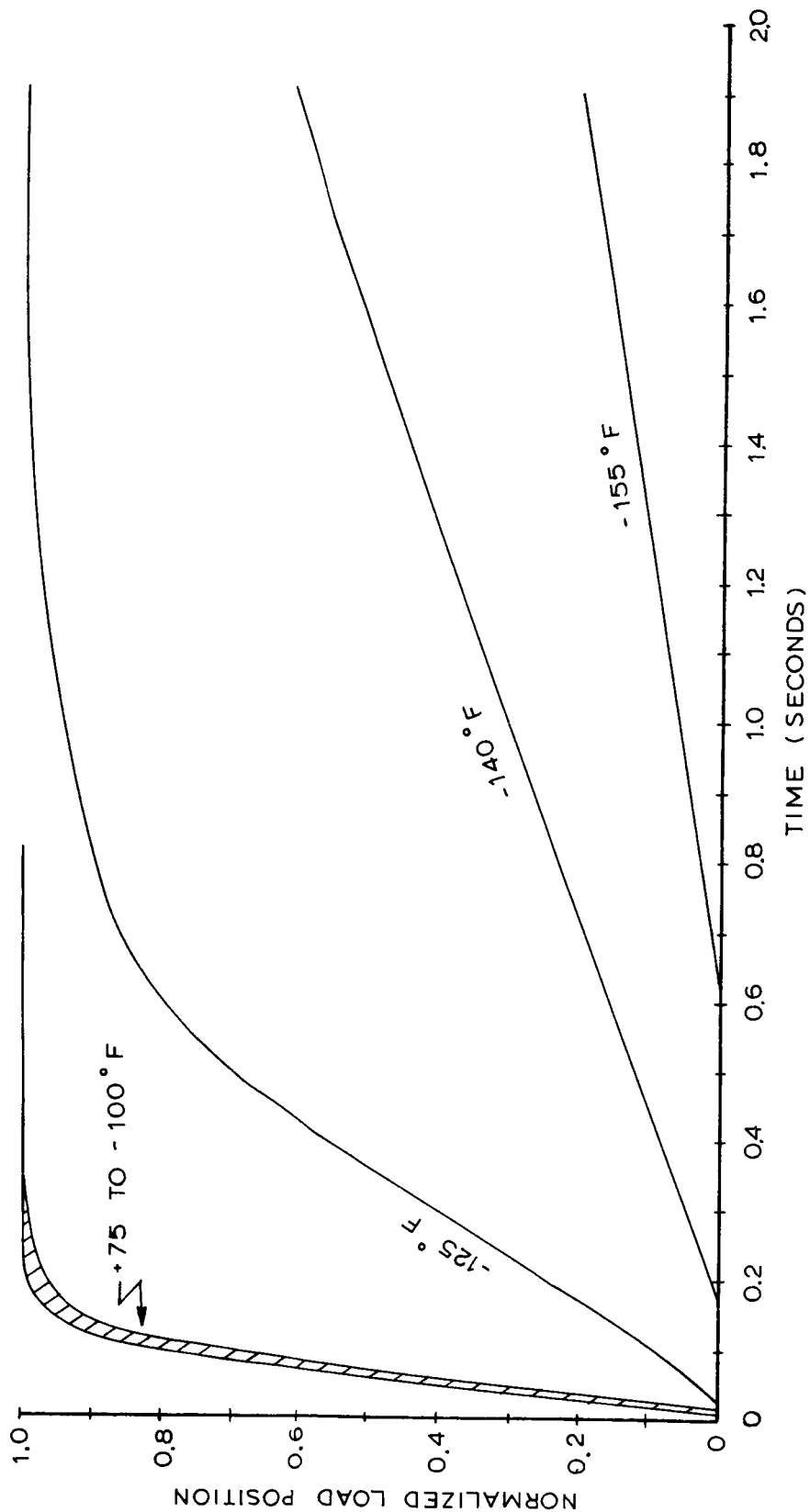


Figure 55: Actuation System Low Temperature Step Response

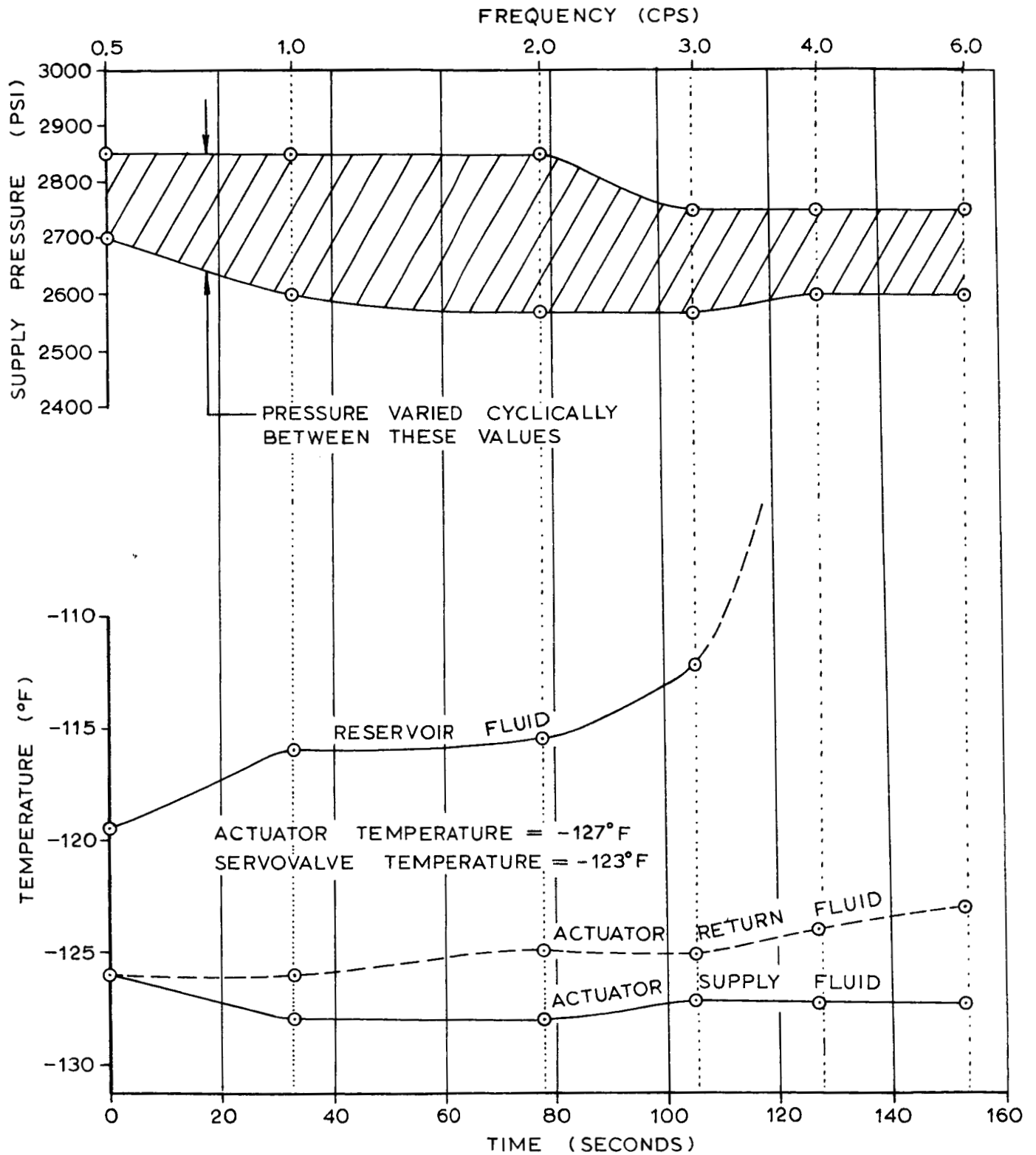


Figure 56: Fluid Pressure And Temperature During
A Typical Low Temperature Test Run

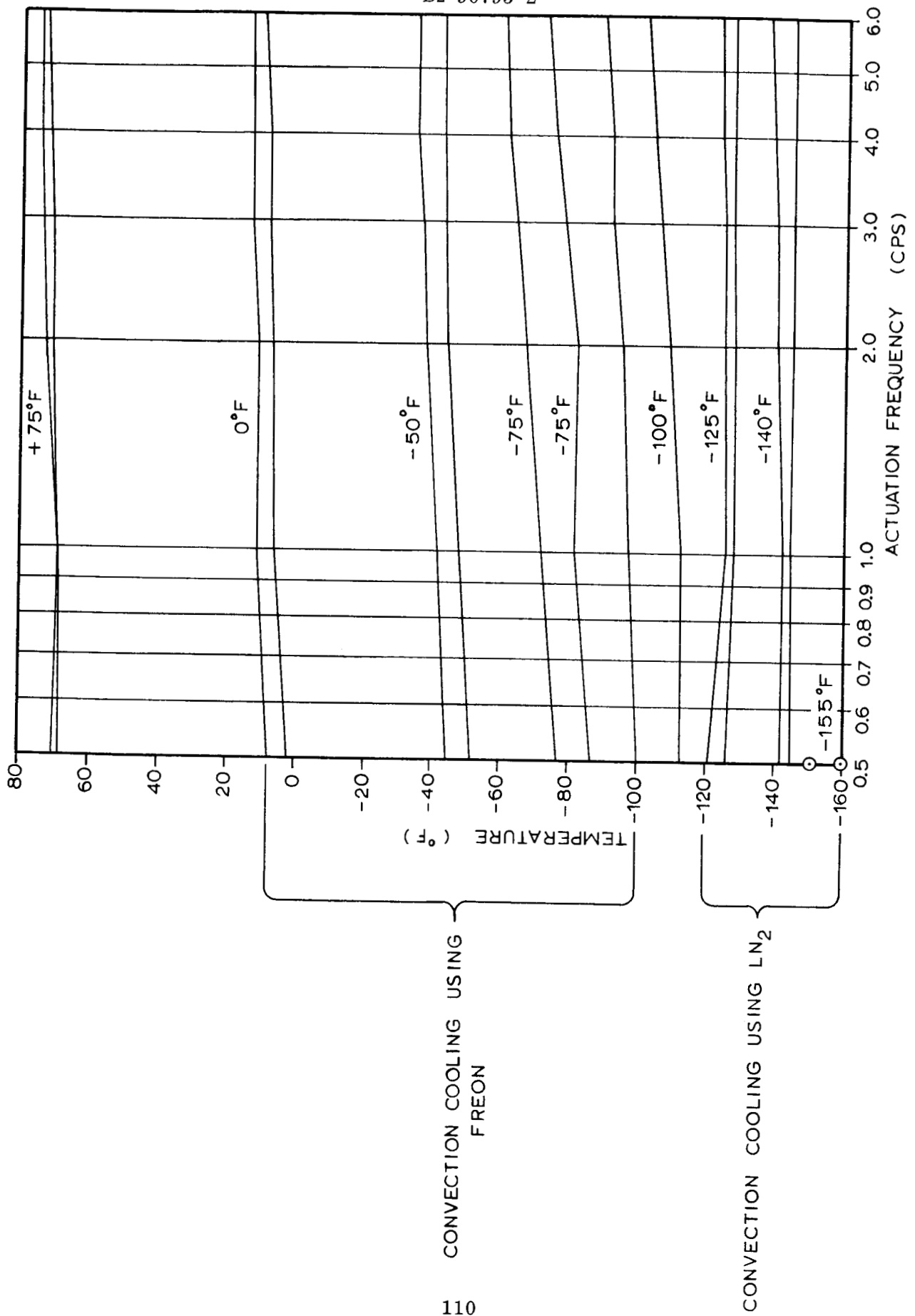


Figure 57: Low Temperature Tests-Temperature History

Fluid leakage past the dynamic seals was an order of magnitude less than the tolerable limit for missile systems. Further efforts to reduce operational leakage do not appear to be required except in space applications where extremely long mission durations using intermittently active hydraulic systems with low fluid capacity is a design requirement. Investigations toward this goal should consider the effects of squeeze on dynamic elastomeric seals and the resulting abrasion of seals during actuation.

The actuation-system response data indicates that system performance is adequate for flight-control applications at temperatures as low as -100°F . The response at temperatures below -100°F does not meet the TVC test requirements with the break frequency selected for the test system. By increasing the system gain, thereby increasing the break frequency, acceptable response at temperatures down to approximately -125°F would be expected throughout the frequency range evaluated in the test program.

The correlation between the E-3- and 5606-system test data indicates that further study should be devoted to analyzing the possibility of a general relationship between fluid viscosity and system performance. In conjunction with such an evaluation, it is recommended that the effects of fluid viscosity and temperature on servovalve performance, separate from a system, be investigated. Such an investigation could lead to design techniques that would extend the low-temperature capability for flight-control applications.

The baseline tests at the beginning and end of the low-temperature test series showed that no permanent degradation in the system resulted from operation at low temperature. Degradation due to contaminants in the system was eliminated by cleaning the filters. It was concluded that the contaminants were residual in either the reservoir or receiver as a result of construction of these vessels without providing accessibility for adequate internal cleaning. The concern pertaining to residual contaminants that are not detected during contamination level checks should be much greater for low-temperature operation. Degradation of supply pressure during operation at low-temperatures was shown to be due to increased pressure drop through the filters with high-viscosity fluid.

5.3 COMBINED-EFFECTS TESTS

Two combined-effects tests are included — a simulated flight test and a high-temperature test. The simulated flight test will investigate the combined effects of low temperature, vacuum, and intermittent system use. The high temperature test will investigate the use of the E-3 hydraulic system at the maximum expected lunar surface temperature.

5.3.1 SIMULATED FLIGHT TEST

The actuation system for the TVC flight-control task selected for simulation in the test program must be exposed to both low temperature and hard vacuum for about 144 continuous hours during a flight to the Moon. The actuation system will be operated during the flight to perform midcourse maneuvers and near flight termination for braking and landing maneuvers.

5.3.1.1 Objectives

The simulated-flight portion of the combined effects tests was performed to determine the combined effects of low-temperature and hard-vacuum environments on a hydraulic actuation system designed for space application. An equally important objective of the test was to investigate the capability to execute intermittent operational sequences without refurbishment or removal of the system from the space environment between sequences.

5.3.1.2 Facilities

To achieve the hard-vacuum requirements, the actuation system tested for low-temperature effects (Section 4.2) was installed in the CA-4 space chamber shown in Figure 58. The chamber can be evacuated to a vacuum of 8×10^{-9} torr when it is clean, dry, and empty. Access is provided by rolling the chamber back on rails from an adapter that contains connections to roughing pumps and a steam ejector. Final pumping is by a 35-inch-diameter, 50,000-liter-per-second oil diffusion pump. A liquid-nitrogen cooled baffle in the adapter prevents diffusion-pump oil from entering the test chamber. Penetrations to the chamber are available for supplying power and instrumentation and are also used as structural supports for mounting the system.

During testing, cooling of the test system was accomplished by radiation to the cold walls of the cooling container enclosing the test system. This container has been previously discussed in Section 4.3. A change in the method used to regulate liquid-nitrogen flow through the four cooling zones on the cooling container was made to provide automatic temperature control. A schematic diagram of the automatic temperature-regulation system is shown in Figure 59, and the photograph in Figure 60 shows the regulation equipment used.

A copper-constantan thermocouple sensed the temperature of each cooling zone. This temperature was then compared to a desired temperature for that zone by the controller. The desired zone temperatures were established to maintain near constant temperature distribution inside the cooling container. Each temperature controller actuated solenoids that allowed either liquid nitrogen or warm gaseous nitrogen to pass through the cooling coils of a particular cooling zone. Liquid nitrogen was allowed to flow when additional cooling was required and gaseous nitrogen when heating was required. The outlets from the cooling coils for all zones were brought into a common line and exhausted from the space-simulation chamber.

Prior to the simulated flight testing, the operational test system was disassembled for cleaning, inspection, and refurbishment of the loading apparatus. The actuator seals were inspected and all actuator dynamic seals and valve-interface seals were replaced. The lead pads on the load fixture were also replaced. The test system was reassembled and enclosed in the cooling container, and the entire package was mounted in the CA-4 space chamber.

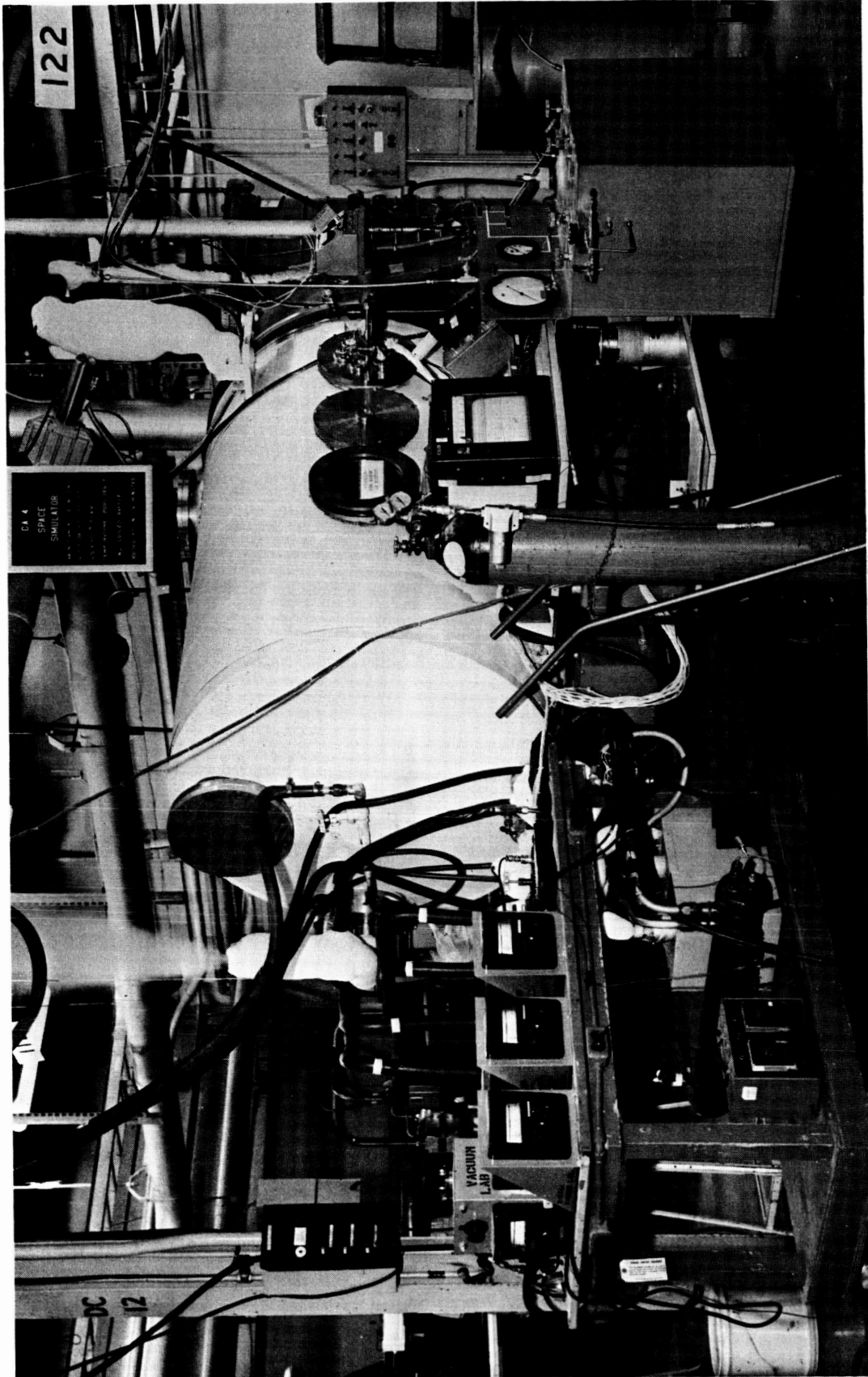
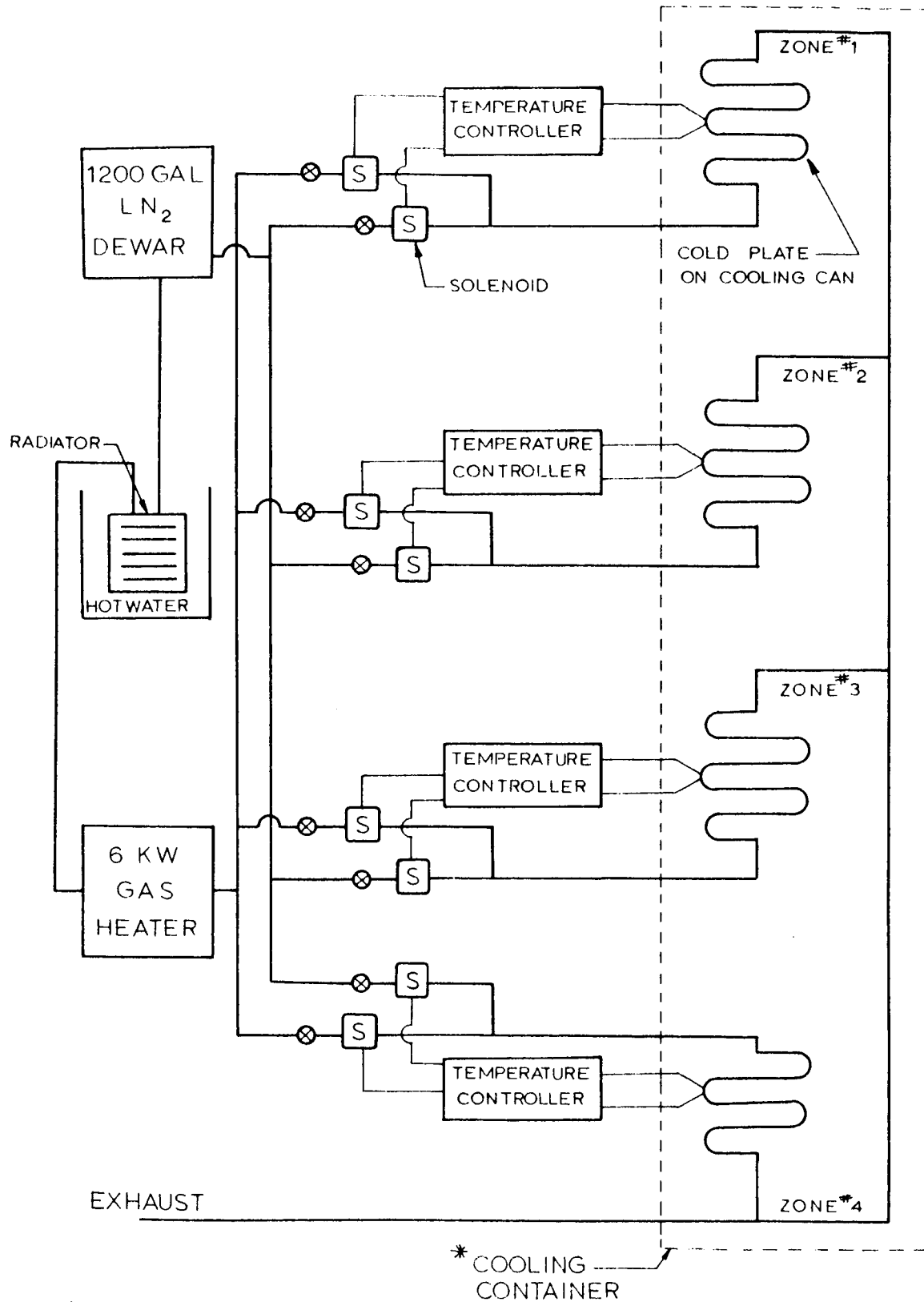


Figure 58: Space Simulator Facility



*SEE SECTION 4.3.3 FOR COOLING CONTAINER DESCRIPTION

Figure 59: Automatic Cooling System

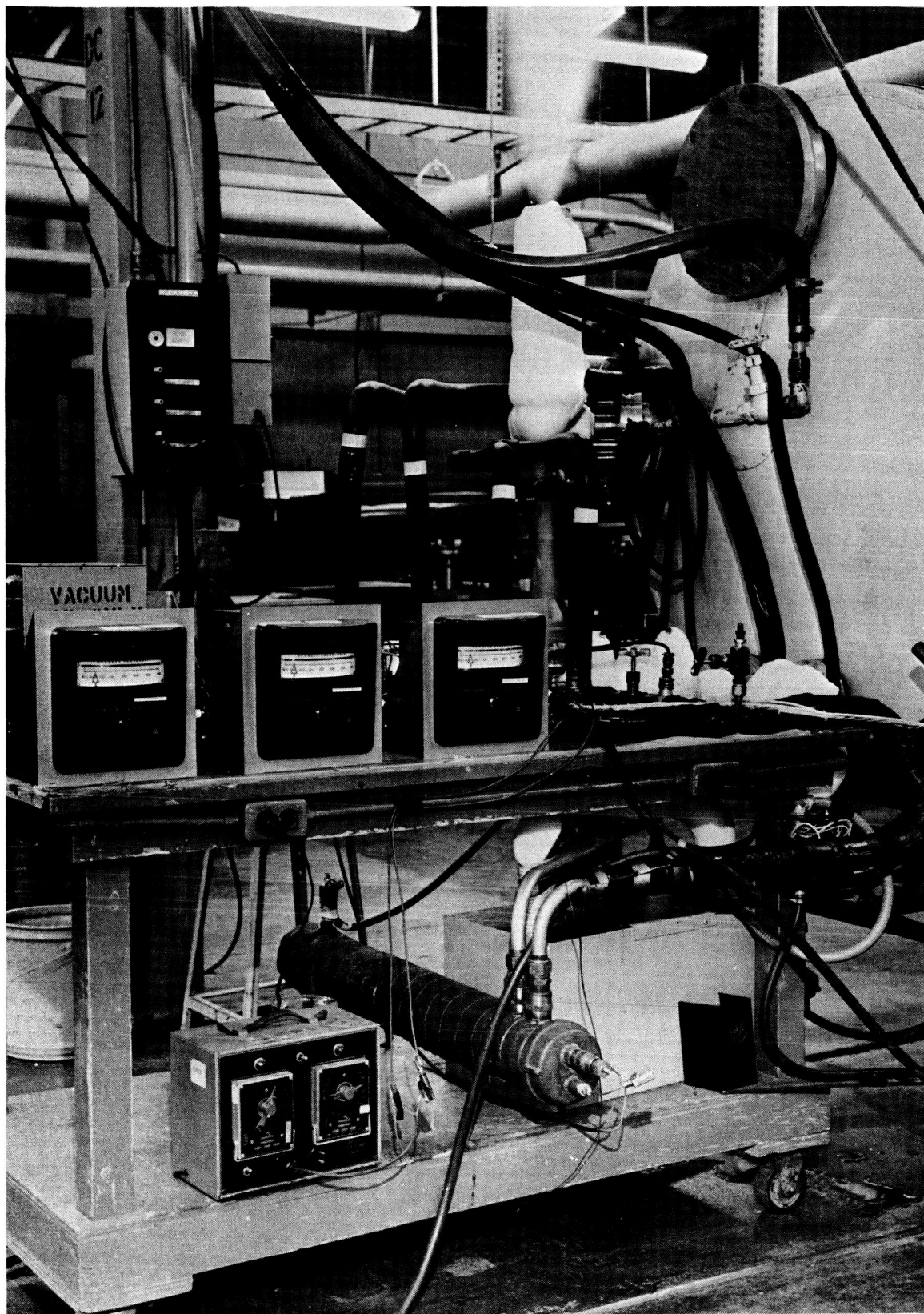


Figure 60: Automatic Temperature Controller

5.3.1.3 Procedure

The simulated flight test was designed to simulate the environmental soak and operational sequence for the RL-10 thrust vector control (TVC) function during flight and landing of a lunar vehicle. Environments to which the TVC actuation system would be exposed during such a lunar flight are -240°F and 10^{-13} torr vacuum pressure during the 144-hour flight. The actuation system would be operated at 72 hours to perform midcourse correction and at 144 hours to perform landing maneuvers. (These operational requirements are discussed in detail in Volume I, Section 5.3). The contract required simulated flight testing using environments of -240°F and approximately 10^{-8} torr vacuum. The test system was not capable of operation at -240°F , being limited to -140°F , as shown in Section 5.2, due to the high viscosity of the E-3 fluid. The simulated flight in the CA-4 chamber, therefore, reflects continuous protection of the actuation system by thermal conditioning to -140°F . The test system was subjected to the maximum vacuum capability of the CA-4 chamber. The instrumentation used in this test was described in Section 5.1.1 and is identical to that used in the low-temperature tests with the addition of environmental pressure measurement within the CA-4 test chamber.

Testing was initiated by performing an operational checkout, as described in Section 5.1.3, at room temperature and pressure. The friction load was adjusted to the same value used in the low-temperature tests (559 pounds) and the checkout repeated. The chamber and contents were then precooled to -95°F to evaluate the automatic cooling system. A vacuum sealing inspection was performed by reducing the CA-4 chamber pressure to within the 10^{-5} torr range.

During the test, temperatures were sampled at half-hour intervals throughout the inactive portion of the test and recorded continuously during the actuation periods of the test. Test-chamber pressure was sampled throughout the test at half-hour intervals, with readings taken immediately before and after the actuation periods of the test.

After 72 hours of soak in simulated space environments, the simulated midcourse correction maneuvers were attempted. Energizing of the servoactuator centering signal failed to result in motion of the actuator piston and load. The test was aborted and the valve filter was removed and found to be clogged. The servovalve filter was sonically cleaned in isopropyl alcohol and replaced. The micronic filter in the high-pressure line was also removed, cleaned, and replaced.

The contaminant removed from these filters was retained in filter paper for further investigation. The system was then reassembled, cycled to purge the system of any entrapped air, and the filters were rechecked to ensure that they remained clean. The chamber and contents were again precooled to -140°F , the chamber evacuated to minimum attainable pressure, and the 144-hour lunar flight simulation test restarted. The actuation sequence representing midcourse correction maneuvers was repeated at 72 hours without difficulty. At 144 hours, the system operational sequence was performed per Section 5.1.3 while maintaining the simulated space environmental conditions.

Subsequent to this operational sequence, the test chamber and contents were returned to room temperature and pressure and the operational sequence again performed. Leakage at the collection ports was measured. No problems were encountered during these operational sequences.

5.3.1.4 Results

Test conditions at the 72-hour aborted operational test showed that the differential pressure across the actuator piston was steady at 400 psi, while approximately 1400 psi was required to overcome the 559-pound friction load. The 0.5-cps sinusoidal signal also failed to vary the differential pressure from 400 psi. Since the differential pressure did not change, it indicated that the valve spool was not moving because of being stuck or because insufficient differential pressure was available to move it. This was caused by a clogged servovalve filter. The increased viscosity of the fluid at low temperature and the clogged filter resulted in a pressure below that which was needed to move the valve spool.

Plots of the temperature and pressure within the cooling container in the CA-4 chamber are shown in Figure 61 for the continuous 144 hours of test. It will be noted that the average chamber vacuum (10^{-6} torr) is not as high as the 8×10^{-9} torr maximum capability of the pumping equipment. This is due to the fact that the large amount of equipment installed in the chamber could not be cleaned sufficiently to prevent outgassing. This is evidenced further from the data in Figure 61, showing that the average pressure continued to decrease throughout the 144-hour test.

Fluid leakage by the dynamic seals, measured at the seal gland collection ports, was found to be 0.5 cubic centimeter in each measuring port. This amount of leakage is considered insignificant for the application tested.

The frequency response data obtained during the 72-hour and 144-hour operational tests is shown in Figure 62. Data in this figure also shows the comparison of room-temperature operation before and after the simulated flight test. This data shows a slight decrease in the system response after the test. The data both before and after the simulated flight, however, fall within an envelope of previous room-temperature and pressure test curves obtained during low-temperature testing. The decrease in response noted after the simulated flight test is, therefore, attributed to minor random inconsistencies in the system, not to system degradation. The response data obtained while in space environments was lower than that at room temperature and pressure. The data does not perfectly agree with data obtained during the low-temperature test series. Differences were caused by the effects of such things as refurbishment of the loading system between the low-temperature and simulated flight tests. The data trend, however — showing lower response at low temperature — is the same as that in previous tests. There is no reason to believe that hard vacuum affected the operation of the actuation system.

Investigation of the contaminant in the filters showed that the contaminant was sand, introduced to the system prior to assembly. The sand remained in the system because of difficulty in cleaning the hydraulic fluid reservoir and receiver.

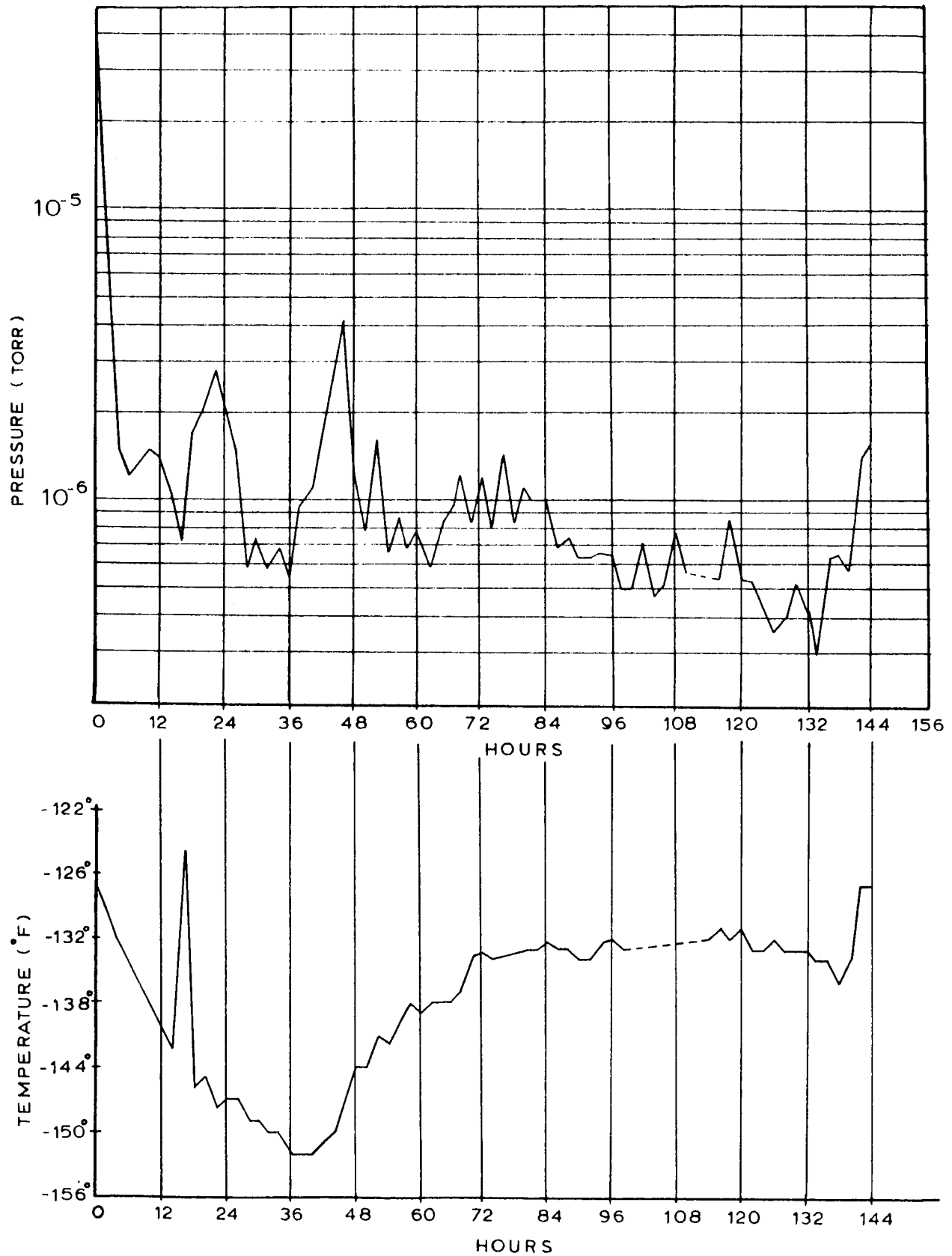


Figure 61: Environmental History — Simulated Flight Test

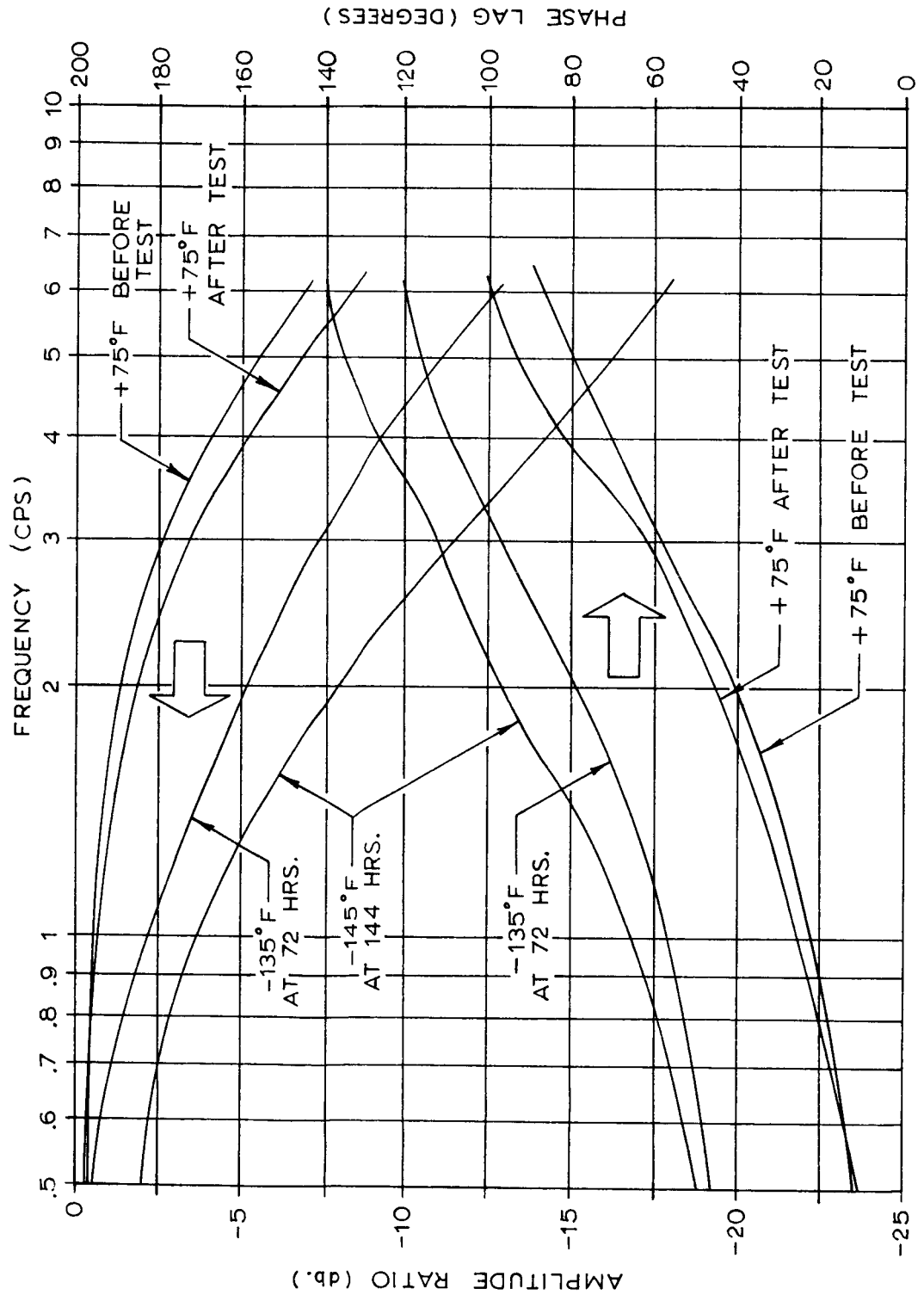


Figure 62: Simulated Flight Test System Response Data

5.3.1.5 Conclusions

This test demonstrates that a hydraulic actuation system using DuPont E-3 fluid with thermal protection to -140°F could be used a number of times in space environments with periods of inactive storage between uses. The hard vacuum and low temperature caused no more than normal seal leakage and the amount of fluid lost would not affect the mission simulated. The effects of the simulated flight test did not produce a change in the operational capability of the system. The system operational response in space environments, compared to room-temperature conditions, is definitely lower because of the increase in E-3 fluid viscosity. The required abort of the test at space environments shows that contamination control is extremely important when fluid viscosity is very high.

5.3.2 HIGH-TEMPERATURE TEST

The usefulness of hydraulic systems in space depends on the capabilities of these systems to operate at high temperature on some applications as well as at low temperature. Because both high- and low-temperature capabilities are needed, the temperature range in which space hydraulic systems are required to operate is greater than that for airborne missile or aircraft applications. The E-3 fluid selected for this test program was chosen for its low-temperature properties, however, its high temperature characteristics were also considered.

5.3.2.1 Objectives

The high-temperature portion of the combined-effects test was performed to determine the effects of a simulated maximum lunar surface temperature environment on the hydraulic test system. The requirement for hard vacuum is not imposed during this test since vacuum exposure for short durations has been shown in Reference 1 to have no effect on system performance.

5.3.2.2 Facilities

No changes in the installation used in the simulated flight test, reported in Section 5.3.1, were made for the high-temperature test. The test was performed immediately following inspection of the system after the simulated flight. The CA-4 space chamber was used as the test facility even though the vacuum capabilities of the chamber were not used. The heating capabilities of the chamber, provided by electrical resistance strip heaters within the chamber walls, were used. These heaters produce a maximum of 350°F ambient temperature within the chamber.

The heating facilities of the CA-4 chamber were supplemented by the injection of hot gaseous nitrogen into the chamber and through the cooling-container coils. The gaseous

nitrogen temperature was regulated by the temperature controllers as described in Section 5.3.1.2 in a manner similar to the control of liquid nitrogen for cooling.

5.3.2.3 Procedure

The temperature of the test system was stabilized at 275°F. An attempt was made to adjust the friction load to provide the total load of 559 pounds used in all previous tests. The load adjusting mechanism did not allow load reduction below a total of 780 pounds, because of the different expansion of materials of the loading components. Because only one test at high temperature was to be performed, this high load was accepted rather than a modification of the loading apparatus.

The test was conducted by operating the system and obtaining data points at discrete actuation frequencies of 0.5, 1, 2, 3, 4, and 6 cycles per second rather than scanning the frequency range. This procedure was used because it required less fluid than the scanning test. With the low viscosity of the fluid at high temperature, the scanning test could not be completed with the fluid capacity in the system. Between each of the frequencies tested, the actuator was centered during reset of the oscillator in the frequency-response analyzer. With the exception of this revised method of input control, the procedures for data acquisition in Section 5.1.1 were followed.

Before and after the high-temperature test, the system was operated at room temperature, using the procedures of Section 5.1.3. The baseline sequence after the high-temperature test was performed at the high-load condition used during the high-temperature test. Comparison of the high-load and normal-load tests was made to adjust the results of the high-temperature test. The system was inspected at completion of the testing, and leakage from the gland leakage collection tubes was measured.

5.3.2.4 Results

Performance of the test system during the operational sequence at high temperature was satisfactory. Seal leakage was 0.05 cubic inches at the rod-end gland and 0.04 cubic inches at the head-end gland. This amount of leakage is insignificant for the simulated application.

Figure 63 shows the comparison of room- and high-temperature system response data at the high-load condition to the corrected response for the normal-loading condition. The system amplitude ratio and phase lag curves at the normal-loading condition are comparable to low-temperature test performance characteristics for a temperature between -100 and -125°F.

Figure 64 shows the response characteristics of the system before and after the high-temperature test for the normal-loading condition. The results of these tests are similar. The operation after the high-temperature test indicates improvement over operation before the test. However, both the before and after test data points fall within the envelope of other baseline runs at 75°F, as shown in Figure 64.

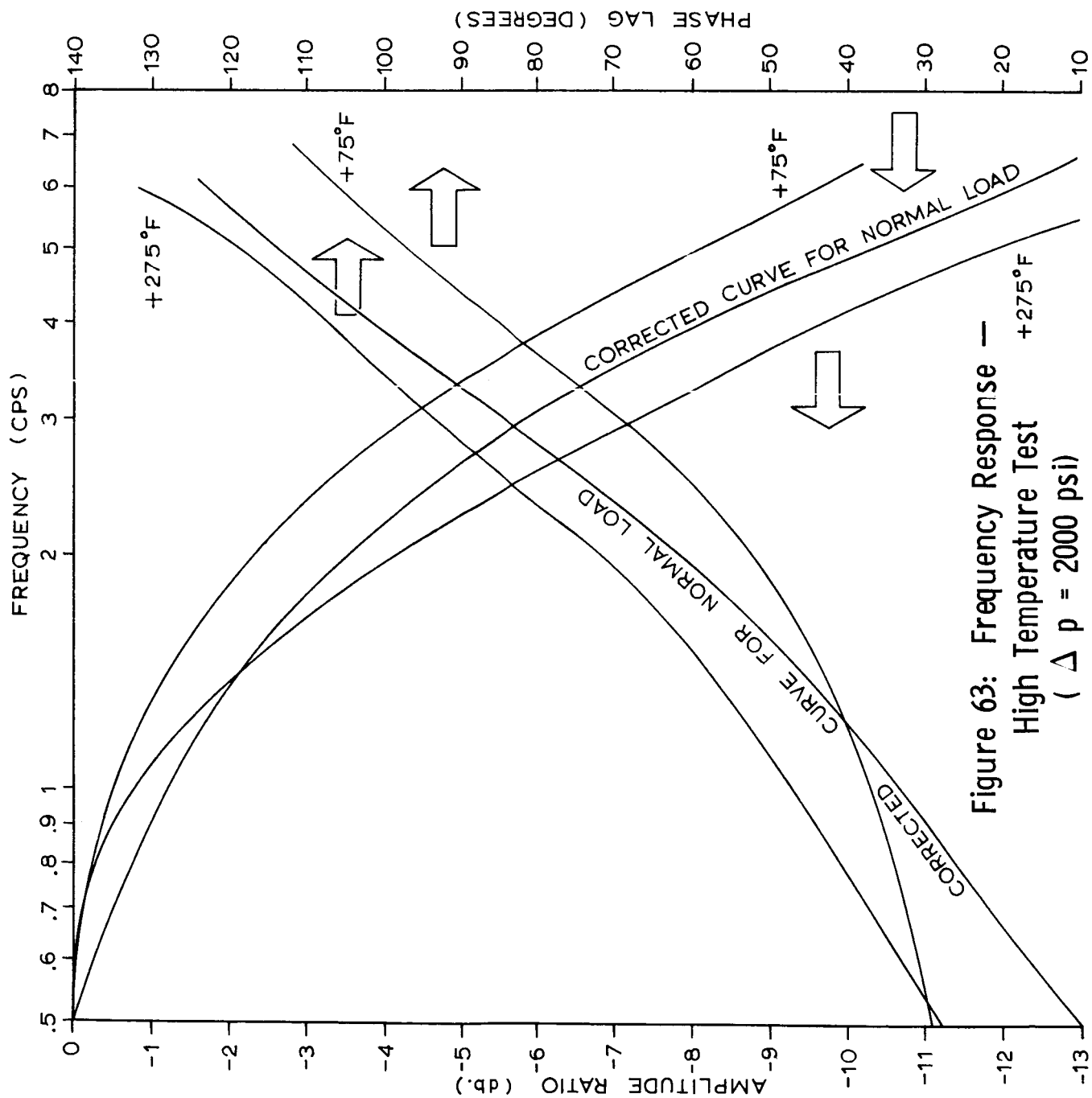


Figure 63: Frequency Response —
High Temperature Test
($\Delta p = 2000 \text{ psi}$)

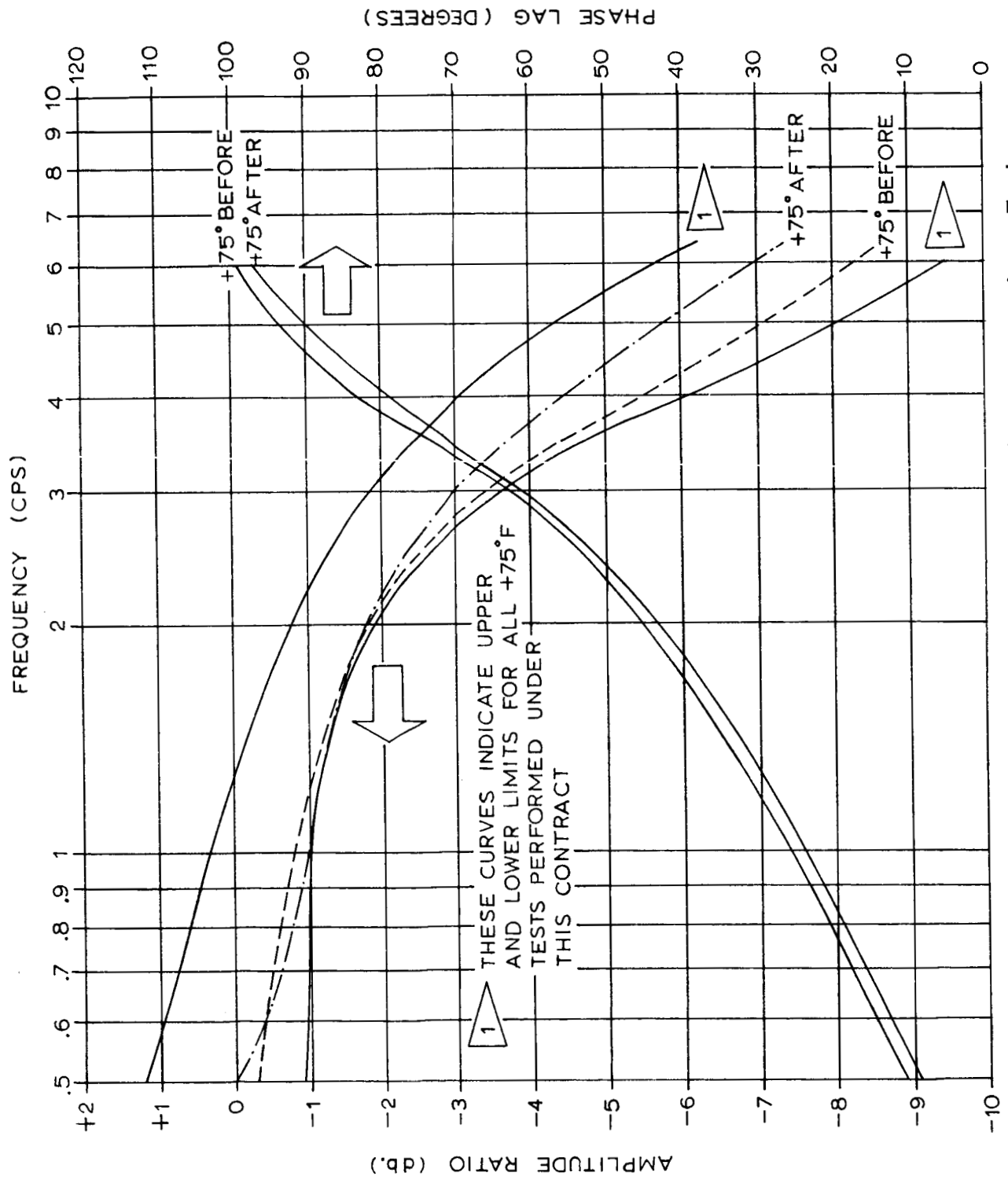


Figure 64: Frequency Response — High Temperature Test

5.3.2.5 Conclusion

The hydraulic actuation system tested was capable of satisfactory operation when exposed to a stabilized environment of 275°F. The effects on the operational characteristics of the system are due to the low viscosity of the fluid and are comparable to effects caused by high viscosity at low temperatures.

Because the test system was a single-pass blowdown system, the low fluid viscosity of 0.3 centistoke did not produce operational problems. Further investigation of the potential problems with the operation of recirculating systems using low-viscosity fluids is necessary prior to incorporation of such systems in space applications. In a recirculating system, The E-3 fluid viscosity resulting from the 275°F environment would be further decreased by temperature increases resulting from pumping and throttling losses. It is not known whether fluids at such lower viscosities can be pressurized by existing piston pumps, especially if the pump is also required to maintain fluid flow at viscosities of 3000 centistokes or greater at low temperatures.

5.4 THERMAL CYCLING TEST

An environmental condition for the TVC system on the lunar landing vehicle is the exposure of the inactive system to the cyclic variation of lunar surface temperatures. The system must be able to withstand this thermal cycling if it is to be used during return to orbit from the lunar surface.

5.4.1 OBJECTIVES

The objectives of the thermal cycling test were to determine the changes that would occur in the operational characteristics of a hydraulic system as a result of 100 hours of cycling between +275°F and -240°F. The +275°F and -240°F temperatures were selected as the maximum and minimum system environmental temperatures expected in lunar applications if suitable reflective coatings were the only thermal protection.

5.4.2 FACILITIES

The thermal cycling test required both high cooling and high heating rates to control temperature fluctuations. These rates could not be provided using the cooling container with liquid and gaseous nitrogen flowing in the coils. The temperature regulation system used for the thermal cycling test is shown in Figure 65. The servoactuator was wound with a coil of perforated copper tubing and wrapped with a blanket of insulating material. Liquid nitrogen or hot gaseous nitrogen was supplied to the copper tubing by direction of a temperature controller. Temperature sensing for the controller was provided by a copper-constantan thermocouple on the actuator. Thermal control of the hydraulic-fluid reservoir was accomplished by winding the reservoir with alternate coils of copper tubing and electrical-resistance heating tape. The heating tape was used because the rate of temperature rise could not be attained using only gaseous nitrogen, due to the large mass of fluid requiring heating. Temperature controllers were used to direct liquid or gaseous nitrogen flow in the tubing and to control current flow in the resistance

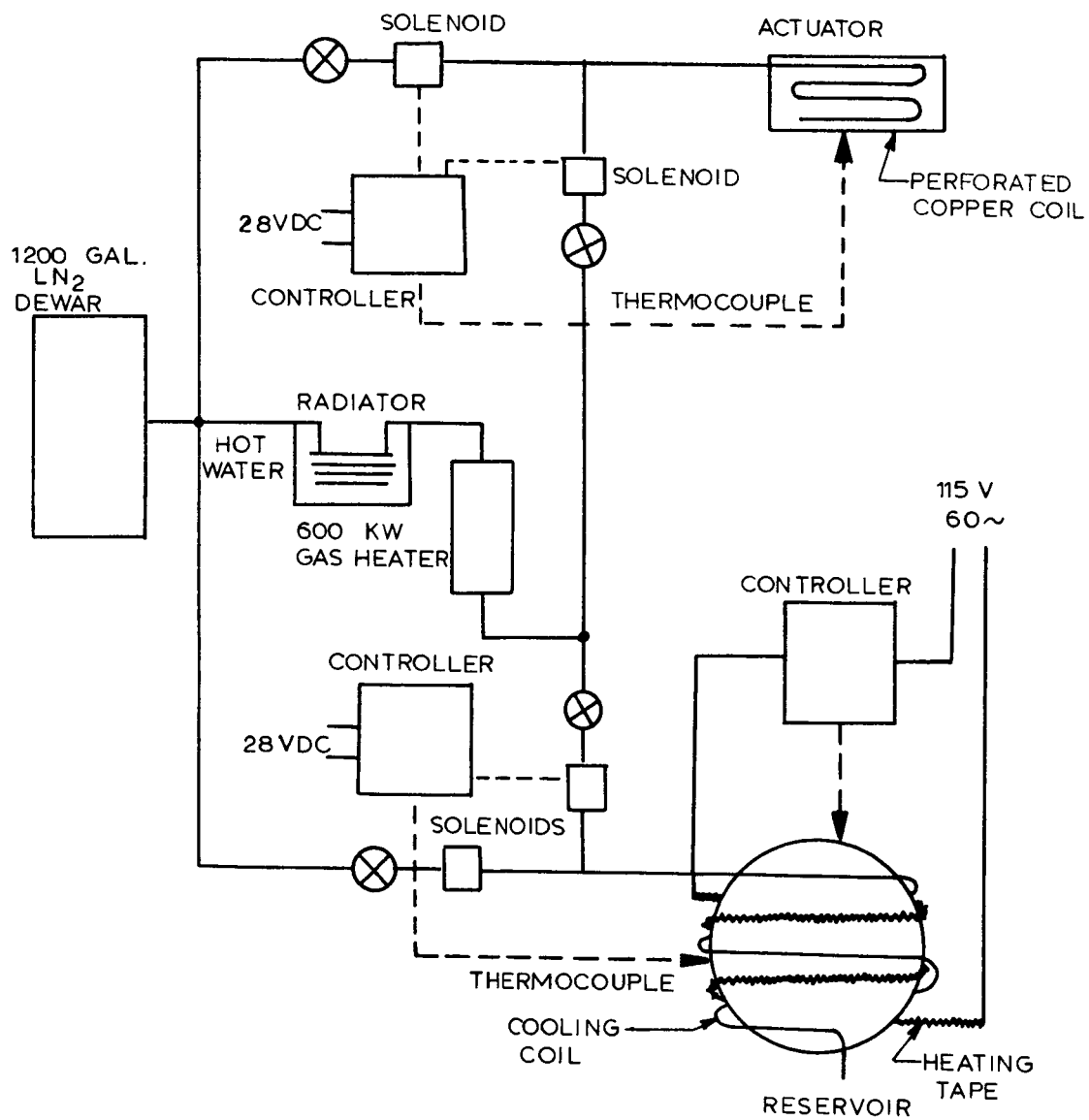


Figure 65: Thermal Cycling Temperature Control

heating tape. The short lengths of tubing connecting the reservoir to the filter and the filter to the actuator acted as conductors to heat or cool this portion of the test system.

5.4.3 PROCEDURE

Before thermal cycling, a test was performed at room temperature, as described in Section 5.1.3, to establish operational characteristics for comparison with a duplicate room-temperature operational sequence after the test.

The 100-hour test requirement was divided into 15 cycles of 7 hours (totaling 105 hours), as shown in Figure 66. By considering the 3.5 hours above 0°F as a lunar day and the 3.5 hours below 0°F as a lunar night, the 105 hours of testing simulates more than 2 years of thermal cycling on the Moon's surface near its equator. Some experimenting was necessary to determine the proper temperature-controller settings to achieve the time-temperature relationships shown in Figure 66. The actuator body temperature was used as the control point for the test, and the reservoir was programmed to follow this control as accurately as possible. Temperatures throughout the system were monitored each 15 minutes on a multiple-point stamping recorder. The remainder of the data acquisition system is described in Section 5.1.1 and was not changed from previous tests. Following room-temperature operational testing after completion of thermal cycling, the Number 1 servoactuator was removed from the test installation, disassembled, inspected, and stored.

5.4.4 RESULTS

Twenty thermal cycles were completed, the first five being used to adjust the temperature controllers and to determine temperature reversal times. Figure 67 shows the time-temperature history for the last 15 cycles, which were performed in a continuous test. The operational characteristics of the system before and after thermal cycling are shown in Figure 68, which indicates that no permanent changes in the system resulted from the effects of thermal cycling. No leakage was found in the leakage collection tubes.

The only signs of wear revealed by the actuator disassembly were in the elastomeric rod-gland seals and the piston seal. Photographs of these seals are shown in Figure 69. The wear represents abrasion during the simulated flight, high-temperature and thermal cycling tests, and operational checkouts and calibrations performed between these tests. The black-ring deposit on the piston seal was a chrome and nickel compound, which was also found on the actuator seal following the low-temperature series of tests.

5.4.5 CONCLUSIONS

Thermal cycling between the temperature limits that constitute the probable minimum and maximum temperatures to be encountered on the lunar surface caused no change in the operational capabilities of the hydraulic actuation system. The test showed that the fluid in a space actuation system can be allowed to freeze without damage or detrimental effects on the system. Cycling did not affect the elastic properties of the seals or cause increased fluid leakage.

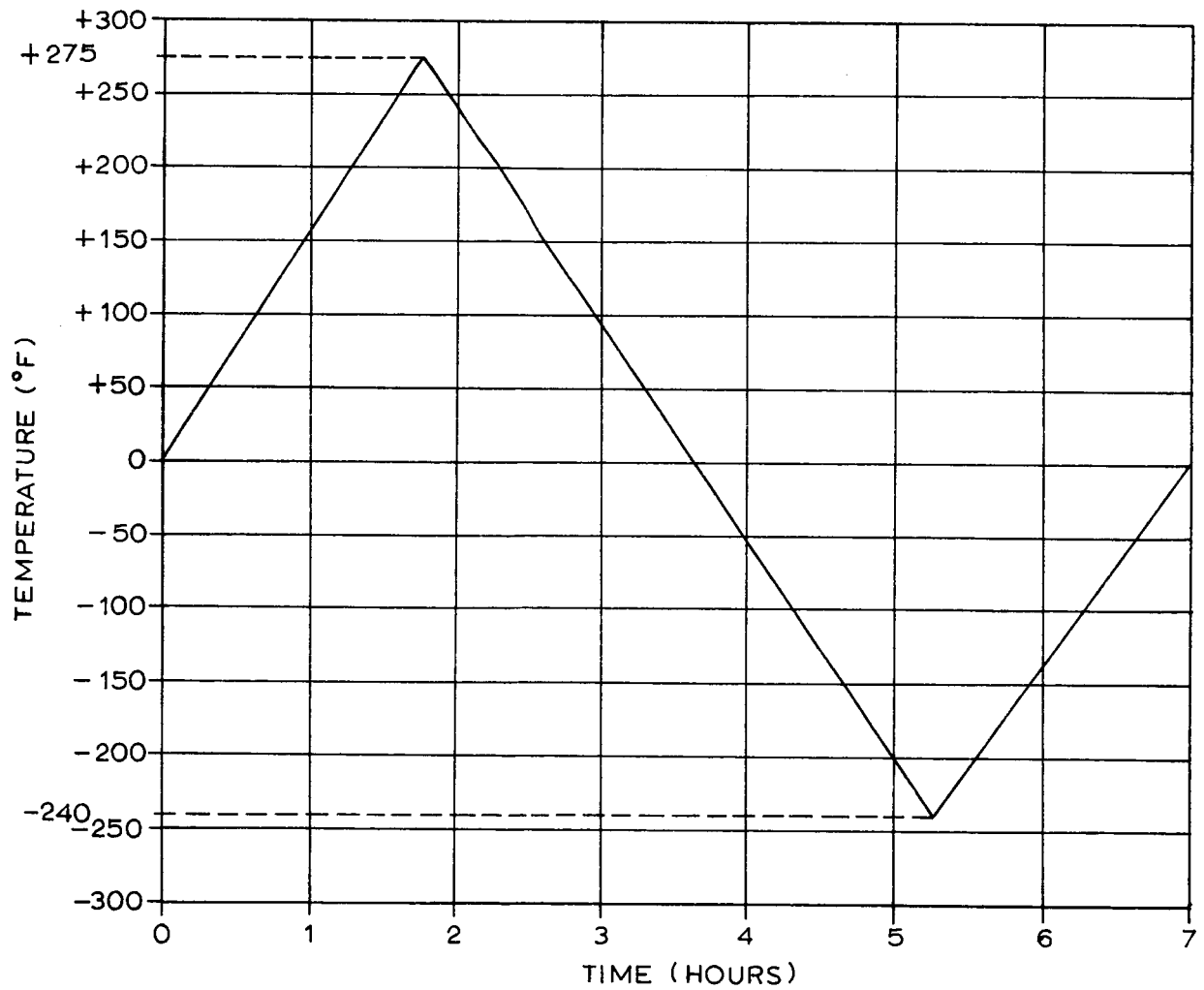


Figure 66: Typical Thermal Cycle

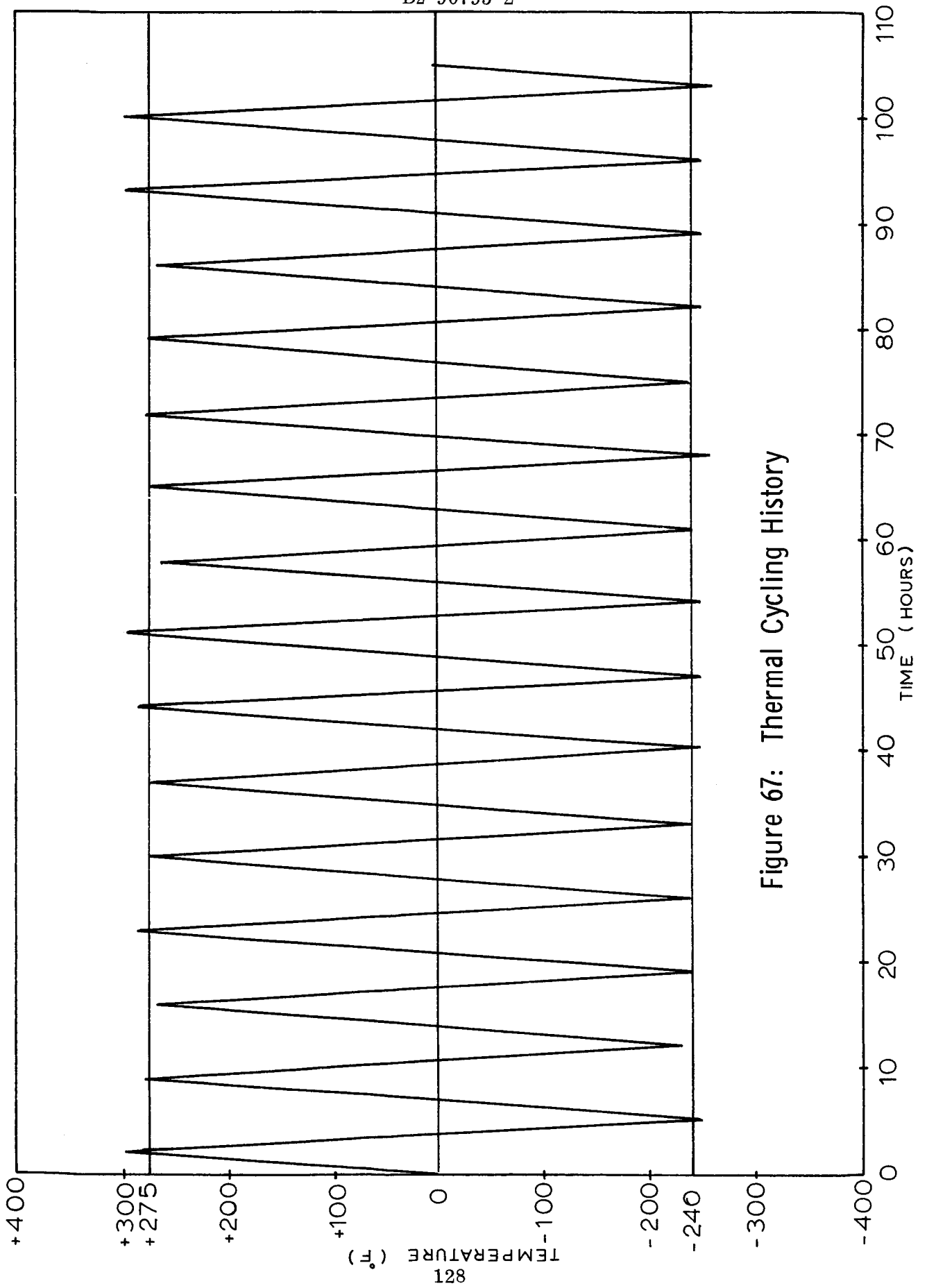


Figure 67: Thermal Cycling History

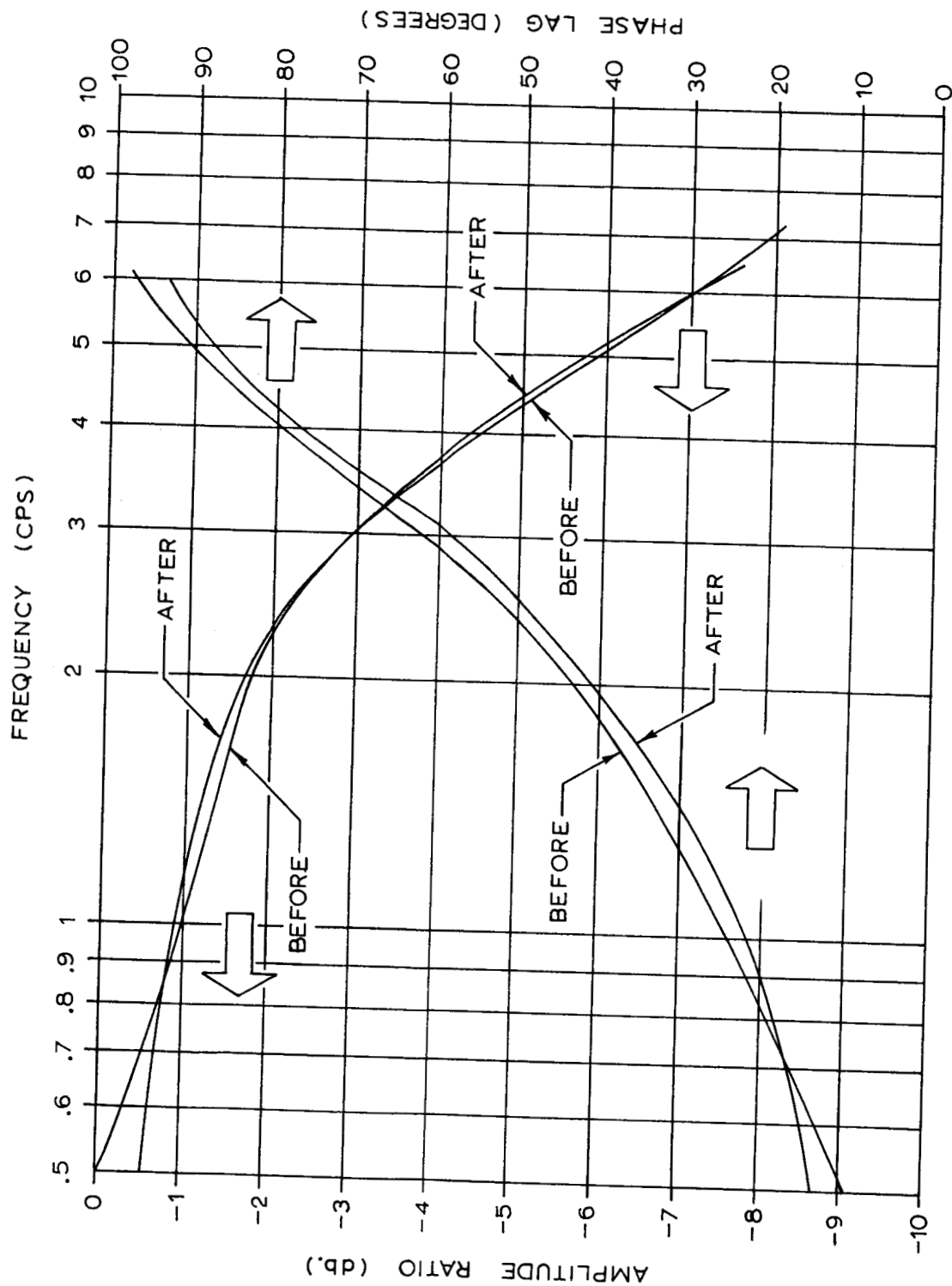


Figure 68: System Response-Thermal Cycle Test

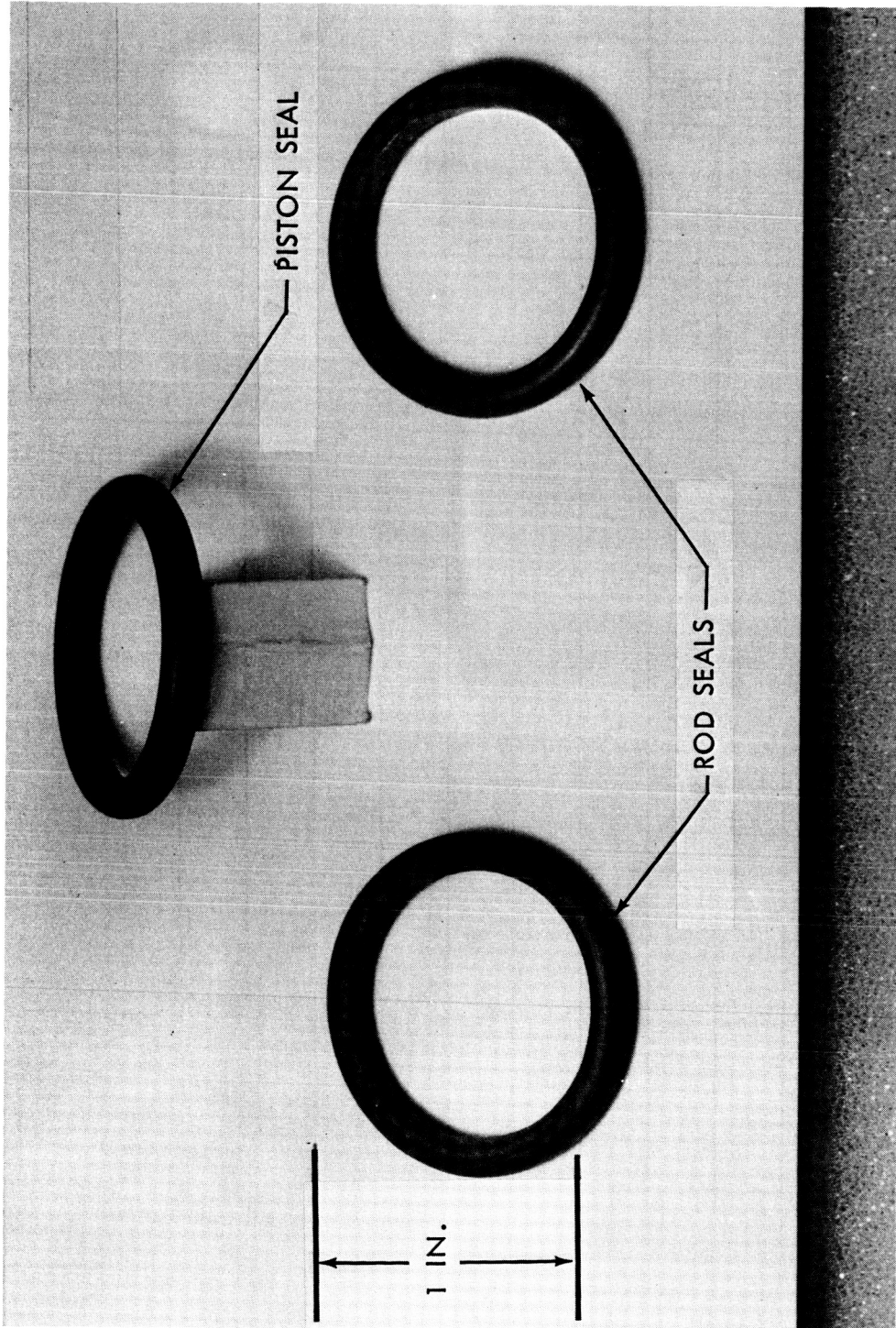


Figure 69: Seal-Wear Actuator Number 1

5.5 VACUUM TESTS

The hard-vacuum environment encountered by hydraulic systems in space imposes requirements that have not been investigated. The effect of elastomeric-seal exposure to hard vacuum for long durations is unknown. Short-term tests of potential hydraulic-system materials that outgas in a hard vacuum have shown no evidence of deterioration in these materials. One such test is described in Reference 1.

5.5.1 OBJECTIVES

The objectives of the vacuum tests conducted in this contract were to determine the deteriorating effects of continuous long-term hard-vacuum exposure on elastomeric seals and other outgassing materials used in a typical space hydraulic system. The seriousness of hydraulic fluid leakage encountered during such long-term storage was also evaluated.

5.5.2 FACILITIES

The vacuum container described in Section 4.3.1 as part of the vacuum storage assembly described in Section 5.1.2.3 was the major facility item used during the vacuum tests. This container provided the means of isolating the servoactuator at hard vacuum during the storage portion of the test and during transfer and installation of the vacuum storage assembly into the operational-test-system load fixture. The storage portion of the vacuum tests was performed with the vacuum test assembly installed on a small pumping system to maintain a hard-vacuum environment. A schematic of this installation is shown in Figure 70, and a photograph of this vacuum storage station is shown in Figure 71.

The pumping portion of the vacuum storage station employs a 6-inch oil-diffusion vacuum pump with a liquid-nitrogen-cooled cold trap to prevent diffusion pump oil from entering the vacuum storage container. The 6-inch diffusion pump is capable of 7×10^{-7} torr vacuum pressure under no-load conditions without the cold trap. Addition of the cold trap allows approximately 10^{-8} torr vacuum to be pumped. The oil-diffusion-pump fluid, heated to form a vapor, rises from a boiler through concentric chimneys from which it is then projected downward through nozzles at supersonic speed. These streams of vapor trap the gas molecules from the chamber being evacuated and propel them forward in the direction in which the roughing pump is drawing gas. The vapor then condenses on the cooled walls of the pump, returns to the boiler, and the cycle is repeated. The gas molecules are exhausted by the mechanical roughing pump. To increase the reliability of the pumping system, a 4-inch diffusion pump was added in series with the 6-inch pump, between the 6-inch pump and the 13-cfm rotary mechanical roughing pump.

The operational portions of the vacuum tests were conducted in the CA-4 space chamber, described previously in Section 5.3.1.2, and used for all tests except the low-temperature series tests. The operational test system, described in Section 5.1.2.2, less the Number 1 servoactuator, was retained in the CA-4 chamber for this test and was connected to the hydraulic support assembly, described in Section 5.1.2.4, located outside the test chamber.

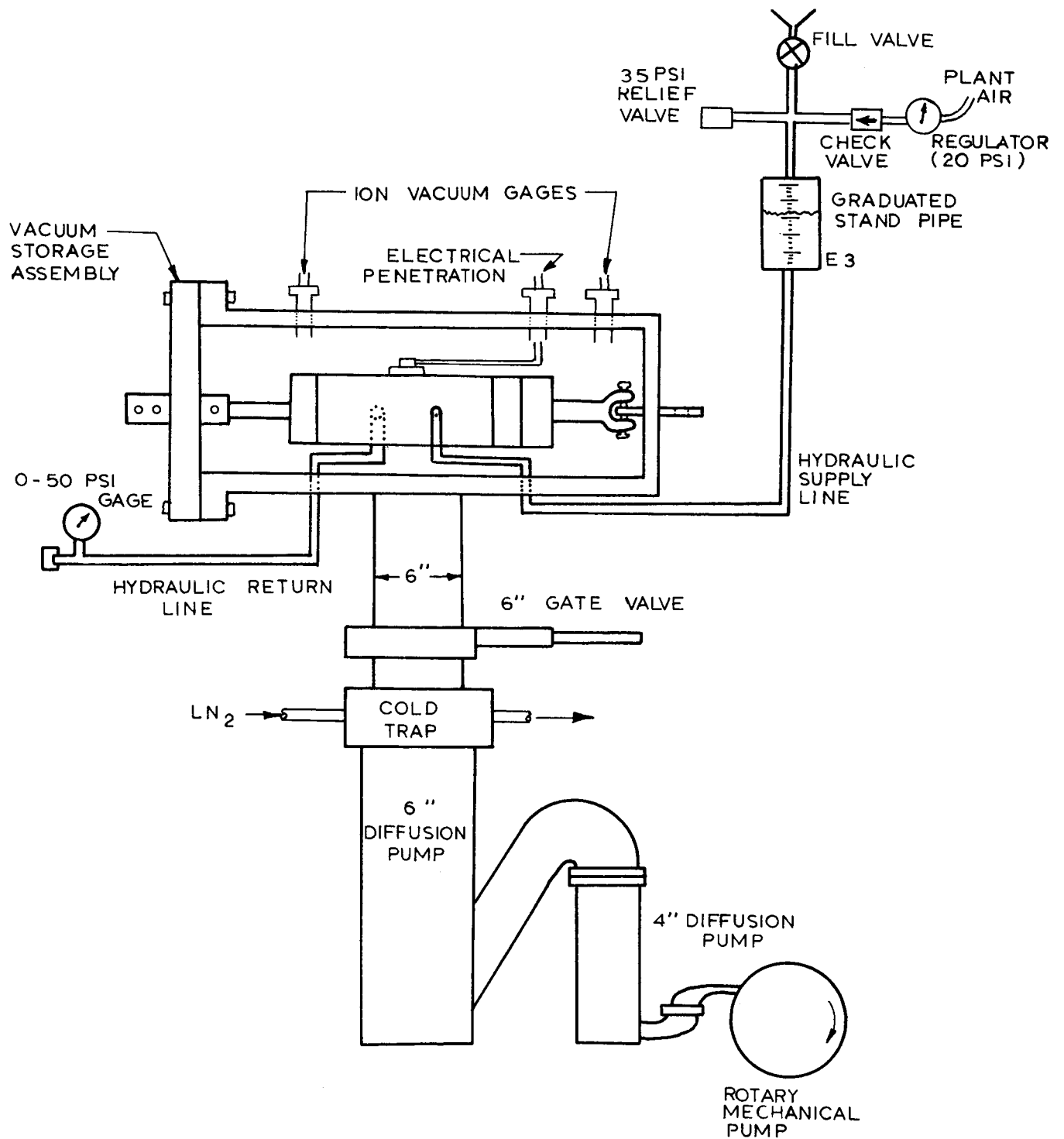


Figure 70: Vacuum Storage Station Schematic

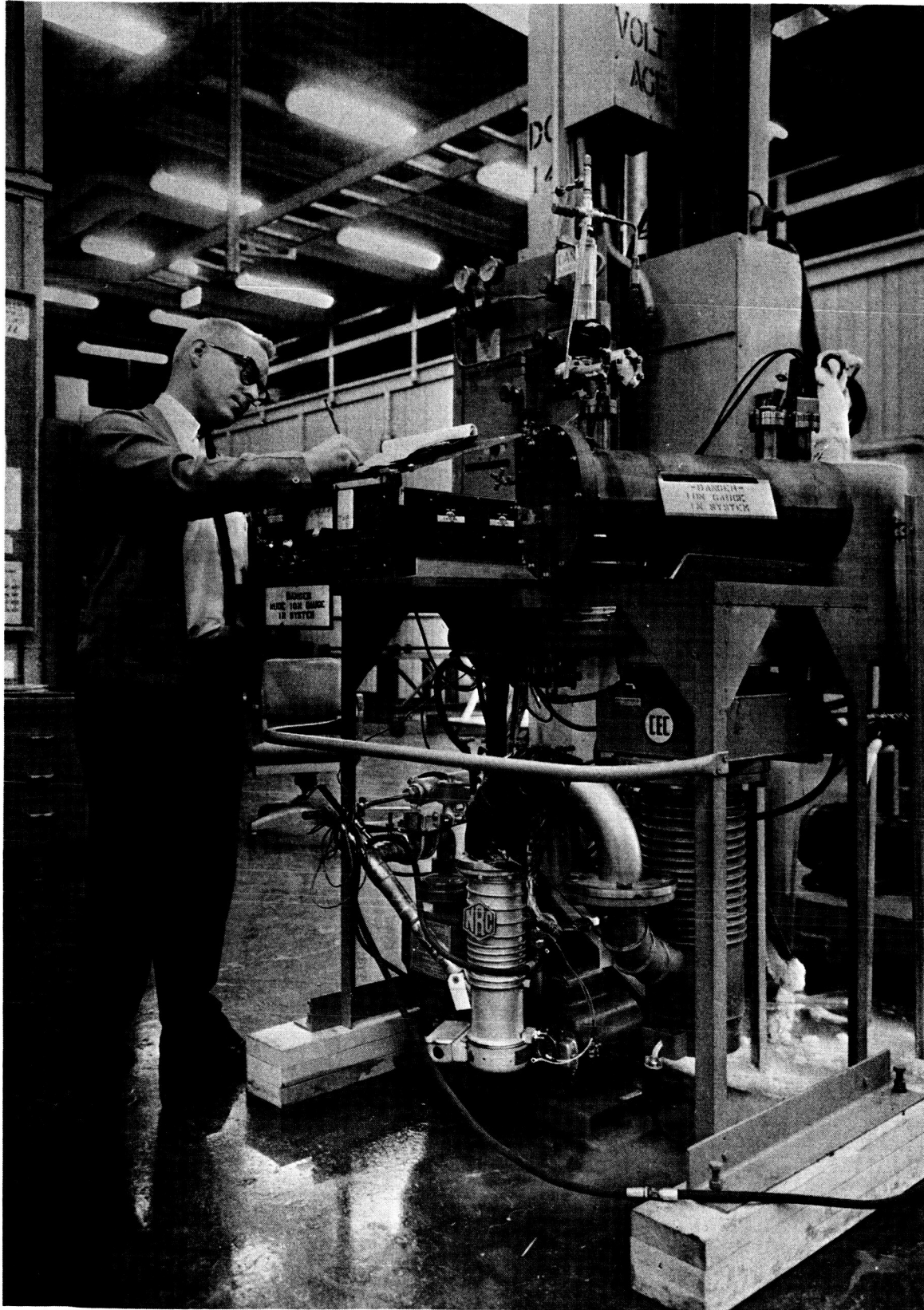


Figure 71: Vacuum Storage Station

5.5.3 PROCEDURE

The method selected to accomplish the test objectives was to store the Number 2 servo-actuator in hard vacuum for 5 months. Subsequent to storage, the actuator would be operated as part of the test system, without removing it from the vacuum environment, to evaluate seal deterioration, possible vacuum effects on leakage rate, and permanent degradation in servoactuator operation. The servoactuator was selected as the component for storage because both static and dynamic seals were exposed to hard vacuum, as were electrical leads and potting materials in connectors for input control to the valve.

The servoactuator was stored at room temperature. In this condition, material molecular activity and outgassing are more severe than at low-temperature vacuum storage, and do not alter the test results other than to accelerate the possibility of material deterioration.

A baseline operation test of the Number 2 servoactuator was performed before vacuum storage. After placing the vacuum storage assembly on the pumping station, the pressure within the vacuum container was reduced to about 10^{-5} torr within 1 hour. Pressure measurements were read manually from the readout instrument for the hot cathode ionization gage installed in the assembly. The fluid stand pipe was pressurized to 20 psi. After 48 hours of storage, a rise in the environmental pressure indicated saturation of the cold trap with condensed E-3 leakage. At the end of 5 days, the storage test was suspended to clean the cold trap and to investigate this leakage problem. The fluid leakage rate past the seals was evaluated by increasing the fluid pressure to determine whether this would assist sealing or increase leakage.

The servoactuator was disassembled, all seal grooves cleaned, and new seals installed with the addition of an O-ring in the redundant groove of each seal gland. Subsequent to parts assembly of the actuator, a helium leak check was performed. The vacuum storage assembly was reassembled and mounted on the test station. Pressurization of the fluid in the stored actuator was discontinued to improve the ability to maintain a hard vacuum. The E-3 fluid in the stand pipe was vented to the atmosphere by leaving the cap on the pipe loosely threaded to ensure that the fluid would remain at atmospheric pressure.

The vacuum storage test was restarted, and the maximum possible vacuum condition was maintained for 134 days. After completing the storage portion of the test, the gate valve was closed and the storage assembly was installed in the load fixture of the CA-4 test chamber. The bolts attaching the lid to the vacuum container were removed and the CA-4 chamber was closed. The pressure in the CA-4 chamber was then reduced to the maximum attainable vacuum under this condition (8.3×10^{-6} torr). This chamber vacuum is not as low as possible because of the large amount of equipment in the chamber and the difficulty in cleaning the equipment to prevent outgassing. The extension of the actuator rod and attached storage container lid during the initial step of the operational sequence, as described in Section 5.1.3, equalized the vacuum environment in the CA-4 chamber with that of the storage container. The remaining operational sequence was completed, and the test chamber was pressurized to 1 atmosphere. The operational sequence that preceded the vacuum storage was repeated for comparison purposes.

The load adjustment during the operational sequences was not conducted because installation of the Number 2 servoactuator in the vacuum container necessitated elimination of the differential piston pressure measurement. The adjustment used to calibrate the friction load was to measure the length of the loading spring corresponding to the desired load, as determined using the Number 1 actuator, with the installed pressure transducers.

After completion of the testing, the actuator was removed, disassembled, and the components and seals inspected. The actuator and other parts of the test system were then cleaned and stored.

5.5.4 RESULTS

The fluid leakage rate and the accompanying container environment during the initial 5 days of storage are shown in Figure 72. It was found that 2100-psi pressurization increased the leakage rate by a factor of 10 over the leakage at 20 psi. The actuator disassembly following these 5 days showed the presence of a black flaky residue on the O-rings and in the grooves of the glands and piston. This material was residual masking or plating material used during plating of the glands and piston and was removable by flushing. Parts were thoroughly swabbed to remove this material before reassembly.

The helium leak check after reassembly showed that a small amount of helium could be detected at the valve/actuator interface and at the leakage measuring ports. The helium check showed no indication that E-3 leakage would occur at these locations, but provided evidence of potentially weak sealing installations.

When clean, dry, and empty, the vacuum storage container was pumped down to 10^{-8} torr on the vacuum storage station. The vacuum achieved during the storage test, shown in Figure 73, had a limit of 10^{-6} torr. This limit was due to some leakage from the seals and the position of the actuator, which partially blocked the exit of gas molecules from the storage container to the diffusion pumps.

Figure 74 is a graph of the fluid lost from the beginning of the continuous vacuum storage period. Total fluid lost during the 134 days of vacuum storage was 1.23 cubic inches. Leakage rates at various times in the vacuum testing are shown in the table below.

<u>Leakage</u>	<u>Fluid Pressure</u>	<u>Leakage Rate (in.³/day)</u>
During 5-day checkout	20 psig	0.205
Before adding redundant rod seal	2100 psig	2.05
After adding redundant rod seal (first day of continuous storage)	14.7 psia	0.032
Average for 134-day storage period	14.7 psia	0.0093

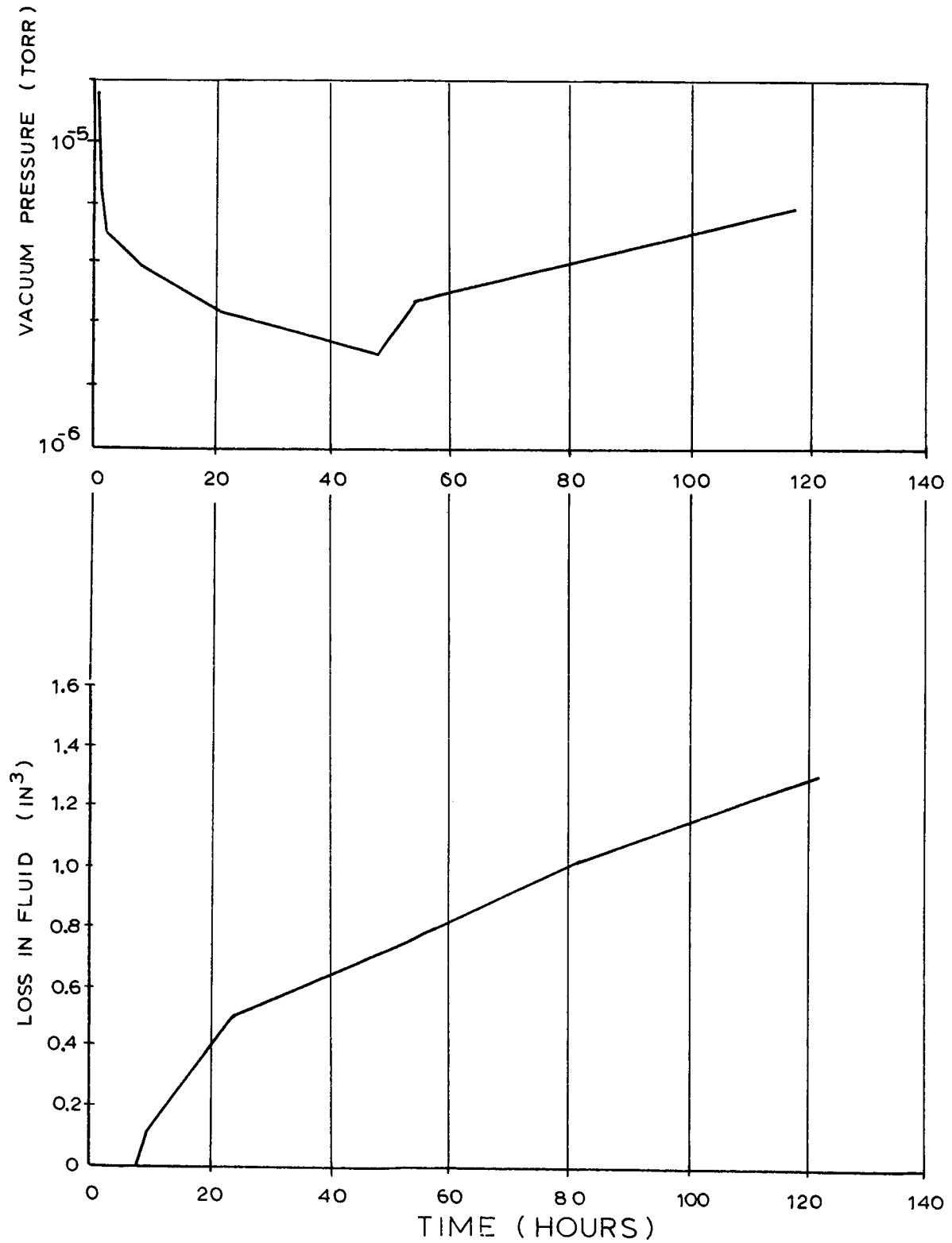


Figure 72: Leakage Effects on Vacuum-Container Pressure

D2-90795-2

DAYS

APRIL

MAY

JUNE

JULY

AUG

START

1

2

END

PRESSURES (TORR)

1 CHANGE OF PRESSURE GAGE

2 DIFFUSION - PUMP - HEATER SHORT CIRCUIT

Figure 73: Vacuum Storage Pressure Log

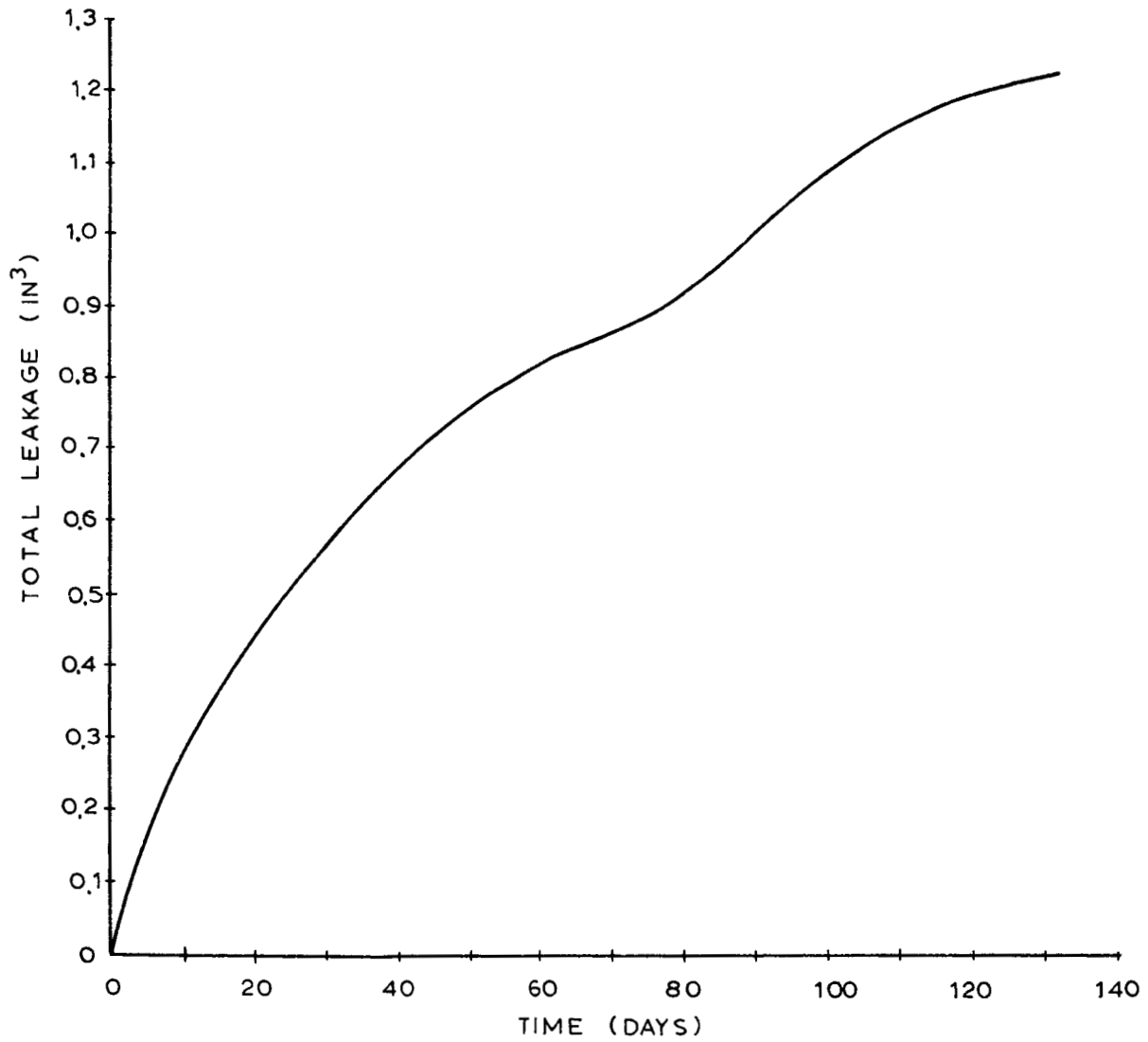


Figure 74: Vacuum Storage Test-Fluid Leakage

The system response curves for the operational sequence tests performed during the vacuum tests are shown in Figure 75. Because the installation of the actuator in the vacuum storage container necessitated the elimination of load-measuring instrumentation, insufficient data was available to explain the departure of the response in hard vacuum from the normal response.

The response data obtained during the room-pressure test at the completion of vacuum testing indicates a decrease in the friction load. This was confirmed by an accurate load calibration check after this test run. The run was not repeated due to the complexity of the disassembly performed to calibrate the friction load.

The Number 2 servoactuator disassembly showed some abrasion of the dynamic rod gland seals and piston seal. The abrasion was, however, less severe than evidenced on seals removed from the Number 1 actuator and pictured in Figures 48 and 69. The static seals showed no deterioration as a result of vacuum storage or subsequent use. A smear of sticky red material was observed on the nonexposed surface of the piston rod. Insufficient material was available for chemical analysis.

5.5.5 CONCLUSIONS

Long-term inoperative storage of a space hydraulic-actuation system in a hard vacuum of 10^{-6} torr is not detrimental to elastomeric seals or some insulation materials. The ability to further evaluate hydraulic systems at harder vacuums will depend on the development of zero-leakage dynamic seals. Such seals do not appear to be necessary for flight applications because the amount of leakage evidenced in the vacuum tests is considered to be tolerable. The vacuum-seal design requirements for vehicle system PFRT chamber testing are much more severe than the design requirements for a flight application; therefore, seal development efforts must be related to the need for chamber testing at higher vacuums. The vacuum-test-system response deviation from data obtained in other tests is caused by a problem within the control or loading system and is not a result of vacuum storage. The baseline test results before and after the vacuum tests indicate no permanent degradation in system operational characteristics due to vacuum storage.

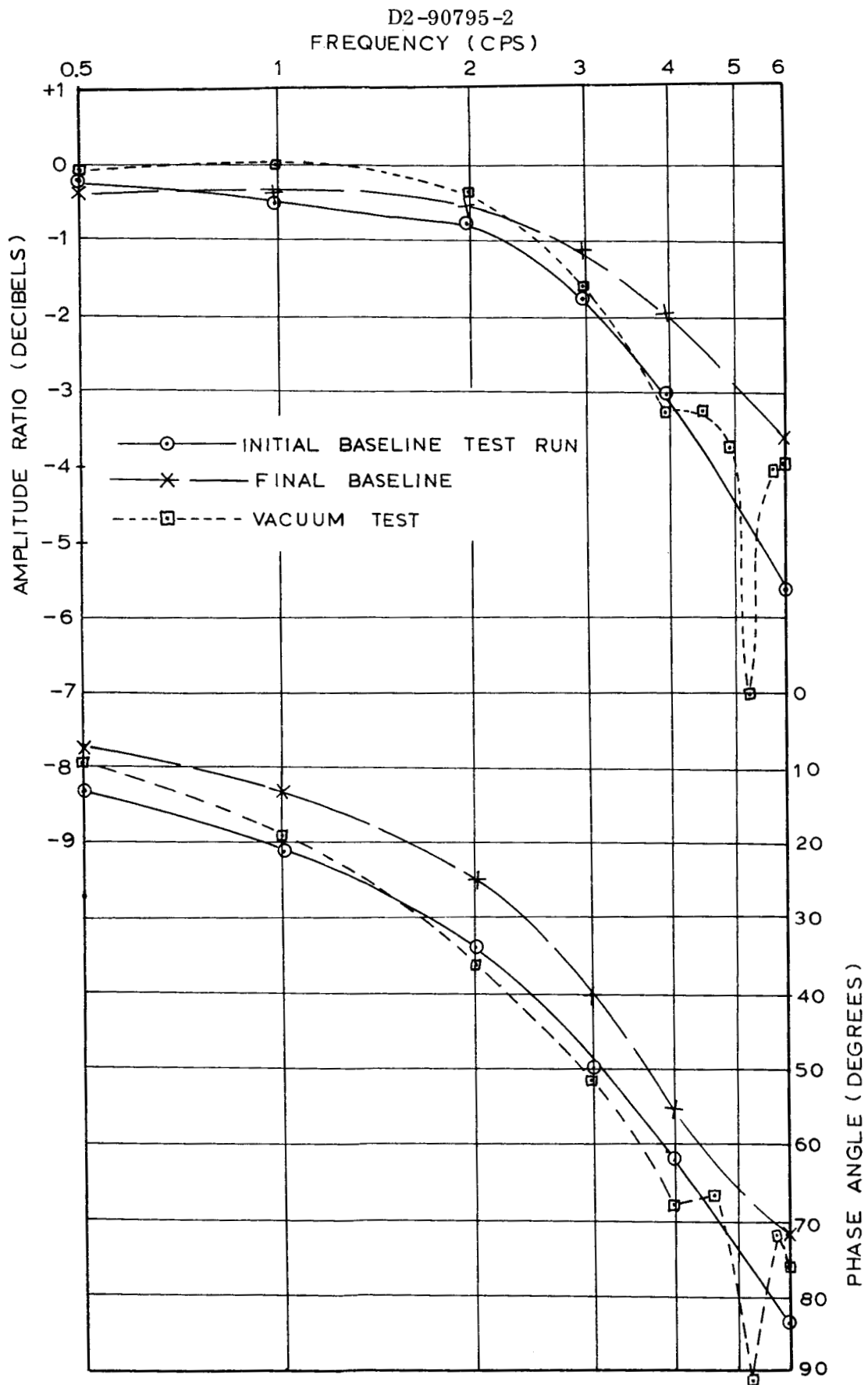


Figure 75: System Response With Vacuum Stored Actuator

6.0 TEST PROGRAM CONCLUSIONS

The results of the test program show that hydraulic systems using presently available advanced fluids are capable of performing many space actuation tasks. Functioning of the advanced hydraulic single-pass system using DuPont E-3 fluid is possible at temperatures as high as 275°F and as low as -140°F, although response at -125°F and below does not meet the requirements established for the test system. However, by increasing the system gain, thereby increasing the break frequency, acceptable response at about -125°F should be obtained throughout the frequency range evaluated in the test program. Performance improvements aimed at satisfying control tasks in temperatures and pressures at or near the environments on the lunar surface require development of new low-temperature fluids and possibly new compounds for elastomeric seals. Research to develop a generalized analysis of the low-temperature performance relationship to fluid viscosity is considered necessary to assist designers in establishing hydraulic system requirements for applications on future vehicles.

The thermal conditioning analysis showed that the penalty to condition to -100°F is an insignificant increase over the penalty for -150°F. Though practical conditioning is possible at either of these temperatures, the hydraulic development objective is to provide systems that do not require conditioning. Such unconditioned systems have an improved reliability and eliminate the delays in usage due to warmup of the system.

The material selection of 304LC stainless steel for use in the actuator was a satisfactory choice for use in a test system. The second choice of Inconel X is preferred for flight applications because, although it is more costly, it does not require the handling precautions necessary with 304LC steel at room temperature.

Fluid leakage past seals and deterioration of seal materials in space environments were not as severe as initially feared. Though seal installations in the test actuator were designed with extra squeeze (20 percent nominal rather than 8 to 13 percent). No leakage was encountered as the result of 105 hours of thermal cycling between +275 and -240°F indicating compatibility of seals with a wide range of temperatures during inoperative storage at one atmosphere pressure. The leakage present during storage at vacuum environment was well within a tolerable limit for leakage of elastomeric dynamic seals but was sufficient to reduce the ability to test to the hard vacuum desired. It is concluded that the sealing conditions required to test at hard vacuums (greater than 10^{-6}) will demand nearly zero leakage past the elastomeric seals. This condition is not required in flight applications, so the necessity for seal development will depend on the desire to test the effects of harder vacuums before flight usage.

The presence of residual contaminants in the system resulting from inability to properly clean the reservoir or receiver tank provided valuable data not intentionally planned as part of the program. Contamination in filters can prevent fluid passage at low temperatures where fluids have high viscosities even though passage is possible under the same conditions at higher temperatures and viscosities. This fact indicates that contamination control is a serious concern because the use of fine-mesh filters might not be

advisable at very low temperatures. The cause of the presence of the contaminants in the test system resulting from the inadequacy of the design of the reservoir and receiver to provide accessibility for cleaning are particular only to components of the blowdown breadboard system tested. The recirculating systems, which would be more acceptable for the majority of space applications, would not be so designed.

Pressure drop through filters increases rapidly with an increase in fluid viscosity. This establishes a serious problem that conflicts with filtration in the system as a means of contamination control. Further investigation of pressure drop in filters with high-viscosity fluids is advised before selection of flight application hardware.

Tests of recirculating hydraulic systems in space environments are needed as a continuation of the efforts initiated with the blowdown system. Proof of the adequacy of hydraulic systems for space applications depends on such testing. The development of a pump usable with both high- and low-viscosity fluids is a critical item. The existence of a great number of space-actuation applications demands the need for continuation of investigations that will culminate in the development of hydraulic hardware for flight systems.

The pleasing results of the test portion of the program reflect that conservatism was exercised in the hydraulic considerations in the trade study reported in Volume I. If the test program had been completed before the trade study analysis, a somewhat more favorable grading toward hydraulics in the parameters of reliability, cost, and availability would have resulted.

REFERENCES

1. Boeing Document D2-23419, "Low Temperature and Vacuum Effects on MIL-H-5606 Hydraulic Servo Actuation System Performance."
2. Boeing Document D2-3017-1, "Space Properties of Seal Materials," March 1965.
3. ASTM Standards, 1961, Part 7, and 1962 Supplement, "Petroleum Products and Lubricants."
4. Pennsylvania State University Contract Report AF ML TDR 64-68, "Fluids, Lubricants, Fuels, and Related Materials," February 1964.
5. ASTM Standards, 1961, Part II, and 1962 Supplement, "Rubber, Electrical and Insulation."
6. Aerospace Structural Metals Handbook, prepared by Syracuse University Research Institute for Aeronautical Systems Division, Contract AF33(616)-7792.
7. Cryogenic Materials Data Handbook, National Bureau of Standards, AF04(647)-59-3.
8. Boeing and North American Quarterly Progress Report No. 3, "Thick Section Fracture Toughness, Exhibit B," AF33(657)-11461.
9. Boeing Document D2-100006, "Lunar Excursion Module, Propulsion and Flight Dynamics," September 30, 1962 (Confidential).
10. "Model Specification 2272D-RL10-A3," Pratt & Whitney Aircraft, August 1962.
11. "Friction in High Vacuum," by A.E. Hanwell, Laboratory for the Physics and Chemistry of Solids, Cambridge, Great Britain.
12. Boeing Drawing 25-50851, "Actuator Assembly, Low Temperature Hydraulic System."
13. "Unfired Pressure Vessels," Section VIII, ASME Boiler and Pressure Vessel Code, 1962.
14. L.S. Marks, Mechanical Engineering Handbook, fifth edition, 1961.
15. ARP 785, "Procedure for the Determination of Particulate Contamination in Hydraulic Fluids by the Control Filter Gravimetric Procedure," Society of Automotive Engineers, February 1, 1963.
16. EL-4 Technical Bulletin, "Freon, E-3 Fluorocarbon Liquid," E.I. duPont De Nemours and Co.